Analysis of structure and function of Chriz complex in *Drosophila melanogaster*

D i s s e r t a t i o n

zur Erlangung des akademischen Grades
d o c t o r r e r u m n a t u r a l i u m (Dr. rer. nat.)
im Fach Biologie

eingereicht an der Lebenswissenschaftlichen Fakultät
der Humboldt-Universität zu Berlin

von
Diplom-Biologe Alexander Glotov

Präsident der Humboldt-Universität zu Berlin
Prof. Dr. Jan-Hendrik Olbertz

Dekanin/Dekan der Lebenswissenschaftlichen Fakultät
Prof. Dr. Richard Lucius

Gutachter/innen:
1. Prof. Dr. Harald Saumweber
2. Prof. Dr. Ann Ehrenhofer-Murray
3. Prof. Dr. Gunter Reuter

Tag der mündlichen Prüfung: 04.12.2015

Table of Contents

Abstract (German)

Die Struktur des Chromatins spielt eine bedeutende Rolle bei der Stadien- und Gewebs-spezifischen Genexpression. Der epigenetische Status von Chromatindomänen wird mit Hilfe einer Anzahl von Proteinen und Histonmodifikationen etabliert und aufrechterhalten. Das Ziel der vorliegenden Arbeit ist die Untersuchung der Bedeutung und Funktion des Chriz Protein Komplexes bei *Drosophila*, der spezifisch in dekondensierten Regionen von Interphase Chromosomen gebunden ist. Mehrere Proteine waren als Bestandteile des Chriz Komplex bereits bekannt, darunter das Zink-Finger Protein Z4 und die H3S10 Kinase Jil1. Meine RNAi Experimente an embryonalen S2 Zellen zeigten, dass die Rekrutierung von Z4 und der Kinase Jil-1 an das Chromatin sowie dessen H3S10 Phosphorylierung während der Interphase von der Gegenwart von Chriz abhängen. Diese Ergebnisse lieferten einen eine starken Hinweis auf eine Ähnlichkeit bei der Bildung des Komplexes in polytänen Zellen und diploiden S2 Zellen. Ich führte eine vergleichende Analyse der Bindungsprofile von Proteinen des Chriz Komplex zwischen Speicheldrüsen im 3.Larvenstadium und S2 Zellen im chromosomalen Intervall 61C7-8 durch. Dabei fand ich heraus, dass die Chriz Bindungsprofile im proximalen Teil der Domäne konserviert waren. Dagegen beobachtete ich eine veränderte Chriz Bindung im distalen Teil, die mit einem veränderten Transkriptionsprofil in dieser Region übereinstimmte. Verfügbare genomweite Daten zeigen eine Tendenz, dass Chriz in der Nähe von Transkriptionsstart-Stellen (TSS) und Promotoren aktiver Gene bindet. Ich untersuchte daher die Korrelation zwischen der Chriz Bindung an Promoter Regionen von elf in S2 Zellen und Speicheldrüsen differentiell exprimierten Genen. Chriz und Z4 RNAi Experimente in S2 Zellen führten zu einer Veränderung der Expression vieler Chriz- und Z4-bindender Gene. Mittels Co-Immunpräzipitation und Protein „Pull-down“ konnte ich die Bindung der Insulator Proteine BEAF-32 und CP190 im Chriz-Komplex nachweisen und die für die Protein-Protein Interaktion notwendigen Proteinabschnitte grob kartieren. Schließlich überprüfte ich die Möglichkeit einer Rekrutierung des Chriz Komplexes durch BEAF-32 mit Hilfe von BEAF-32 RNAi bzw. nach Induktion von Punktmutationen in bekannten BEAF-32 Bindemotiven. Meine Ergebnisse wiesen eine Wechselwirkung zwischen Chriz und Insulator Proteinen nach und zeigten, dass der Chriz-Komplex eine wichtige Bedeutung bei der strukturellen Organisation von Chromatin Domänen besitzt.

Abstract (English)

Chromatin structure is important for the correct stage and tissue-specific expression of the genetic material. The epigenetic state of chromatin domains is established and maintained by a number of proteins and histone modifications. The aim of current thesis is to investigate the role and function of Chriz protein complex, specifically bound to decondensed regions of interphase chromosomes in *Drosophila*. Several proteins were known to compose Chriz complex - chromodomain protein Chriz, zinc finger protein Z4 and H3S10 kinase Jil-1. I performed RNAi experiments on S2 cells which demonstrated that recruitment of Z4 and Jil-1 kinase to chromatin and interphase H3S10 phosphorylation are dependent on the presence of Chriz, and pointed to the high similarity of complex assembling between polytene cells and S2 diploid cells. I accomplished the comparative analysis of binding profiles of Chriz complex components between 3rd instar larvae salivary glands and S2 cell culture within 61C7-8 chromosomal interval. I found that Chriz binding profiles between two tissues are conserved at proximal part, however variant Chriz binding in distal part of 61C7-8 domain coincides with differences in transcription profile in the same region. Publicly available genome-wide data shows a tendency of Chriz to bind near Transcription Start Sites (TSS) and promoter regions of active genes. I investigated the correlation of Chriz binding to promoter regions of 11 differentially expressed genes with the expression of these genes in S2 cells and in salivary glands of 3rd instar larva. Chriz and Z4 RNAi experiments, performed in S2 cells resulted in expression changes of many Chriz- and Z4-binding genes. Using co-immunoprecipitation and pull-down assays, I identified insulator proteins BEAF-32 and CP190 to be present in the Chriz complex and performed rough mapping of interacting domains. Using BEAF-32 RNAi and introduced point mutations to BEAF-32 binding motifs I examined the possibility for recruitment of Chriz complex by BEAF-32. The obtained results revealed the interplay between Chriz and insulator proteins and point to important architectural role of Chriz complex in organizing chromatin domains.

Acknowledgements

I wish to express my sincere appreciation to my supervisor, Professor Harald Saumweber. I consider it a great opportunity to do my doctoral research under his guidance and to learn from his research expertise. I hope that I could be as lively, enthusiastic, and energetic as Harry and to someday be able to manage a research group as well as he can.

I thank all the present and former members of our Cytogenetic group whom I had a chance to work with for their friendly help, comments and suggestions. Thomas Zielke, Dandan Zhao, Ansgar Klebes, Dereje Negeri, Jenni Jammrath, Hussein Baaj, Shaza Dehne, Jorge Ferreira – you are the best colleagues I've ever known. We've got a really great atmosphere in the group, which I will definitely miss.

A big "Thank you!" also goes to Petra Binting and Irina Passow for their brilliant technical assistance.

I would also like to take this opportunity to thank all the students, to whose bachelor or master project I had a possibility to contribute to as a practical supervisor. Sorry for being strict with them sometimes.

I especially thank my Mom, Dad, and Sister. I love them so much and I would not make it this far without them.

Finally, I thank God for letting me through all the difficulties.

1. Introduction

1.1 Chromatin architecture

Large genomes of eukaryotic cells are densely packed into chromatin to fit inside nuclei that have diameter of few microns. One of fundamental questions in molecular biology is how such a compacted structure is established and maintained in a way to provide correct and virtuously regulated expression of encoded genetic material.

The fundamental unit of chromatin is a nucleosome comprising 147 base pairs (bp) of DNA wrapped around a histone octamer core in ≈1.67 left-handed superhelical turns as shown on the Fig. 1 (Cutter et al. 2015). The four core histones (H2A, H2B, H3 and H4) are relatively small (11–15kDa), very basic proteins that are highly conserved among eukaryotic species (White 2001). N-terminal "tails" of histones protruding out of nucleosomal core are strikingly prone to such post-translational modifications as acetylation, methylation or phosphorylation in a multitude of residues (Bannister et al. 2011; Feng et al. 2011).

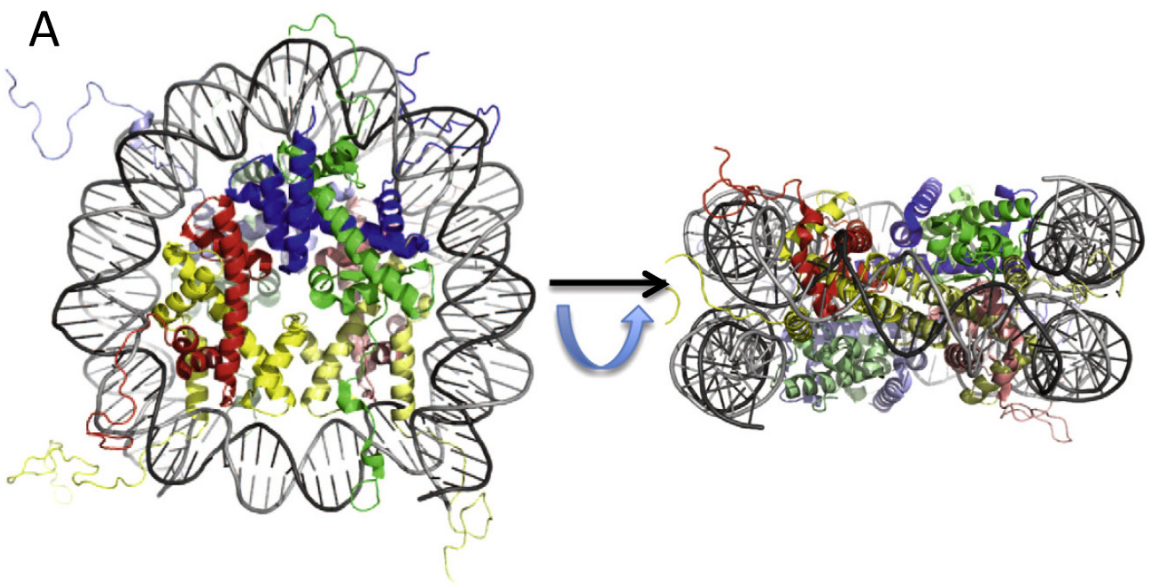

Fig. 1. Structural details of a nucleosome core. (A) Model of a nucleosome core. A view down the superhelical axis, and a view rotated 90˚ about a horizontal axis. H2A, green, H2B, blue, H3, yellow, H4, red. Proteins in lower half of nucleosome are lighter in color (Cutter et al. 2015).

The core DNA is in tight association with the core histones and is protected from nuclease digestion whereas the linker DNA is rapidly digested. This fact determined historically the term ''nucleosome core particle'', which was originally defined as the product of extensive micrococcal nuclease digestion of native chromatin (Ausio et al. 1989).

The nucleosomal folding reflects the first 'beads on a string' fiber level of DNA compaction with a diameter of 10 nm. Linker histones (H1 and H5) bind to the DNA linker regions in close proximity to the sites of DNA entry, and organize the nucleosomal particles into a more

condensed 30-nm chromatin fiber, which represents the second level of DNA compaction (Thoma et al. 1979; Widom et al. 1985).

To describe three-dimensional organization of nucleosomes into 30-nm chromatin fibers, a number of models, including the solenoid (Finch et al. 1976), twisted-ribbon (Worcel et al. 1981), cross-linker (Staynov et al. 1983), and superbead (Zentgraf et al. 1984) models, had initially been proposed, based on the early studies of native chromatin in nuclei or isolated from nuclei by various biochemical and biophysical studies. Despite three decades of intense research, the precise structure of the 30-nm chromatin fiber remains elusive, however, recently Guohong and coworkers proposed 3D-cryo-EM structure which showed a left-handed twist of the repeating tetra-nucleosomal structural units with a two-start ‘‘Zig–Zag’’ configuration (Guohong et al. 2015) (Fig. 2).

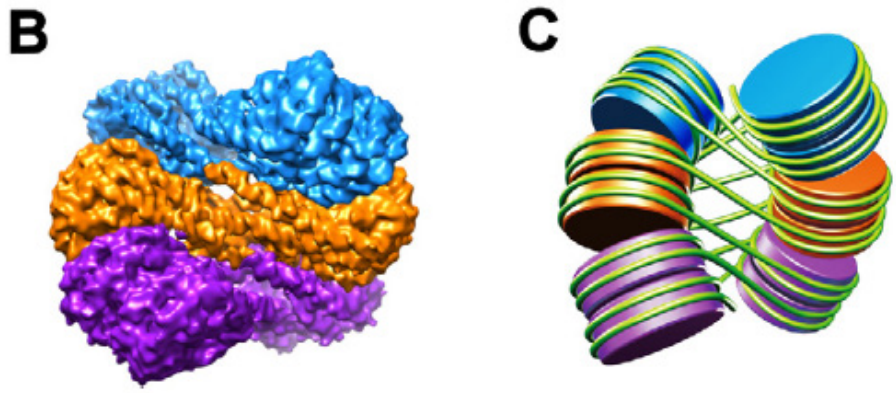

Fig. 2. 3D structure of 30-nm chromatin fiber. (B) The three tetranucleosomal structural units of the 30-nm chromatin fibers reconstituted on 12 x 187 bp DNA arrays are highlighted in different colors. (C) A schematic representation of the cryo-EM structure of a 30-nm chromatin fiber as shown in B. (Guohong et al. 2015)

The 30 nm fibres could be further compacted or coiled, or just be arranged side to side, forming a hierarchy of folding levels, resulting in fibres of 60– 300 nm (Daban 2000).

Other microscopy-based studies suggested complex topologies co-existing within linear interphase chromosome structures (Bian et al. 2012). Based on cryo-EM and ESI contrast for conventional EM, the existence of an in vivo interphase chromosome structure which consists nearly entirely of 10 nm fibers, locally dispersed or concentrated in compact local domains was proposed (Bian et al. 2012).

During the interphase, chromatin is folded into domains 300-700 nm sizes, which comprise a chromosome territory. The structure and organization of chromatin loops inside a chromosome territory remain still unclear and was proposed to exist in the form of solenoid, or zigzag, or nucleosomes, or a hybrid of those. According to the chromonema model, chromosome structure arises from three helical folding levels of chromatin fibres. Fibres of 60–80 nm in width are coiled into fibres of 100– 130 nm which are further coiled to the 200–300 nm structure of the metaphase chromatid (Heun et al. 2001) (See Fig. 3).

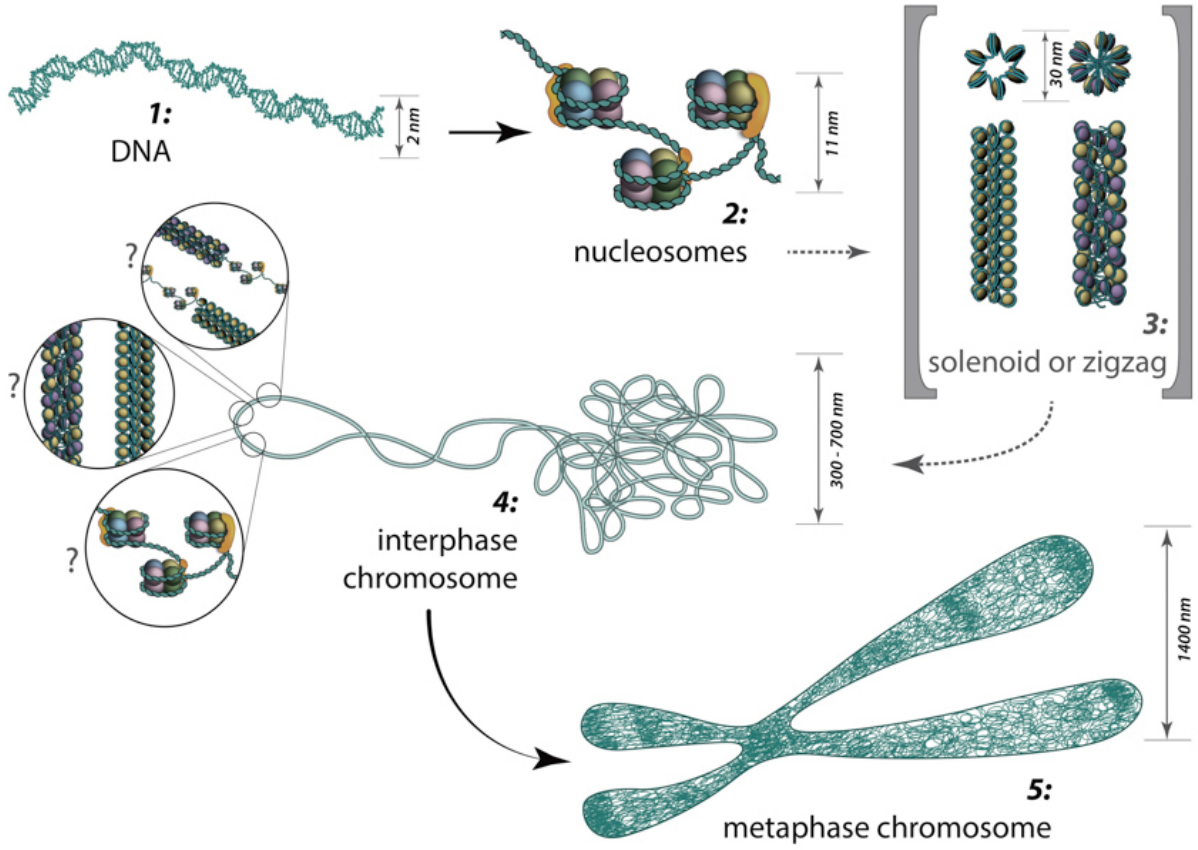

Figure 3. From DNA to metaphase chromosome: The major structures in DNA compaction. (MBInfo).

During such processes as transcription or replication chromosomal organization is highly dynamic, varying both between different cell types and during the cell cycle. Recent studies revealed importance of spatial nuclear disposition of different chromatin regions and their relationships to the nuclear envelope for regulation of gene expression (Bickmore et al. 2013). However the exact logic of chromosome organization at the sub-megabase scale, which is the level where most gene regulatory landscapes and long range interactions are thought to occur (Kleinjan et al. 2009, Sanyal et al. 2012) had remained somewhat of a blackbox.

Chromosome conformation capture (3C) experiments have uncovered the presence of an additional level of compartmentalization of the genome (Dekker et al. 2002). Chromosomes of a wide range of species were found to be organized as a string of so called Topologically Associated Domains (TADs), which are characterized by preferential chromatin interactions within them, and spatial separation of loci located in different domains (Dekker et al. 2015). In mammalian genomes these domains are several hundred kb in size, up to 1–2 Mb (Dixon et al. 2012), whereas they are smaller in bacteria (~170 kb) (Le et al. 2013) and in flies (~60 kb) (Hou et al. 2012). TADs (also named as “physical domains”) were found to correlate strongly with epigenetic features, including active gene density, association with the nuclear

lamina, replication timing, nucleotide and repetitive element composition (Sexton et al. 2012). Analyzing of expression patterns of genes located within the same TAD across ES cell differentiation, Nora and coworkers revealed that genes united in the same TAD show similar dynamics of expression during differentiation, whereas genes located in different TADs were less correlated (Nora et al. 2012).

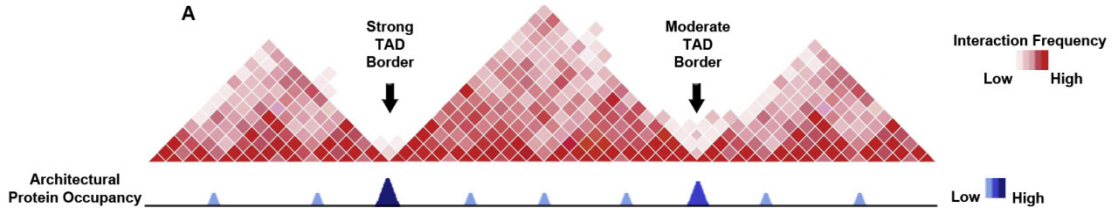

Figure 4. Architectural proteins mark TAD borders. Cartoon schematics depicting regions of highly associating chromatin called TADs, which are separated by TAD borders. Interaction frequency is shown as a continuum from white to dark red. (A) The strength of a TAD border, defined as the ratio between intra- and inter-TAD interactions around border sequences, depends on architectural protein occupancy (occupancy shown by peak size and a continuum from light to dark blue) (Cubenas-Pottis et al. 2015).

Moreover, the calculated physical domains from the Hi-C contact map strongly correlated with numerous linear epigenetic profiles describing enrichment for histone modification or such DNA-binding factors as chromodomain protein Chriz, insulator proteins CP190, BEAF-32 and dCTCF (Sexton et al. 2012) (See Fig. 4). These findings support the statement that TADs are critical chromosome structural units of long-range gene regulation (Sexton et al. 2012, Cubenas-Pottis et al. 2015).

1.2 Histone modifications

Interphase chromatin is not static. Although nucleosomes themselves are stable and have limited mobility, a number of remodeling complexes can mobilize and/or eject the nucleosome to regulate access to DNA (Saha et al. 2006). Moreover, depending on the needs of the cell, the N-terminal and C-terminal tails of histones may undergo reversible post-translational modifications that change their interaction with DNA and convert them to “docking stations” for different classes of nuclear proteins (Martin et al. 2005)

To date, a wide variety of histone post-translational modifications (PTMs) are known, including methylation, acetylation, phosphorylation, glycosylation, carbonylation, ubiquitylation, biotinylation, sumoylation, citrullination, ADP-ribosylation, N-formylation, crotonylation, propionylation, and butyrylation, as well as proline and aspartic acid isomerization (Sadakierska-Chudy et al. 2015). Known enzymes, which execute this huge variety of modifications are listed in Table 1.

Enzyme	Activity[1]	General Role
Deacetylases		
RPD3	H3K9, H3K14, H3K27, H4	Repression
HDAC3	H4	Repression
HDAC4		Repression
HDAC6	H4	Repression
HDACX		Repression
SIR2	H3K56, H4	Repression
Acetyltransferases		
dGCN5	H3K9, H3K14, H4K12	Activation
Tip60		Repression
Chm	H4	Activation and repression
MOF	H4K16	Activation, dosage compensation
dCBP	H3K18, H3K27, H3K56	Activation
TAF1	H3 and H4	Activation
Lysine Methylases		
Trx	H3K4	Activation
Ash1	H3K4, H3K9, H3K36, H4K20	Activation
Trr	H3K4Me3	Activation
dSet2/dHybp	H3K36Me3	Activation, dosage compensation
dMes-4	H3K36Me2, Me3	Activation
dDot1/Grappa	H3K79Me1, Me2	Activation
Su(var)3-9	H3K9Me2	Heterochromatin
dSETDB1	H3K9	Heterochromatin
dG9a	H3K9, H3K27	Repression
E(z)	H3K27Me1, Me2, Me3	Repression
PR-Set7	H4K20Me1	Repression
Suv4-20	H4K20Me2, Me3	Repression
Lysine Demethylases		
Su(var)3-3	H3K4Me1, Me2	Heterochromatin
LID	H3K4Me3	Activation and repression
dKDM4A	H3K9Me3, H3K36Me3	Repression
dKDM2	H3K4Me, H3K36Me2	Repression
dUTX	H3K27Me2, Me3	Activation
Arginine Methylases		
DART1	H4R3Me2	Repression
DART4/CARMER	H3R17Me2	Activation
Ubiquitinases		
dRING	uH2A	Repression
dBre1	uH2B	Activation
TAF1	uH1	Activation
Deubiquitinases		
Calypso	uH2A	Repression
Scrawny	uH2B	Repression
USP7	uH2B	Repression
Nonstop	uH2A, uH2B	Activation
Kinases		
JIL-1	H3S10	Activation
TAF1	H2BS33	Activation

Table 1. Histone modifying enzyme activity. [1] Histone or residue if known. (Modified from Swaminathan et al. 2012)

Phosphorylation, in general, represents one of the major forms of histone post-translational modifications. It can be found at, threonine (North et al. 2011), tyrosine and histidine

(Besant et al. 2012), but more often at serine residues (Sotero-Caio et al. 2011) in each or the four core histones. In particular, phosphorylation of histone H3 at serine 10 is observed frequently. This modification is observed both at interphase chromatin and during mitosis and is linked with different processes, such as transcription activation or mitotic chromatin condensation (Nowak et al. 2004). During interphase in *Drosophila*, the majority of H3S10 phosphorylation is performed by JIL-1, an essential, ubiquitously expressed, nuclear tandem kinase (Jin et al. 1999) (will be discussed later). At mitosis, genome-wide H3S10ph (and also H3S28ph) marks are established by Aurora B kinase and erased by PP1 phosphatase (Giet et al. 2001, Goto et al. 2002).

Histone acetylation in *Drosophila* is known a while ago to be associated with transcription activation (Allfrey et al. 1964). To date, several histone acetyltransferases have been identified and grouped into three main families - MOF (KAT8), chameau (KAT7) and Tip60 (KAT5) belong to the MYST HAT family. dGCN5 (KAT2) and Elp3 (HAT9) represent members of the GNAT HAT family, while nejire (KAT3) is the single *Drosophila* CBP/p300 homologue (Lee et al. 2010, Boros 2012).

Methylation of histones may occur at lysine and arginine residues and is associated both with transcription activation and repression (Martin et al. 2005). Lysine methylation, which is more characterized, was found at five positions of histone H3 and at single position of histone H4. Methylation of H3K4, H3K36 and H3K79 was identified in association with active transcription, whereas H3K9, H3K27 and H4K20 methylation associated with repression (Sims et al. 2003, Martin et al. 2005).

In *Drosophila* methylation of H3K4 is executed by several enzymes. To date, Trx, absent, small and homeotic di*scs* 1 (Ash1), and Trithorax-related (Trr) have been identified as H3K4 methyltransferases. Little imaginal di*scs* (LID) and Su(var)3-3, the *Drosophila* homolog of LSD1, are H3K4 specific demethylases (Swaminathan et al. 2012)

Histone H3 lysine 27 trimethylation, was specifically found to play an important role in polycomb-mediated gene silencing. It is known to be found at repressed genes containing PREs – Polycomb Response Elements, which recruit PcG proteins. Trimethylation of H3 K27 spreads out from this sites by enzymatic activity of E(z), the SET domain-containing subunit of PRC2 (Muller et al. 2002).

As can be seen, the majority of histone modifications can be associated with two opposite processes, namely transcriptional activation and repression (Cohen, 2011). However, regulation of these processes is tightly connected with another important task – determination of chromatin state (Brower-Toland et al. 2009).

Heterochromatin is generally repressive and deprived of such histone modifications as acetylation. In metazoan, two types of heterochromatin can be defined – *facultative* heterochromatin which contains developmentally or tissue-specifically silenced genes (for instance, homeotic genes, *Antennapedia* or *Bithorax* complexes) sometimes marked by

H3K27me3, and H3K9 methylated *constitutive* heterochromatin, which contains permanently silenced genes in genomic regions such as the centromeres and telomeres. Active genes and their regulatory regions are located in more open, decondensed **euchromatin**, containing a number of typical histone modifications, such as H3S10 phosphorylation or H3K9 acetylation. However, high degree of overlap between different histone modifications is observed, proposing, that there are no simple rules governing their localization and function (Bannister et al. 2011).

A simplified scheme of euchromatic and heterochromatic regions, established by action of distinct histone modifying enzymes is shown on Fig. 5.

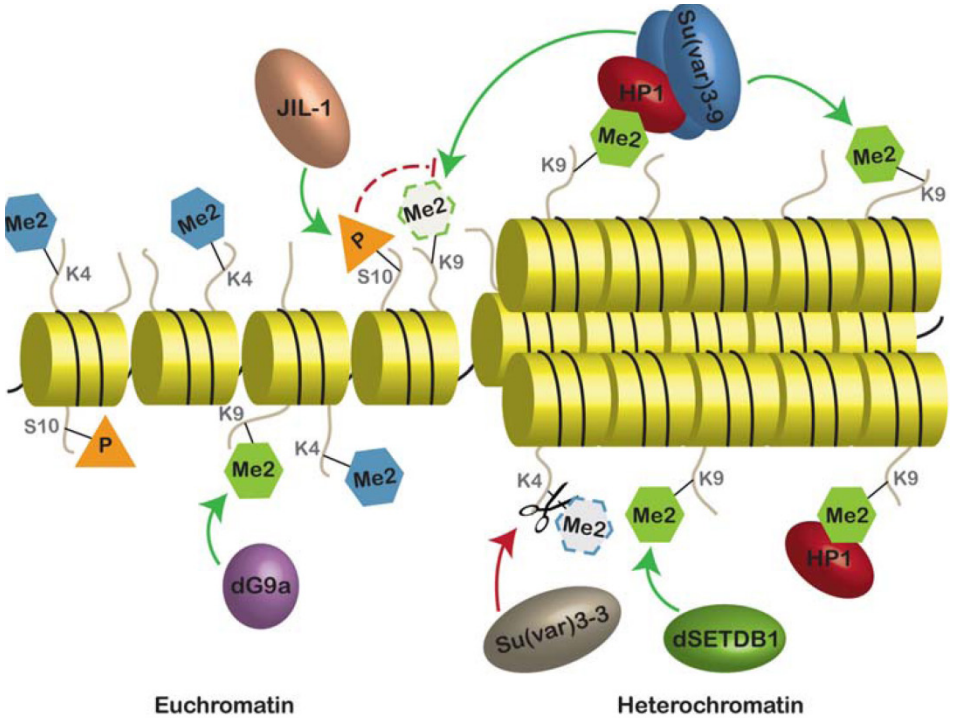

Figure 5. Chromatin states with typical histone modifications. The major enzymes and their location of action are indicated. Green arrows indicate the addition of the mark and red arrows with scissors indicate the removal of the specified modification. Dashed arc indicates an indirect effect. Dashed lines and margins indicate disappearance of the mark (Swaminathan et al. 2012, modified).

Genome-wide profiles identifying the location of the histone marks, as well as analysis of phenotypes resulting from altered levels of the modifying enzymes indicate the existence of "cross talk" between certain modifications where, for instance, one mark facilitates another or is even required for the second mark to occur or when one modification prevents the modification of a second residue (Lee et al. 2010).

Such comparative analysis required systematic collection of a rapidly increasing amount of genome-wide data. In 2007 over 2 000 datasets containing the information about positions

of modified histones and other chromatin marks, origins of DNA replication, RNA transcripts and the transcription factor binding sites of *Drosophila* were combined to a single database by modENCODE Consortium (2007-2012) aimed to discover and provide biologically informative characterizations of as many genomic elements as possible (Brown et al. 2015). The modENCODE platform provided unique possibilities for epigenetic studies purposed to reveal the principles of underlying chromatin regulation (Schubeler et al. 2010).

The analysis of genome-wide distribution of numerous epigenetic factors leaded to a statement that functional state of chromatin may be accompanied by a certain local combinations of bound proteins and/or histone modifications (Filion et al. 2010). The development of such ideas resulted in establishing of several “maps of chromatin state” (Filion et al. 2010; Kharchenko et al. 2011; Zhimulev et al. 2014), which were attempted to identify the necessary epigenetic features for chromatin structure determination. Active chromatin types in their models were accompanied with local enrichment of Pol II, active transcription and presence of such modifications as H3K9Ac and H3K4me3. Repressive chromatin types featured Polycomb group protein binding, lamin association, H3K27me3, etc. Using the available database Zhimulev and coworkers reported correlations found for a number of regions between the cytogenetic structure of polytene chromosomes and selected features of inactive/active chromatin of S2 cells (Vatolina et al. 2011; Demakov et al. 2011).

1.3 Polytene chromosomes

Polytene chromosomes of *Drosophila* have been used for epigenetic studies since 1934 (Turner et al. 1992). Due to chromatid amplification, polytene chromosomes of larval salivary glands provide a precious possibility of direct visualization of chromosomal architecture during interphase, location of proteins bound and modified histones involved in the regulation of chromatin structure and expression of genetic material.

On microscopic squash preparations of polytene chromosomes a reproducible pattern of clearly distinguishable compacted bands interrupted by less compacted interbands can be observed (See figure 6) (Painter et al. 1934; Beermann et al. 1972).

Heat-shock or steroid hormone treatment leads to local loosening of polytene chromatin structure known as “puffing”, which is associated with the induction of extremely high levels of transcription of steroid response or stress-activated genes located at relevant polytene chromosome regions (Ashburner 1967, 1970).

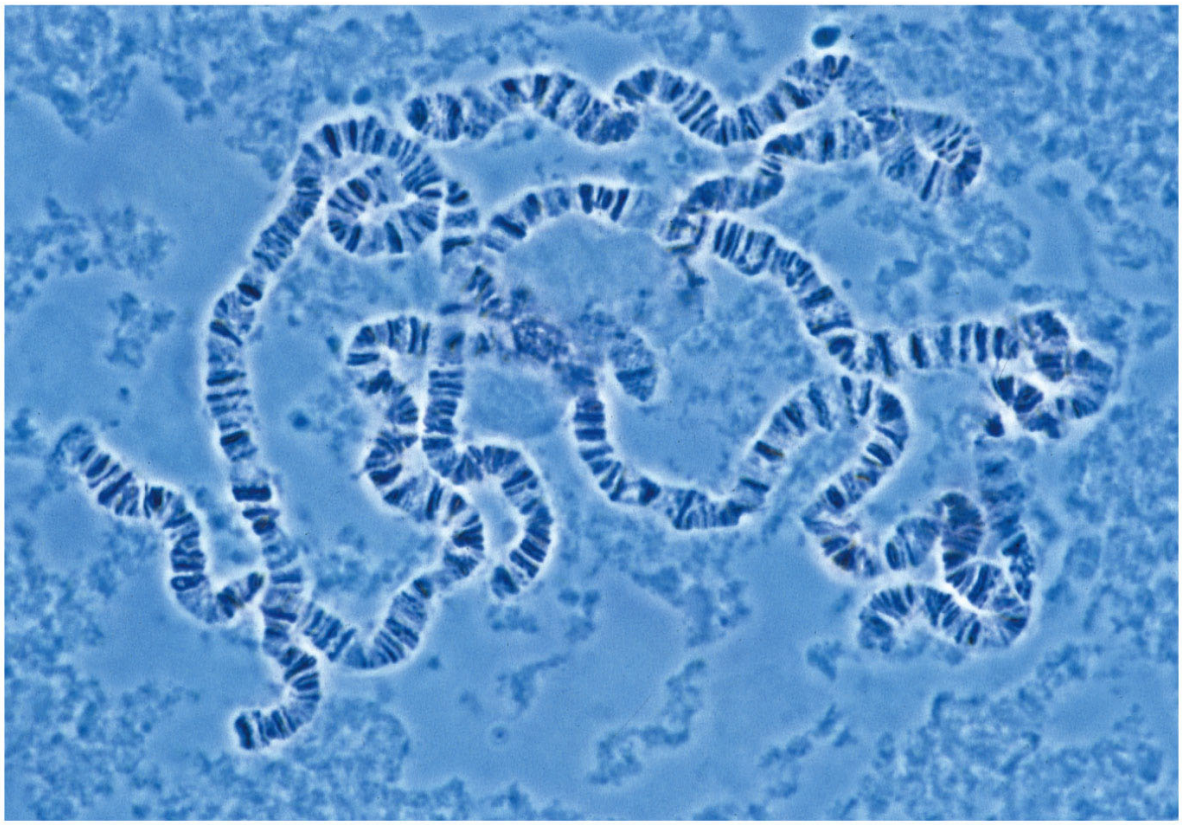

Fig. 6. Polytene chromosomes from *Drosophila* salivary glands. (The Cell, 4th Edition, Fig. 5.26, 2006)

RNA-polymerase enrichment as well as detected ongoing transcription process in interbands pointed to localization of active genes there (Alcover et al. 1982). Till recent time, the hypothesis which postulated interbands as the sites of location of 5' parts of genes, while the 3' gene ends were assigned to the adjacent bands was poplular among cytologists (Zhimulev et al. 2013). However latest findings purposed to merged the cytological observations with molecular biological datasets consider interbands as distinct open chromatin domains, containing active genes (See Fig. 7) (Sexton et al. 2012; Zhimulev et al. 2014; Zielke et al. 2015, in press). Therefore, experimental evidences, strengthening the statement that the boundaries of chromatin marks coincide with borders of the physical domains, are provided (White 2012).

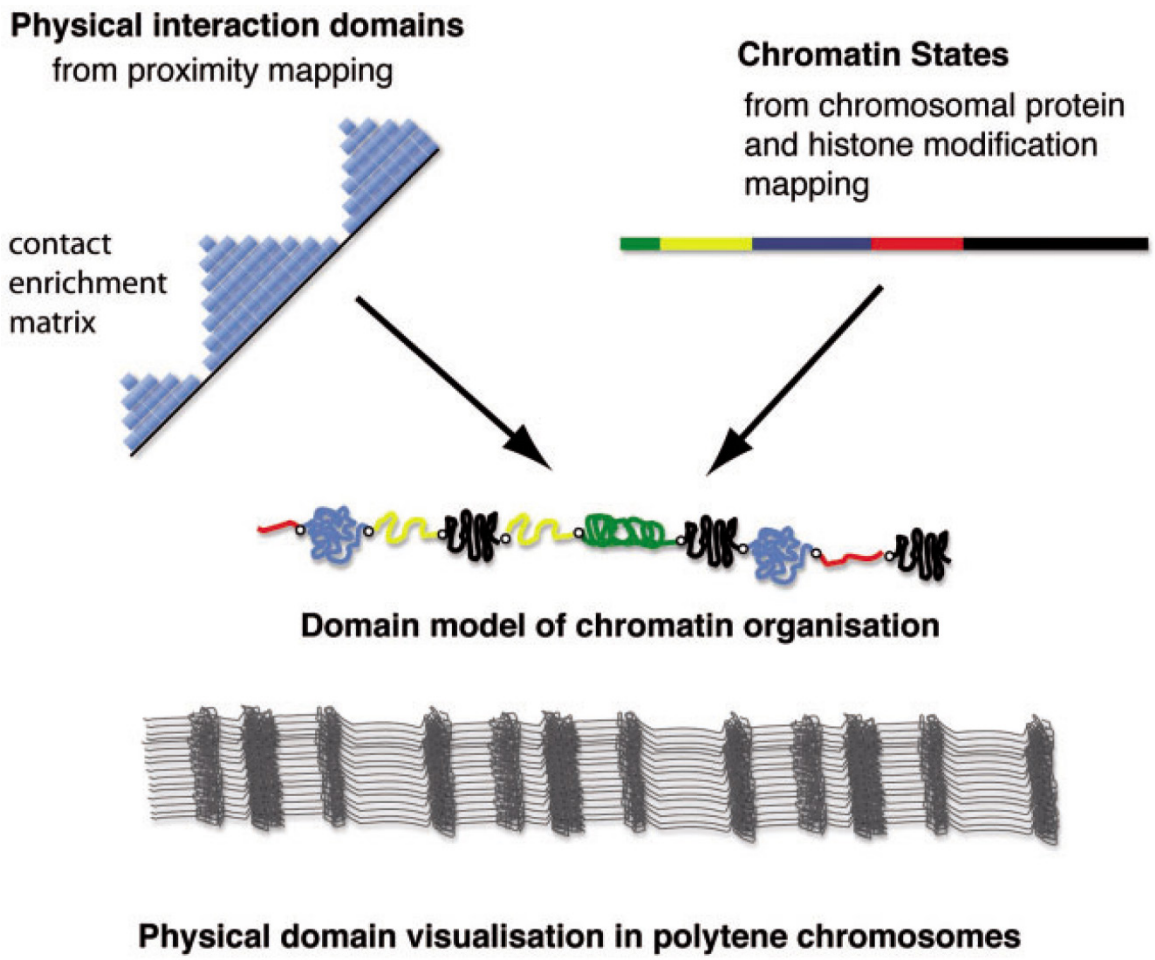

Figure 7: The domain organization of the genome. In the domain model, the different chromatin states are represented by domains of different chromatin folding, separated by boundaries (open dots). Blue, green and black lines corresponds to different types of condensed chromatin, red and yellow – to active chromatin states (according to Filion et al. 2010). Physical domains can be visualized at polytene chromosomes as band/interband pattern (Modified from White 2012).

Continuing technical and methodological advances together with the wealth of existing studies on the *Drosophila* genome make the fly a major model for the analysis of the many remaining questions concerning how genome packaging relates to genome function (White 2012).

1.4 Chriz/Z4/Jil-1 complex

The proper organization of eukaryotic chromosomes determines the manner in which the DNA sequence is interpreted in a large number of cellular processes, such as DNA replication, repair and transcription (Sexton, 2009). Therefore, for keeping the dynamic structure of chromatin, a huge number of proteins and protein complexes are employed. Current study is focused on Chriz complex, discovered in our group in 2004.

Several proteins are known to be part of this complex, however, the “core” consists of zinc-finger protein Z4 and “the chromodomain protein interacting with Z4” - Chriz (also called Chromator by some authors (Rath et al. 2004).

Chriz has a calculated molecular weight of 100 kDa (apparent 130-140 kDa), and can be divided into two main domains, an amino-terminal domain containing the chromodomain and a carboxy-terminal domain containing a nuclear localization signal (Fig. 8)(Rath et al. 2004, Gortchakov et al. 2005). Chriz protein is ubiquitous, essential and is known to fulfil several functions during fly development (Gortchakov et al. 2005; Rath et al. 2006; Wasser et al. 2007; Ding et al. 2009). During the interphase Chriz is localized at interband regions of polytene chromosomes, but not in puffs. However, during cell division Chriz redistributes to form a macro molecular spindle matrix complex together with at least three other nuclear-derived proteins Skeletor, Megator, and EAST (Walker et al. 2000; Rath et al. 2004; Qi et al. 2004, 2005). The studies of Gan with colleagues showed that N-terminal part of Chriz is responsible for correct targeting to chromatin (Gan et al. 2011). Same domain later was found to interact with histone H1 (Yao et al. 2012). C-terminal domain was reported to be sufficient for localization to mitotic spindle (Ding et al. 2009).

Figure 8. Schematic picture of the full-length chromodomain protein Chriz (926 amino acid residues). Chomodomain is displayed as yellow box. The extent of the domains is given by aa numbers.

Chriz is required for maintenance of chromatin structure – polytene chromosomes of flies with a combination of hypomorphic mutant alleles showed loss of band/interband structure together with numerous ectopic contacts connecting non-homologous chromosomal regions (Rath et al. 2006)(Fig. 9, 10).

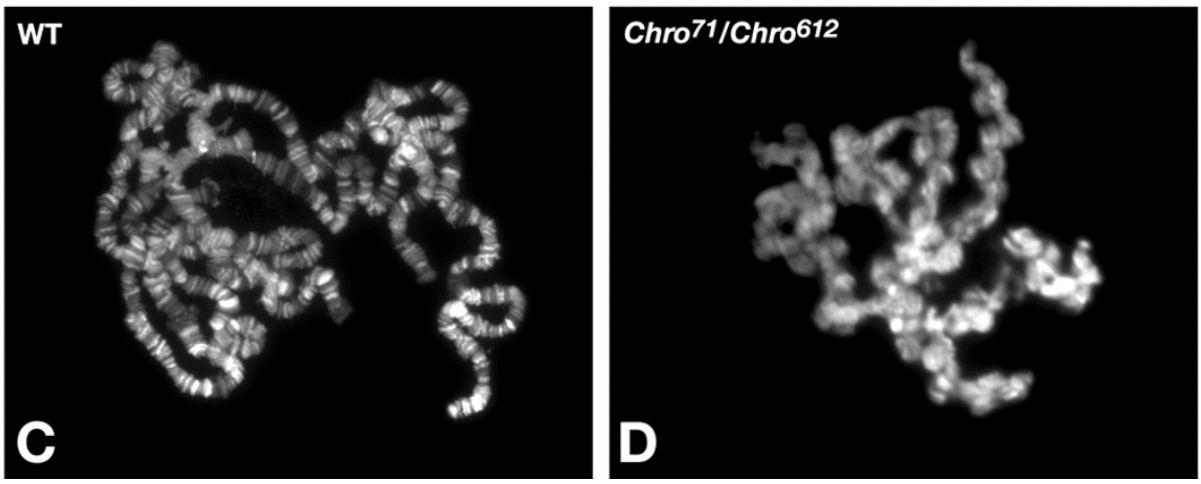

Fig. 9 Localization of Chriz in mutant polytene chromosomes. Polytene chromosome preparations from third-instar larvae were labeled with Hoechst to visualize the chromatin. Preparations are shown from a wild-type female larvae (C) and from a female *Chro*^{71}/*Chro*^{612} mutant larvae (D). Reduced levels of wild-type Chromator protein have a severe effect on the structure and organization of larval polytene chromosomes. Note the disruption and misalignment of interband and banded regions and the extensive coiling and folding of the chromosome arms in *Chro*^{71}/*Chro*^{612} mutant chromosomes (D). (Modified from Rath et al 2006)

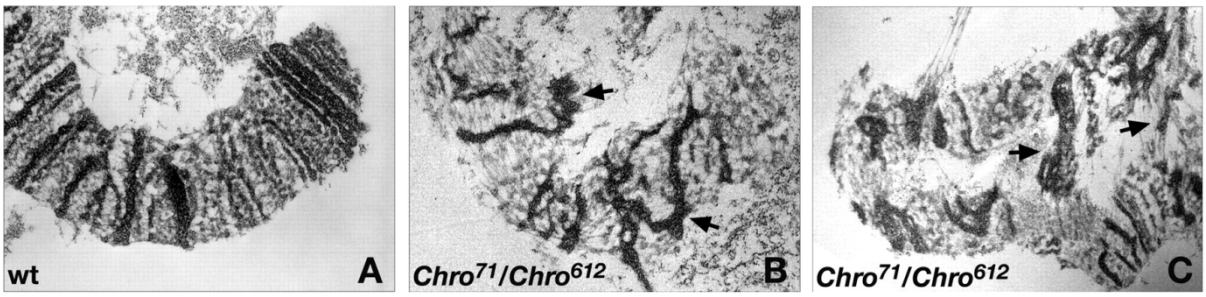

Fig. 10. Ultrastructure of Chro71/Chro612 mutant polytene chromosomes. (A) TEM micrograph of a wild-type polytene chromosome. Note the clear segregation into bands and interbands and the orderly alignment of euchromatic chromatid fibrils. (B,C) Chromosomes from Chro71/Chro612 polytene salivary gland nuclei. The micrograph in B shows the disorganization and misalignment of band/interband polytene chromosome regions (arrows). The micrograph in C shows the folding and coiling of the chromosomes with numerous ectopic contacts connecting non-homologous regions (arrows). (Modified from Rath et al 2006).

Chriz significantly co-localizes and interacts with the tandem kinase Jil-1, which phosphorylates histone H3 at serine 10 residue during the interphase (Rath et al. 2006). Jil-1 was shown to play a significant role in maintaining polytene chromosome structure and is enriched about two-fold on the male X-chromosome (Jin et al. 1999; Wang et al., 2001; Deng

et al., 2005; Zhang et al., 2006). In the absence of JIL-1 non-orderly intermixing of euchromatin and the compacted chromatin banded regions was observed (Deng et al., 2005) along with is a striking redistribution of the heterochromatin markers dimethyl H3K9 and HP1 to ectopic chromosome sites (Zhang et al., 2006). Deng and colleagues demonstrated that ectopic recruitment of JIL-1 to a cluster of Lac operator repeats, mediated by fusion with a lacI DNA-binding domain leaded to local decondensation of polytene chromatin. Their results also provided evidence that observed reorganization of chromatin structure was dependent on the kinase activity of JIL-1 (Deng et al. 2008). Corces and coworkers have proposed that histone H3S10 phosphorylation executed by Jil-1 is required for active transcription by the RNA polymerase II machinery (Ivaldi et al. 2007; Kellner et al. 2012). However, later it was demonstrated that RNA polymerase II mediated transcription occurs at robust levels in the absence of H3S10 phosphorylation (Regnard et al. 2011). Recently, Cai and coworkers provided experimental evidence for the functional role of JIL-1-mediated H3S10 phosphorylation in maintenance of active gene expression by serving as a protective epigenetic mark counteracting H3K9 dimethylation and gene silencing (Cai et al. 2014). It has been shown that the C-terminal domains of Jil-1 kinase and Chriz directly interact with each other (Rath et al. 2006). Consequently, Gan and colleagues demonstrated that Jil-1 requires Chriz for targeting to polytene chromosomes (Gan et al. 2011).

Another component of Chriz complex – seven zinc-finger protein Z4 with a molecular weight of about 160 kDa is essential for fly development and acts in a dose-dependent manner on the development of several tissues (Fig. 11)(Eggert et al. 2004).

Figure 11. Schematic picture of the full-length zinc-finger protein Z4 (996 amino acid residues). Z4 contains 7 zinc-finger (ZnF) domains of the classical C2H2 type (green box). The extent of the domains is given by aa numbers.

Z4 is localized to open interband domains of polytene chromosomes (not in puffs) and is involved in maintenance of chromatin structure; chromosomes from 3rd instar larvae of hypomorphic Z4 mutants loose the organization into bands and interbands and altogether appear as a less compact mass of chromatin (Eggert et al. 2004). Z4 has been shown to be an important cofactor in at least three different pathways related with chromatin remodeling: the NURF and the TRF2/DREF remodeling complexes, where it acts as an activator (Kugler et al. 2007; Kugler et al. 2010); and in the JAK/STAT pathway, where Z4 acts as a co-repressor (Kugler et al. 2011). In the work of Silva-Sousa the role of Z4 in maintenance of telomere stability is discovered (Silva-Sousa et al. 2012).

Chriz and Z4 precisely co-localize in interbands along the whole length of polytene chromosomes (Gortchakov et al. 2005) (see Figure 12) and interact by their central and N-terminal domain, respectively (Gan et al. 2011).

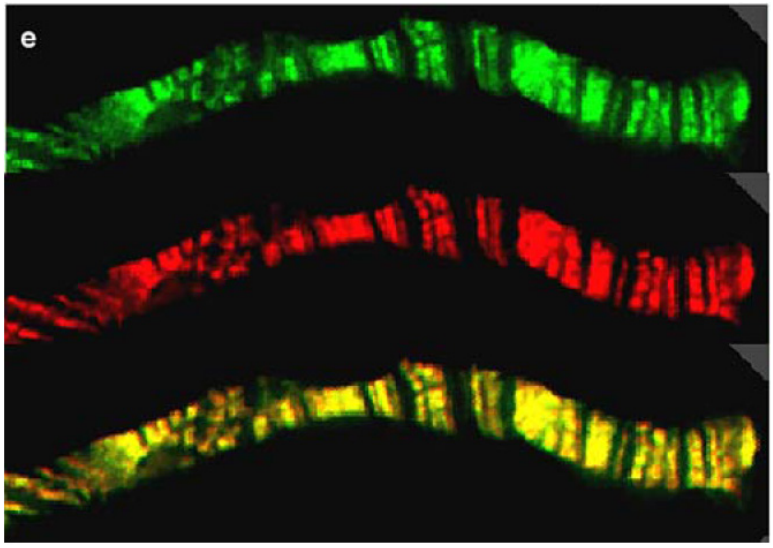

Fig. 12. Z4 and Chriz colocalize on polytene chromosomes; top: Z4 (green); middle: Chriz (red); bottom: colocalization is demonstrated by the yellow color resulting from the overlay of both wavelengths (Gortchakov et al. 2005)

Interestingly, loss of function of Chriz complex components also influences the coherence and organization of bands although neither protein is present in these regions. Rath and coworkers suggested that their function may affect the distribution and/or activity of other molecules important for influencing chromatin structure such as boundary elements. (Rath et al. 2006, Van Bortle et al. 2014)

1.5 Boundary elements

Chromatin insulators play a key role in determining the structural organization of eukaryotic chromatin.

Generally, insulator elements possess two key properties indicative of the capacity to define a chromatin domain, characteristic for each insulator family. The first is termed enhancer blocking, the ability to interfere with enhancer– promoter communication only when placed between the two elements (Reitman et al. 1990; Cai et al. 1995). The second feature is termed barrier activity, the ability to protect a flanked transgene from position-dependent silencing (Kellum et al. 1992). Numerous research work in chromatin studies provided strong support for both types of models, and, therefore defined two major classes of insulators: ‘enhancer blocking’ insulators which block communications between adjacent regulatory elements in a position dependent manner and ‘barrier insulators’ which prevent the

silencing of euchromatic genes by blocking the spreading to nearby heterochromatin. Both types are schematically visualize on Fig. 13

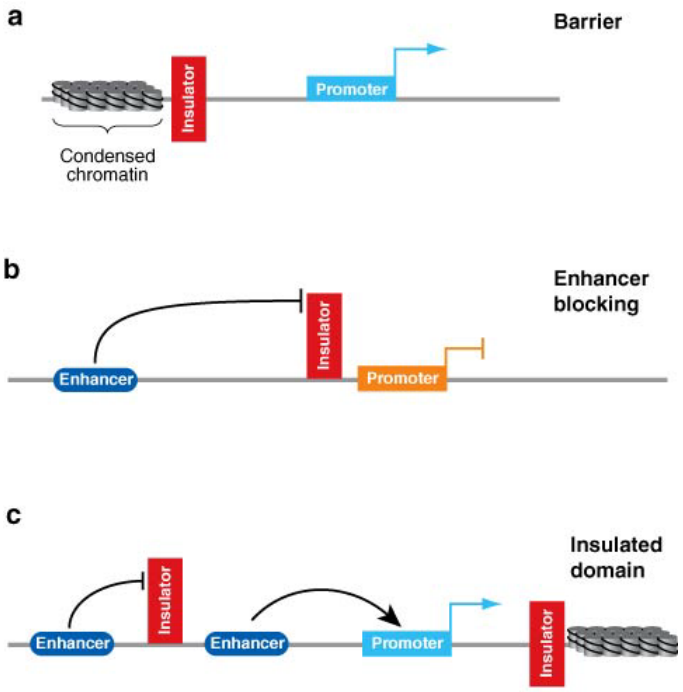

Figure 13. Insulators block enhancer and silencer elements in a position-dependent manner. (a) Barrier elements block the linear spread of silenced chromatin protecting the reporter gene from silencing. (b) Enhancer-blocking elements interfere with enhanced transcription when placed between an enhancer element and the promoter. (c) Flanking a transgene with insulator elements generates a functionally independent domain protected from position effects. Regulatory interactions can occur within the domain whereas the insulators block external signals (Valenzuela et al. 2006).

Pioneer studies on boundary elements were focused on the 87A7 locus in *Drosophila*. This locus contains two divergently transcribed heat shock genes (*hsp70*) actively transcribed at increased temperature and reflected by puffing in salivary gland polytene chromosomes. DNAse sensitivity analysis of DNA regions flanking the 87A7 locus identified two zones with an unusual chromatin structure, called *scs* and *scs*' (specialized chromatin structures) (Udvardy et al. 1985). These regions were shown to be located very close to the border between the decondensed 87A7 locus and the flanking condensed chromatin. Further research on these elements identified them as insulators (Kellum et al. 1991). Kellum and coworkers hypothesized that if insulator elements established borders between chromatin domains, they should protect a reporter gene from position effects when integrated into the genome. Random P-element mediated insertion of white minigene with a minimal promoter resulted in flies with a range of eye color from white to red due to position effects. Such position effects were considered to be a consequence of interactions between the promoter of the reporter gene and enhancer and silencer elements present near the integration site. When the white minigene was placed between the *scs* and *scs*' elements, its level of

expression was uniformly low in the transformed lines, indicating that *scs* and *scs*' protected the expression of the miniwhite gene from euchromatin (Kellum et al. 1991).

Several enhancer-blocking assays were designed to test whether these DNA sequences inserted between an enhancer element and a target promoter can prevent them from interacting, and both *scs* and *scs*' were shown to insulate reporter genes from different enhancer elements as well (Kellum et al. 1992). Although they do not share any sequence homologies, both *scs* and *scs*' elements were recently shown to be close to promoters of genes (Avramova et al. 1999). The *scs* insulator is found in a region that contains the promoter for CG31211 whereas the *scs*' insulator maps to the promoter of two divergently transcribed genes, CG3281 and aurora (Glover et al. 1995). Later, two proteins bound to *scs* and *scs*' insulators were characterized, the zinc-finger Zeste-white 5 (Zw5) protein and the "boundary element-associated factor" - BEAF-32 (Gaszner et al. 1999; Zhao et al. 1995).

These studies gave rise to further characterization of function of identified insulator proteins and revealed additional sites throughout the genome as well as protein complexes associated (Hirose et al. 1996, Xu et al. 2004). Distinct families of insulators have been described to date, defined by insulator binding protein that is essential for their activity (Maeda et al. 2007). In *Drosophila* five insulator families were identified: Suppressor of Hairy-wing [Su(Hw)], boundary element-associated factor (BEAF), Zeste-white 5 (Zw5), the GAGA factor (GAF) (Maeda, 2007), and dCTCF, a homologue of mammalian CTCF (Moon, 2005). Each category of insulator complexes also contains the common centrosomal protein 190 (CP190) (Matzat et al. 2014).Genome wide analysis identified thousands of binding sites for most of these proteins (Bushey et al. 2009; Schwartz et al. 2012; Van Bortle et al. 2014).

Recent observations proposed a model for insulator function in which direct DNA-binders (BEAF-32, dCTCF, Su(Hw)) provide DNA specificity and serve as "first layer proteins", whereas such proteins as CP190, Mod(mdg4) or Chriz may interact with them and form a "second layer" being responsible for the physical interactions required for long-range contacts (Vogelmann et al. 2014).

In the current study we will focus on two insulator proteins – BEAF-32 insulator and CP190.

The BEAF-32 insulator protein is known to have two isoforms, A and B, which differ in their N-terminal part, where two slightly different atypical C2H2 zinc-fingers, termed BED fingers are located (see Fig 14) (Aravind et al. 2000). C-terminus of BEAF-32 contains BESS domain and coiled-coil CC-domain, involved in protein-protein interactions (Hart et al. 1997). Gilbert and colleagues showed that this domain is necessary for BEAF-32 self-interaction and, demonstrated the capacity of BEAF-32 to form trimers (Gilbert et al. 2006).

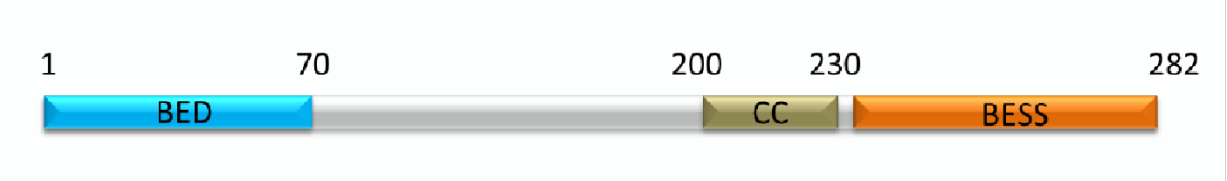

Figure 14. Schematic picture of the full-length boundary element – associated factor BEAF-32 (282 amino acid residues). BEAF-32 contains BED domain (blue box) at the N-terminus , coiled-coil domain (brown box) and BESS domain (orange box) at the C-terminus. The extent of the domains is given by aa numbers.

According to ChIP studies both isoforms bind specifically to *scs*' as well as many other sites in the genome, however the more abundant BEAF-32B protein apparently is associated with more sites than BEAF-32A (Jiang et al. 2009). It was shown experimentally that a number of BEAF-32 binding sites possess enhancer blocking activity (Hart et al. 1999; Schwartz et al. 2012), supporting the statement that BEAF-32 is a general insulator factor. BEAF-32 was found to bind DNA directly and is preferentially associated with a CGATA motif (Hart et al. 1997). Same DNA motif is also bound by the DREF transcription factor proposed to compete with BEAF-32 for chromatin binding (Hart et al. 1999). Comparative analysis of the genome-wide binding profile of BEAF-32 with the distribution of its binding motif suggests that BEAF-32 prefers to bind to dual clusters containing two or three individual binding motifs, totaling five or six sites, spaced by a 200 bp central AT-rich region (Emberly et al. 2008). These "dual cores" as well as the majority of BEAF-32 binding sites correspond to transcription start sites (Jiang et al. 2009). Furthermore, BEAF-32 has a clear tendency to bind at promoter regions of head-to-head oriented genes (Jiang et al.2009). Yang and colleagues hypothesized that BEAF-32 may play an evolutionarily conserved role in preventing undesired transcriptional regulatory crosstalk between the individual genes forming the pair (Yang et al. 2012). Knockdown studies of BEAF-32 in cell culture have provided insight into its role in regulation of gene expression. RNAi of BEAF-32 in cells results in few changes in gene expression with no apparent growth arrest (Schwartz et al. 2012; Van Bortle et al. 2012). However, after longer time of BEAF-32 depletion, growth arrest is observed, as well as increase in cellular DNA content and chromosome segregation defects (Emberly et al. 2008). These effects may partially result from relief of competitive binding with DREF, which activates a subset of cell cycle control genes (Matzat et al. 2014). Interestingly, global H3K9me3 rises in BEAF-32 knockdown cells, in contrast, to unchanged global H3K27me3 levels or gene expression within H3K27me3 islands bordered by CTCF sites (Van Bortle et al. 2012). In addition to DREF, BEAF-32 also overlaps considerably with other insulator proteins, particularly centrosomal protein CP190 (Bushey et al. 2009).

CP190 is a protein of 1,096 amino acids with a predicted molecular weight of 121 kDa and an apparent molecular weight of about 190 kDa. The protein contains an N-terminal BTB/POZ (Broad-complex, Tramtrack and Bric-abrac/Poxvirus and Zinc Finger) domain; an aspartic-acid rich D-domain; three C2H2 zinc finger motifs; and a C-terminal E-rich domain (see Fig. 15) (Ahanger et al. 2013).

Figure 15. Schematic picture of the full-length Centrosomal Protein 190 (1,096 amino acid residues). CP190 contains BTB/POZ domain (light-orange box) at the N-terminus, D-rich (red box), CENT (violet box) and zinc-finger (ZnF) domains (green box) in the center and an E-rich domain (blue box) at the C-terminus. The extent of the domains is given by aa numbers.

CP190 contains a centrosomal targeting domain (CENT) for its localization to centrosomes during mitosis (Whitfield et al. 1995). The BTB/POZ, the aspartic-acid rich (D-rich) and the C-terminal glutamic-acid rich (E-rich) domains are essential for its association with insulator subclasses and insulator function. The E-rich region was shown to be important for the dissociation of CP190 from the chromosome after heat-shock, which may provide a mechanism for regulating insulator function (Oliver et al. 2010). CP190 was identified to be associated with centrosomes throughout the nuclear division cycle in syncytial *Drosophila* embryos (Frasch et al. 1986). However, after the cellularization of the embryo, CP190 is exclusively found in nucleus during the interphase (Callaini et al. 1990). Using indirect immunofluorescence staining of polytene chromosomes from salivary glands, CP190 was found at a number of sites along the entire length of the chromosomes localizing mainly to interbands and band/interband boundaries (Whitfield et al. 1995). Recent genome-wide studies revealed an extensive overlap of CP190 with the target sites of main insulator factors; dCTCF, Su(Hw), BEAF and GAF (Negre et al. 2010). It was demonstrated that 80% robust CP190 binding sites overlap with dCTCF, Su(Hw) or BEAF-32 (Schwartz et al. 2012). The number of sites in the genome where CP190 binds independently of Su(Hw), dCTCF and BEAF-32 were later identified as binding sides for recently discovered proteins IBF1, IBF2, Pita and ZIPIC (Maksimenko et al. 2015; Cuartero et al. 2014).

As can be seen, insulator proteins associate in clusters of overlapping binding sites more often than would be expected by chance, suggesting that these factors could bind as a complex to the same genetic locus (Vogelmann et al. 2014). Significant co-localization of insulator protein BEAF-32 with Chriz complex components on polytene chromosomes was revealed by Gan and colleagues (Gan et al. 2011). Later, this observation was confirmed by computational analysis of overlapped binding sites between insulator proteins BEAF-32, CP190 and Chriz (Vogelmann et al. 2014) (Fig. 16) More detailed systematic screen of chromatin profiles performed by Sexton and coworkers showed that such proteins as Chriz, CP190, CTCF, and BEAF-32 were identified at domain borders. At the same loci, active histone mark H3K4me3 and high DNase hypersensitivity showed a striking enrichment compared to background regions (Sexton et al. 2012). Interestingly, CP190 and Chriz were found to be most represented at the borders of physical domains. Boundary behavior was significant but somewhat weaker at peaks of BEAF-32, H3K4me3, and CTCF and was minimal at peaks of Su(Hw) (Sexton et al. 2012).

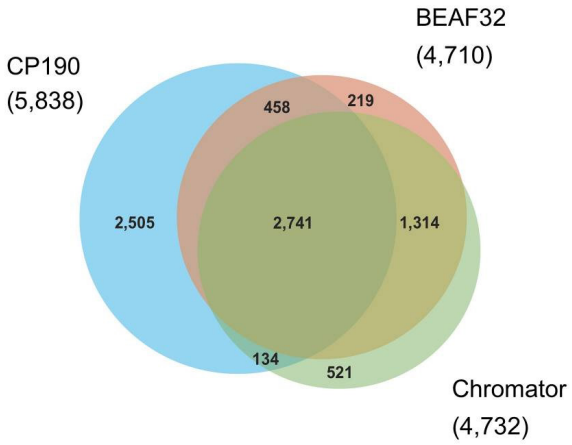

Fig. 16. Venn diagram showing the genome-wide overlap between BEAF-32, CP190 and Chromator (Chriz) in S2 cells. Binding sites were calculated from publicly available modENCODE ChIP-chip data (Vogelmann et al. 2014).

All these findings proposed a possibility of physical interaction between Chriz complex and insulator proteins. Co-IP experiments performed by Gan and colleagues revealed interaction between Chriz complex component Z4 and insulator BEAF-32 (Gan et al. 2011). Direct interaction between Chriz and Mod(mdg4), which is the component of Su(Hw) complex was reported (Golovnin et al. 2014).

The variety of identified connections between Chriz complex and other proteins, allows us to assume that the role, which Chriz complex plays in the cell may not be restricted to maintenance of chromatin structure. It is still unclear to which extent the knowledge about Chriz protein complex obtained on the polytene chromosomes can be extrapolated to diploid cell chromatin. Interactions between Chriz and insulator proteins BEAF-32 and CP190 are still weakly studied and mechanism how Chriz complex is recruited to chromatin remains unknown.

1.6 Therefore, current work has the following **aims**:

1. Determine the interactions between known and putative components of Chriz complex – Z4, Jil-1, BEAF-32, Chriz and CP190.
2. Identify the role of “core” Chriz complex components in gene expression.
3. Compare the composition and localization of Chriz complex in polytene and diploid cells.
4. Explore the possibility of Chriz complex recruitment by identified factors.

2. Materials and Methods:

2.1. Materials

2.1.1 Chemicals

If not specified, standard chemicals from Serva, Roth, Merck and Sigma were used.

2.1.2 Bacterial strains

For cloning and plasmid DNA production *E. coli* strain *XL1-Blue (recA1 endA, gyrA96 thi-1 hsdR17 supE44 relA1, lac [F', proAB, lacIqZDM15, Tn10 (Tetr)]c)* was used.

For protein expression *E. coli* strain *BL-1-DE3 (B F– dcm ompT hsdS(rB– mB–) gal λ(DE3))* was used.

For *E. coli* cultivation the following media were used:

LB-Medium (Luria/Miller)	LB-Agar (Luria/Miller)
10 g/l Trypton	10 g/l Trypton
5 g/l Yeast extract	5 g/l Yeast extract
10 g/l NaCl	10 g/l NaCl
	15 g/l Agar-Agar

2.1.3 Cell culture

Drosophila S2 cells were kept in 10-50 ml tissue culture flasks in commercial *Drosophila* S2 medium (Gibco, Lot 1627148) with 10% FCS under conventional conditions at 28 ˚C. Cells were split 1-2 x weekly.

2.1.4 Fly work

Drosophila strains were kept in standard media at 18˚C (see receipt in the table below). Crosses were performed at 25˚C.

Standard fly media (Bloomington)	
39l	Water
675g	Yeast
390g	Soy flour
2,85g	Cornmeal
225g	Agar-Agar
3l	Sugar syrup
188ml	Propionic acid

In current work the following *Drosophila* strains were used

Name	Marker	Chr.	Notes
WT-Oregon			Wild type
Tft/CyO		2	Balancer strain
TM3/TM6		3	Balancer strain
Tft/CyO; TM6/MKRS		2,3	Balancer strain
G231.1 Gal4		2	Gal4 salivary gland specific driver (Dr. U. Hinz, Cologne)
G61 Gal4		X	Gal4 salivary gland specific driver (Dr. U. Hinz, Cologne)
ΔKG12 Chriz		3	Chriz deletion (Gortchakov et al. 2005)
42pattP		2	(Zielke, Saumweber 2014)
BEAF RNAi		2	Bloomington, 35642
CP190 RNAi		3	Bloomington, 33903
Chriz RNAi		2	(Gortchakov et al. 2005)
UAS-NB		2	y1 w*; P{UAS-Nslmb-vhhGFP4}2 , Bloomington, 38422

2.1.5 Crossing schemes:

Double BEAF/CP190 double RNAi strain was obtained by the following crossing scheme:

$$P_{BEAF}: \frac{BEAF^{RNAi}}{BEAF^{RNAi}};\frac{+}{+} \quad X \quad \frac{CyO}{If};\frac{TM6,Tb}{MKRS,Sb} \qquad P_{CP190} \quad \frac{+}{+};\frac{CP190^{RNAi}}{CP190^{RNAi}} \quad X \quad \frac{CyO}{If};\frac{TM6,Tb}{MKRS,Sb}$$

$$F_1: \frac{BEAF^{RNAi}}{If};\frac{MKRS,Sb}{+} \quad X \quad \frac{CyO}{+};\frac{CP190^{RNAi}}{TM6,Tb}$$

$$F_2: \frac{BEAF^{RNAi}}{CyO};\frac{CP190^{RNAi}}{MKRS,Sb} \quad X \quad \frac{BEAF^{RNAi}}{CyO};\frac{TM6,Tb}{+}$$

$$F_3: \frac{BEAF^{RNAi}}{CyO};\frac{CP190^{RNAi}}{TM6,Tb} \quad X \quad \frac{BEAF^{RNAi}}{CyO};\frac{CP190^{RNAi}}{TM6,Tb}$$

OR

$$F_3: \frac{BEAF^{RNAi}}{BEAF^{RNAi}};\frac{CP190^{RNAi}}{TM6,Tb} \quad X \quad \frac{BEAF^{RNAi}}{BEAF^{RNAi}};\frac{CP190^{RNAi}}{TM6,Tb}$$

$$\text{Final Stock: } \frac{BEAF^{RNAi}}{BEAF^{RNAi}};\frac{CP190^{RNAi}}{CP190^{RNAi}}$$

Crosses were performed during a lab rotation project by M. El Genedy under my supervision.

The Chriz-GFP strain was obtained using the following scheme:

$$\text{P: } \frac{w^-}{w^-};\frac{\text{ChrizGFP}, w^+}{\text{ChrizGFP}, w^+};\frac{+}{+} \quad \text{X } w^- \ \frac{\text{CyO}}{\text{If}};\frac{\text{TM6, Tb}}{\text{MKRS, Sb}} \qquad \frac{w^-}{w^-};\frac{\text{ChrizΔKG12}}{\text{ChrizΔKG12}} \quad \text{X} \quad w^- \ \frac{\text{CyO}}{\text{If}};\frac{\text{TM6, Tb}}{\text{MKRS, Sb}}$$

$$F_1\text{: } \frac{w^-}{w^-};\frac{\text{ChrizGFP}, w^+}{\text{CyO}};\frac{\text{TM6, Tb}}{+} \quad \text{X } w^- \ \frac{\text{CyO}}{+};\frac{\text{ChrizΔKG12}}{\text{MKRS, Sb}}$$

$$F_2\text{: } \frac{w^-}{w^-};\frac{\text{ChrizGFP}, w^+}{\text{CyO}};\frac{\text{TM6, Tb}}{\text{ChrizΔKG12}} \quad \text{X } w^- \ \frac{\text{CyO}}{\text{ChrizGFP}, w^+};\frac{\text{ChrizΔKG12}}{\text{TM6, Tb}}$$

$$F_3\text{: } \frac{w^-}{w^-};\frac{\text{ChrizGFP}, w^+}{\text{ChrizGFP}, w^+};\frac{\text{ChrizΔKG12}}{\text{ChrizΔKG12}}$$

DeGradFP strain 1 was obtained using the following scheme:

$$\text{P: } \frac{\text{Gal4}, w^+}{\text{Gal4}, w^+};\frac{+}{+};\frac{+}{+} \quad \times \ w^- \ \frac{\text{CyO}}{\text{If}};\frac{\text{TM6, Tb}}{\text{MKRS, Sb}}$$

$$F_1\text{:}\frac{\text{Gal4}, w^+}{w^-};\frac{+}{\text{CyO}};\frac{\text{TM6, Tb}}{+} \quad , \quad \frac{\text{Gal4}, w^+}{w^-};\frac{+}{\text{If}};\frac{+}{\text{MKRS, Sb}} \times w^-;\frac{\text{ChrizGFP}, w^+}{\text{ChrizGFP}, w^+};\frac{\text{ChrizΔKG12}}{\text{ChrizΔKG12}}$$

$$F_2\text{: } \frac{\text{Gal4}, w^+}{\text{Gal4}, w^+};\frac{+}{\text{CyO}};\frac{\text{TM6, Tb}}{+} \quad \times \quad \text{Gal4}, w^+;\frac{\text{If}}{\text{ChrizGFP}, w^+};\frac{\text{MKRS, Sb}}{\text{ChrizΔKG12}}$$

$$F_3\text{: } \frac{\text{Gal4}, w^+}{\text{Gal4}, w^+};\frac{\text{ChrizGFP}, w^+}{\text{CyO}};\frac{\text{ChrizΔKG12}}{\text{TM6, Tb}}$$

$$F_4\text{: } \frac{\text{Gal4}, w^+}{\text{Gal4}, w^+};\frac{\text{ChrizGFP}, w^+}{\text{ChrizGFP}, w^+};\frac{\text{ChrizΔKG12}}{\text{ChrizΔKG12}} \times w^-;\frac{\text{UAS}-\text{NB}, w^+}{\text{UAS}-\text{NB}, w^+};\frac{\text{ChrizΔKG12}}{\text{TM6, Tb}}$$

$$F_5\text{: } \text{Gal4}, w^+;\ \frac{\text{UAS}-\text{NB}, w^+}{\text{ChrizGFP}, w^+};\frac{\text{ChrizΔKG12}}{\text{ChrizΔKG12}}, \qquad \frac{\text{Gal4}, w^+}{w^-};\ \frac{\text{UAS}-\text{NB}, w^+}{\text{ChrizGFP}, w^+};\frac{\text{ChrizΔKG12}}{\text{ChrizΔKG12}}$$

DeGradFP strain 2 was obtained using the following scheme:

$$\text{P: } \frac{y^{10}}{y^{10}};\frac{+}{+};\frac{\text{ChrizΔKG12}}{\text{TM6, Tb}} \quad \times \ w^- \ \frac{\text{CyO}}{\text{If}};\frac{\text{TM6, Tb}}{\text{MKRS, Sb}}$$

$$F_1\text{: } y^{10};\ \frac{+}{\text{CyO}};\frac{\text{MKRS, Sb}}{\text{ChrizΔKG12}}$$

$$\text{P: } \frac{w^-}{w^-};\frac{\text{UAS}-\text{NB}, w^+}{\text{UAS}-\text{NB}, w^+};\frac{+}{+} \quad \times \quad w^- \ \frac{\text{CyO}}{\text{If}};\frac{\text{TM6, Tb}}{\text{MKRS}^{\text{Sb}}}$$

$$F_1: \frac{w^-}{w^-}; \frac{UAS-NB, w^+}{CyO}; \frac{+}{TM6, Tb} \quad \times \quad y^{10}; \frac{+}{CyO}; \frac{MKRS, Sb}{ChrizΔKG12}$$

$$F_2: w^-; \frac{UAS-NB, w^+}{CyO}; \frac{ChrizΔKG12}{TM6, Tb} \times \frac{w^-}{w^-}; \frac{UAS-NB, w^+}{CyO}; \frac{ChrizΔKG12}{TM6, Tb}$$

$$w^-; \frac{UAS-NB, w^+}{UAS-NB, w^+}; \frac{ChrizΔKG12}{TM6, Tb}$$

Both DeGradFP strains were established by Y. Rehn under my supervision.

2.1.6 Primers:

Name	Sequence 5'-3'	Name	Sequence 5'-3'
Primer used for ChIP/qPCR:			
cg3523ChrizF	TTCCAGTTTTACTCGCGTGGT	rev1ChrizF	GCGAAAAGAGAGTTGCCACA
cg3523ChrizR	ATTTGCCCGCCATAGTCGGA	rev1ChrizR	TCGAAGTAGCCGCCCTG
tctpChrizF	GTTCGCCTTAATATTCCCT	cg6405ChrizF	ATAAACTTTATTCTTGCGCCAT
tctpChrizR	GACCTGCCACGCGCTCA	cg6405ChrizR	AAATCAAGTGAAAACCGTTACC
galeChrizF	TACCACCCCTATTCGCGTCTC	spz4ChrizF	ACAAAGTGCACAGTTTCGC
galeChrizR	CCACGCGACATGGCT	spz4ChrizR	CCCAAGTCCCACGGCAAA
cg25cChrizF	CCGTCGCCCATCCGTTC	cg9040ChrizF	TACTAGCAGGTCGCCTAACGC
cg25cChrizR	GCCCCATCTTCACTCGT	cg9040ChrizR	CGTCTTAATTTTCGGTGGCT
baccChrizF	ATCAACAGAAAGATTGGCACA	sgs7ChrizF	AACATTTTACATGCCCTT
baccChrizR	TGCAACCCCATAAGATTCGAAA	sgs7ChrizR	ATTTCAGTGAGCACATCCAA
cg3402ChrizF	TTGTCGCCCACAACAAACTCT	sageChrizF	ACTGCCGGACAACTGGAC
cg3402ChrizR	ACTAAGAAACATTGCCAAACAG	sageChrizR	GCGATGACGGATCAACTGCT
med30ChrizF	ATTACCCTGGTTTTGACCGTA		
med30ChrizR	TGGTAATTTAAAACCCGCGACT		
Primers used for qRT-PCR in correlation experiments:			
q_cq6405-F	GGAAATCAACGAGAGTCTCTGTC	q_cg3523-R	GCGTCAATAATAGCTTCATGGGT
q_cq6405-R	AATCTTGTGTTCCAATCGGTGT	q_tctp-F	TGATCTACGAGGTGTACGGAAA
q_cg9040-F	TATTGGTTGCCTTCGTAACGG	q_tctp-R	TCGGTGGTTAAGCACAACATC
q_cg9040-R	CCGAACTGGACTCTACATCAGA	q_gale-F	TCAATGCGGGCTACAACGTC
q_sgs7-F	TTCTCCGATCTAGCCCTGGG	q_gale-R	CCGGTGATTTCCTGCACCC
q_sgs7-R	AAAGTTGGGGCTTTTCGGGA	q_cg25c-F	AGGGCGAAATGGGTTTCCC
q_sage-F	GGGCTTGGAATGCAACAAACC	q_cg25c-R	CCCTTATCACCACGCTGTCC
q_sage-R	GTGCTATTGGCTATACTACCGC	q_spz4_F	CGGCGATGTAAGGCACATTTC
q_cg3523-F	TGACCAACAGTTCTTCGGTGT	q_spz4_R	GTCCGCCATCCTTGCTATATC
q_ef1-F	GCGTGGGTTTGTGATCAGTT	q_bacc-F	AATCCGCAGAATCAAAGAAGGC
q_ef1-R	GATCTTCTCCTTGCCCATCC	q_bacc-R	TCGCTCTCGATTTCACTGTCG
q_med30-F	AGCACGGCAATATGCAGCA	q_cg2402-F	ATGGCGAAAATGGCATTCCAG
q_med30-R	CAGGTCCTTGGGGATTCATCT	q_cg2402-R	GCCGCACTTGAGGATCTCG
q_rev1-F	ATgACCCgCgATgAggATAAT		
q_rev1-R	ggTCCgACTTgCgAAATggAT		
Primers used for ChIP/qPCR of 61C7-8 domain:			
F61C7-8_10	ACCGTTCAATGACGAATTTTACAG	F61C7-8_21	AAGCAAAAACTCAGCGCCAC
R61C7-8_10	CAGCTCTTCTCGCGTTTTCC	R61C7-8_21	CCACAGAGAAGCGAAGAACG
F61C7-8_11	ACAACACATAGGAAAACGCGAG	F61C7-8_22	TGCGTGAAAAACGCTCAGATG

R61C7-8_11	CACAAACAAACCGACACTGCC	R61C7-8_22	ACCATCGGAATGTGGAATGTGG
F61C7-8_12	GCAGTGTCGGTTTGTTTGTG	F61C7-8_23	CCAGTCGGATCGAGATGGGG
R61C7-8_12	GACTTCGTAAAAAGTTGTACCTTTCG	R61C7-8_23	AACATGTGGTCAGCATCGGC
F61C7-8_13	GATGAAAGATCGGCGCAAAAG	F61C7-8_24	GTATTTTGTACGCCATGTCTTGTG
R61C7-8_13	GAACCGCTTTCCCGTGTTTA	R61C7-8_24	CCAACTCGCCTTGGGATGAC
F61C7-8_14	TCAGTGTGCCAGTGTATGTG	F61C7-8_25	TGGATGTTGGACGTGGAGAAT
R61C7-8_14	CATGCTGTGTGTGAATTCCG	R61C7-8_25	GTCTTCGCAACGTTATCAGCG
F61C7-8_15	CACACAACGCCGTTTATTGG	F61C7-8_26	GCGCTGATAACGTTGCGAAG
R61C7-8_15	GTTCCCATTCACGTTCTGGC	R61C7-8_26	CAACGTGCTCCACTTTGTCG
F61C7-8_16	AGACAGGCGAGACGGCAATA	F61C7-8_27	GTGGAGCACGTTGGACAGAG
R61C7-8_16	GCTGCAAAGAATATACGAGTTCAG	R61C7-8_27	GTGCATGCTGATTAGCACCTTG
F61C7-8_17	GCAGCAATACTGTGGTTAAACG	F61C7-8_28	CGTACATGCGATGGATTCGG
R61C7-8_17	CGGGATAAGTCTGAGCGAAG	R61C7-8_28	GGAGTCGTCGCTCCAGTTTG
F61C7-8_18	GGGAGAACCGATTTTTCGGG	F61C7-8_29	CGCTTGGATATGGGGTGAC
R61C7-8_18	GCAGACCGTAGCATTAACCG	R61C7-8_29	ATAACTGCCCACTAAGTCGC
F61C7-8_19	TCGCCGCTCAATAGAAAGTTTG	F61C7-8_30	TGCTATGCCTCATTAGGATGGATG
R61C7-8_19	TGTGTGGGAAAGTATGCGCC	R61C7-8_30	ATTTGAGCACCGAATGCACG
F61C7-8_20	CCTTCGCACGCTTTCCTCTC	F61C7-8_41	GCGCGTGTACTCCACTTAC
R61C7-8_20	GGGTGGGGGACATGAACTG	R61C7-8_41	GAACCACCAATGCCACCAAT
F61C7-8_31	CGTGCATTCGGTGCTCAAAT	F61C7-8_42	GGCAGAAAAGTTCAGAAGAGTGG
R61C7-8_31	GGCCATTTACAACACTTGGATCG	R61C7-8_42	CGCATGGCCCGTCTAAAAG
F61C7-8_32	GAATCGATCCAAGTGTTGTAAATGG	F61C7-8_43	GCCAGAAAACGTCACGAAATATG
R61C7-8_32	GCGAGTGTAGCGACAATTGT	R61C7-8_43	TGCGTTCCCTCAAAAGAGAC
F61C7-8_33	TTGAGCCGAAACACAAACGG	F61C7-8_44	CGGGCACAAACAATAATGCG
R61C7-8_33	CTAGCGTCTGCAAACCGTC	R61C7-8_44	CCGGCCCGTTAGCTATGTC
F61C7-8_34	CTAGACGGCGGTAAATGTGTC	F61C7-8_45	CCAACTCTCGGACCGAACTG
R61C7-8_34	TGGCTGCAGCTACATCTGTA	R61C7-8_45	GAATTGGAAAGAGAAAGACAGAACG
F61C7-8_35	CACCGGAGGCTCTGCTAATG	F61C7-8_46	GCGACTCTGACTGTGCAAAT
R61C7-8_35	GTAGCCGCGTTTCCTTTTGC	R61C7-8_46	CCGCAAGACCATGCTTACC
F61C7-8_36	CCGGAAACTTGCAGGAAATTG	F61C7-8_47	CCGAAGCAGTATTTTACGGTTTG
R61C7-8_36	CGCCAAATCAGCACAACTCG	R61C7-8_47	TGGCATTTGACCGGCTTTAT
F61C7-8_37	CGCCGGGGAATAAGATTCGG	F61C7-8_48	CGCTGCGCAAATACATTCTC
R61C7-8_37	CCCCTCGGGGCATGTTTATTG	R61C7-8_48	ACAACAAACTTCAGTACAATGCG
F61C7-8_38	AGGCAGCCAACAGACAACTA	F61C7-8_49	CAGAAGCACATGGCAGTGATG
R61C7-8_38	CTATTGATGGCGGTGGCAATG	R61C7-8_49	AGACGCGAATAGGGGTGGTA
F61C7-8_39	CCGATCCCCGATTCCGTTC	F61C7-8_50	CGAGACGAATCCCACTGTGC
R61C7-8_39	GGCAAAACTACCACAAAGGC	R61C7-8_50	CATCCTTATCGCCGCTGACC
F61C7-8_40	CACTGACAACTGGAAACTTGCG	F61C8_11	GCTCATCGCGGTAGGGAATC
R61C7-8_40	GGCGTTACGGAAAGAGTTCCC	R61C8_11	TTCCAGGAGGTCTTCGCCTC
F61C7-8_51	TCGACCAAGTCAGCCTGC	F61C8_12	AGCATATTGTTGCTGCCCCC
R61C7-8_51	GCTAACCCGTTTCTTGCACT	R61C8_12	GTGCCCCAACAAGGAGTGG
F61C7-8_52	GCGGAATCGTTTCAAGGGC	F61C8_13	CACCCATCGGCATCATGTTG
R61C7-8_52	CACACGAAATTAGGCCACACG	R61C8_13	GCGAGCATACAGTTTCAGCG
F61C7-8_53	CCCTTTCGCCACTTAGGATG	F61C8_14	CCATGCGAAAAGAGAGTTGCC
F61C7-8_53	CTTCTTGCCGGTGATTTCCT	R61C8_14	AGTAGCCGCCCTGAAAAGAG
F61C7-8_54	GAGTGGACATCACGGACAGG	F61C8_15	CCCTATCTGCTGTACACGAACC
R61C7-8_54	CCGCCACTTGAGCAAACAAC	R61C8_15	CCACAGCCTGCTGCAAATTC
F61C7-8_55	GCAAATGTGCCAACTGGATACC	F61C8_16	TGCTTCTTTGTGTCCGTGGG
R61C7-8_55	GGGAGCTGTTGTGGATGTGG	R61C8_16	ACCTTTTCCGCCTTGTCTCC
F61C7-8_56	CGAGCAGGTTATCACGCATTC	F61C8_17	TCCAAAACGGGATGTCCGTG
R61C7-8_56	GCGCGTAAGCACAAAGCTG	R61C8_17	CCCACACCGGGCAGTAAATC
F61C7-8_57	GCACTATCAACAGCTATTTAAAGAACAC	F61C8_18	TTCGCTTTACCAACTCGGTCG
R61C7-8_57	GTCGATTTTGTGCTGAAAGGG	R61C8_18	ATTATATCGCAAACTCCGTGGC

F61C7-8_58	CCACTTTGCCGCCCTGAAG	F61C8_19	GGAGCGCAAGGAGCAAGAG
R61C7-8_58	CGATGTACAGTTGCCCGTGG	R61C8_19	TCCACGTCATTCGGCTTTGG
F61C8_1	GCAAGTCTGACAAGGTAGGAGG	F61C8_20	CCAGTGTGGCTCTTTCCCAC
R61C8_1	GCCACCTGTGCGATGTAGG	R61C8_20	CATATTACAGCCGTCGCAGC
F61C8_2	GCCCTACATCGCACAGGTGG	F61C8_7	TCTGGCTACATGTGTGTGCG
R61C8_2	ACGCCGGTGCCCAAATTGTA	R61C8_7	GGGCGTGACCTCCACATAAG
F61C8_3	AGATGTGGCCACTTGCTATG	F61C8_8	CTGCAGGATCTTGTCGTGG
R61C8_3	CAGGCGTAGTAACTCAGGAAC	R61C8_8	TCCGGGCATAAAAGAGAGCT
F61C8_4	CGCCTGATAATGGCTCAGGTAG	F61C8_9	TGAAGCCGCACTTGAGGATC
R61C8_4	ATTGGCACGCGTCAATGATG	R61C8_9	GCGAACGAACTAAACCTGGC
F61C8_5	GGTGGCACTGGGAGATTACAC	F61C8_10	CGGCCTGGTGCTGGAATG
R61C8_5	ATGTGCGAAGAAGGCGCATC	R61C8_10	CGCTGGCAACAATCGCATTA
F61C8_6	TTCAACAACTCTGCGTTCGG		
R61C8_6	CGATTTCTTTGCCTCTCCATCAC		
Primers used for qRT-PCR in RNAi experiments:			
Z4RTF	GGCGTGCTCACCTGAATCCAA	Socs36E-RAf	CAAGCCCATCGACCAGAACACC
Z4RTR	AGTGACCGCTCCGCTACTGA	Socs36E-RAr	GCTGCCGCTCTCCACGTCCTC
Actin 42aF	AGCGGATAACTAGAAACTACTCC	spi-REf	CTGTTTGAACGATGCCCATTGCT
Actin 42aR	CTAAAGCTGCAACCTCTTCGT	spi-REr	TGTATTCGCATCGCTGTCCC
ball-RAf	AGGGCACAGTTTTCACCGATT	Stat92Ef	GAAACACCCCAACCGTTGCAC
ball-RAr	CCCACTTTGCAAGCCGCGTA	Stat92Er	GCTCTTGCTCTACCCGATGGA
CycE-RCf	ATTCAAGCTTCCCCGGCCACC	zip-RBf	ACATGCAGGCCCTTCGTTCCC
CycE-RCr	CGCCCTCATCGCCCAGGTACTCG	zip-RBr	CCCGCAGTTGCTTGACAAGTCC
dos-RBf	TGGATCGCAGTACCCGACCT	qCp190F	ACTTCATGTACACAGGCACCC
dos-RBr	TCGCTCCTCCTTCCTCGGGCAT	qCp190R	GCAGCTTCAACAGCACCGTCA
drk-REf	ATATGTTAGCCAAACCGCTCCC	qBEAF-32F	ACGAGGAGCTCACCAAGGACGAC
drk-REr	AAATCGTGTTTGGCAATCGCTT	qBEAF-32R	ACCGCACGTACATCTTCCGACT
E2f-RBf	AGCGTTCCCGTCACATCGAAG	chrizPP23396f	CGTTCTTGTATGTGGACGATGT
E2f-RBr	AGCCAGATTCTCGCGCATCAGA	chrizPP23396r	GGATCGAGCGATTCCTTCAAAT
Hrb27C-RAf	CACGCAGCCACCCTATGCAAC	z4qrt2F	GCATCAGAGTCCTTCCGCATCG
Hrb27C-RAr	ACGACATGCTACTCCGCTCCT	z4qrt2R	CGCTCAGTGCCTCATCAATGGTC
ImpL2-RAf	CCAGTGCCATTGTGCGCGTCC	Ptp61F-RCf	TCCCTTGCCGCCATTACCCGTA
ImpL2-RAr	TCTTGGAGCCAGTGCGTCCCA	Ptp61F-RCr	CCTCATCGGTGTCGTCCTCGTC
mars-RAf	ATGTGTTGTCCAAGCCGTTCGAG	Sir2-RAf	ACAACGAAGCCACGCCTAGCTAC
mars-RAr	GCACCACCTCCGCCACGTA	Sir2-RAr	CGCTTTCCCCTCTGTTGTGGA
Primer used in cloning of RNAi constructs:			
BEAF-S2-RNAi-F	GTACTCGAGCAAAACCGTGCGGATTACC	Chriz-S2-RNAiF	CAACTCTTCCCGGGTCAC
BEAF-S2-RNAi-R	GGCCTGCAGCCAAGCTAAGTGCAAAATAGT	Chriz-S2-RNAiR	GTCCCGTGCGGTATCTTT
CP190-S2-RNAiF	GTACTCGAGCCTGGCTGTGCCTGAGA	Z4-S2-RNAiF	TTTGCTTCCCGGTTTGGG
CP190-S2-RNAiR	GGCAAGCTTCTGGTAGACTTATGTCCGAAA	Z4-S2-RNAiR	CAAGTGCGGCACTTGTTC
Primer used in cloning of constructs for pull-down assay:			
BEAF-32-2R	GCGATCTAGACTACTCATCCTTGGCAAGCG	CP190-1F	AATGCGGCCGCATGGTGAAGTCAAGTCCGT
BEAF-32-2F	GCATGAATTCTCCAGCAGCAGTAACGAC	CP190-1R	GACGCGGCCGCTTACGAGCCGAGGAATTCT
BEAF-32-3F	AGCAGCTCGGCCAAGCAGCTGAAGA	BEAF3Ph-F	GTCCGATTTTTCGCCAT
BEAF-32-3R	GCTGGAGTGGAGACATCGGTGCCG	BEAF3Ph-R	GGTTGCAGCAATAATGC
BEAF4Ph-F	AATGATTGCGAGGAAGA	pGEXseq	TTCATGTTGTATGACGCTCTTG
BEAF4Ph-R	GTCCGATGGCGAAAAAT	MBPseq	GACTGATGAAGGTCTGGAAGC

2.1.7 Antibodies:

Name	Animal	Clonality	Source	Notes
Primary antibodies				
anti-Chriz	Rabbit	Polyclonal	Biogenes	animal 6177
anti-Z4	Mouse	Monoclonal	Cell Culture Lab	Z4 cell line supernatant
anti-Jil1	Rabbit	Polyclonal	Biogenes	animal 6267
anti-CP190	Mouse	Monoclonal	Cell Culture Lab	BX63 cell line supernatant
anti-BEAF-32	Rabbit	Biogenes	Biogenes	animal 21352
anti-Tubulin	Mouse	Monoclonal	Cell Culture Lab	BX90 cell line supernatant
anti-NonA	Mouse	Monoclonal	Cell Culture Lab	Bj6 cell line supernatant
anti-H3S10P	Mouse	Monoclonal	Abcam	ab14955
anti-H3K4me3	Rabbit	Polyclonal	Abcam	ab8580
anti-H3K27me3	Rabbit	Polyclonal	Active Motif	39155
anti-MBP	Mouse	Monoclonal	New England Biolabs	E8032S
anti-GST	Mouse	Monoclonal	Abcam	ab34589
Secondary antibodies				
anti-mouse IgG-AP	Goat		Jackson Immuno Research	Alkaline Phosphatase conjugated
anti-rabbit IgG-AP	Goat		Jackson Immuno Research	Alkaline Phosphatase conjugated
anti-rabbit Alexa Fluor 555	Goat		Invitrogen	Red fluorophor conjugated
anti-mouse Alexa Fluor 488	Goat		Invitrogen	Green fluorophor conjugated
anti-mouse Alexa Fluor 555	Goat		Invitrogen	Red fluorophor conjugated
anti-rabbit Alexa Fluor 488	Goat		Invitrogen	Green fluorophor conjugated

2.2 Methods

2.2.1 Cloning

Standard molecular biology protocols (Transformation of *E. coli* with plasmid DNA, plasmid DNA isolation, gel electrophoresis, PCR, etc.) were performed according to (Sambrook et al. 2012) and using enzymes and reagents from Thermo Fisher according to manufacturer's protocols. The following kits were used: Peqlab gel extraction kit 12-2500-01, Zymo clean and concentration kit D4033, D4013, Qiagen plasmid DNA midi prep 12843.

2.2.2 SDS-PAGE and western blot

SDS-PAGE and western blotting were done according to "Methods in molecular biology" (vol. 536, 869) using the recommended buffers. In western blotting "wet" transfer to nitrocellulose membrane was used.

2.2.3 Chromatin immunoprecipitation

Chromatin immunoprecipitation was performed according to the protocol of Legube et al. (2006). Chromatin was prepared either from 10^7 S2 cells or 100 pairs of L3 salivary glands. Proteins were cross-linked to the DNA by 0,75% or 2% formaldehyde for S2 cells or salivary glands respectively; afterwards the cross-linking reaction was terminated by adding glycine to a final concentration of 125 mM. Cells were washed with PBS and resuspended in lysis buffer. Lysates were sonicated to shear DNA to an average fragment size of 200 - 1000 bp. The obtained lysates were centrifuged to remove cell debris, pre-cleared by incubation with empty magnetic beads, diluted with RIPA buffer and combined with antibodies. The following antibodies were used: anti-Chriz rabbit polyclonal (own production, animal 6177), anti-BEAF-32AB rabbit polyclonal (own production, animal 21352), anti-H3S10Ph (ab14955, Abcam), anti-H3K4me3 (ab8580, Abcam), anti-H3K27me3 (39155, Active Motif). After 1 h incubation with rotating, magnetic beads were added and incubated with rotation for 2 h. The magnetic beads were washed 3 times with wash buffer and 1 time with final wash buffer to remove unspecific binding. The immunoprecipitated DNA was eluted, decrosslinked by incubation at 65˚C overnight, treated with RNAse A and purified using Chip DNA Clean & Concentrator Kit (Zymo research, D5205). The DNA obtained was amplified by PCR under standard conditions. The primer pairs for ChIP were designed to amplify 180-200 bp fragments covering 639-664 kbp region of 3L chromosome. Relative quantification analysis has been used to determine fold enrichment over mock control. Standard curve quantification was used to determine percent of input precipitated.

Lysis Buffer 50 mM HEPES-KOH pH7.5 140 mM NaCl 1 mM EDTA pH8 1% Triton X-100 0.1% Sodium Deoxycholate 0.1% SDS Protease Inhibitors (SIGMA)	**RIPA Buffer** 50 mM Tris-HCl pH8 150 mM NaCl 2 mM EDTA pH8 1% NP-40 0.5% Sodium Deoxycholate 0.1% SDS Protease Inhibitors (SIGMA)
Wash Buffer 0.1% SDS 1% Triton X-100 2 mM EDTA pH8	**Final Wash Buffer** 0.1% SDS 1% Triton X-100 2 mM EDTA pH8

150 mM NaCl 20 mM Tris-HCl pH8	500 mM NaCl 20 mM Tris-HCl pH8
Elution Buffer 1% SDS 100mM NaHCO3	

2.2.4 RNA expression analysis

RNA for expression analysis was isolated from 20 pairs of third-instar larvae salivary glands or 10^7 S2 cells using Quick-RNA MiniPrep Kit (Zymo Research, R1054). cDNA synthesis was performed using Oligo dT/Random hexamer primer mixture and RevertAid Premium Reverse Transcriptase (Thermo Scientific) following the manufacturer's protocol. *Actin42a* or *EF1* was used as the endogenous control in further qPCR analysis.

2.2.5 Real-time PCR analysis

Quantitative PCR of ChIP and expression analysis was performed using SYBR Green PCR master mix (Applied Biosystem) in a StepOnePlus Real-Time PCR system (Applied Biosystem). The amplification parameters were as follows: 10 min at 95°C, 40 cycles of 15 s at 95°C followed by 1 min at 60°C. At the end of the program the melting curve was recorded. The resulting data were analyzed using StepOne Software v2.3.

2.2.6 RNAi in S2 cell culture

Sequences for RNAi were selected using FlyRNAi database (flyrnai.org). The main criteria were absence of off-targets, positive reference from previous public screenings and the length of product around 500-1000 bp. Selected sequences were amplified from WT cDNA and cloned to pLitmus plasmid for bidirectional transcription. As a control a plasmid with 900 bp part of Orange Fluorescent Protein sequence was used. From each plasmid PCR with T7 primer was performed, the product was purified and used as a template for in vitro transcription.

dsRNA synthesis was performed using T7 RNA polymerase (Thermo Fisher Scientific) according to the manufacturer's protocol. After in vitro transcription DNAse digestion was performed (15 min 37˚C) followed by inactivation of DNAse (2µl 0,5M EDTA added and incubated at 65˚ for 10 min). dsRNA was precipitated with Ammonium Acetate, washed twice with 80% ethanol and resuspended in RNAse free water. For transfection 15 µg of dsRNA per well (6-well plate) was used.

Transfection was performed according to Current protocols in Molecular Biology, (Supplement 65, Unit 26.5, 2004). Cells were passaged 24h hours prior to transfection. At

the day of transfection cells were counted and seeded to 6-well plates, 10^6 cells per well in 1 ml of serum-free media. After adding the dsRNA cells were hand-mixed 15 sec and incubated 60 min at 28˚C. Finally, 2 ml of S2 growth medium (with 10% FCS) were added to each well. To determine optimal knockdown conditions for further experiments, cells were analyzed after 24, 48, 72 and 96 hours.

2.2.7 Co-immunoprecipitation

Co-IP was performed from *Drosophila* Kc cells nuclear extract using magnetic beads (Thermo Scientific, Cat. № 88803). Nuclear extract was pre-cleared by centrifugation 10 min 21 x g followed by 15 min incubation on a shaker with 25µl pre-equilibrated magnetic beads per sample. Next, the nuclear extract was incubated 1 h with 10 µg of antibody at RT with mixing. After adding 25µl of pre-equilibrated magnetic beads the extract was incubated 2h at RT with mixing. Then 3 washing steps with 500µl TEN 125 were performed. Proteins were eluted by adding 80 µl SDS-PAGE reducing sample buffer and further analyzed by western blotting.

TEN125: 10mM Tris-HCl pH 8,0, 1mM EDTA, 125mM NaCl

2.2.8 IIF

Immunostaining of polytene chromosomes from 3rd instar larvae was performed as described by Eggert and coworkers (2004).

Immunostaining of S2 cells was performed according to Sarkar Angshuman (2007) (Cold Spring Harbor Protocols; 2007; doi:10.1101/pdb.prot4760)

2.2.9 Microscopy

For microscopy, a DeltaVision Spectris Optical Sectioning microscope (OSM) equipped with 60x and 100x lenses, a polychroic beamsplitter suitable for DAPI and RD-TR-PE and Filter sets DAPI (EX360/40; EM457/50) and RD-TR-PE (EX555/28; EM617/73) was used. Images were obtained a stack of optical sections that were deconvolved using DeltaVision SofWorx software.

2.2.10 Quantitative image analysis

For the image deconvolution and further analysis DeltaVision SoftWorx and ZIK ImageJ software was used. Determination of signal intensity profile to measure levels of

fluorescence was performed for each wavelength separately from three independent images. After selecting the region of interest, the pixel intensity profiles for this selected area were recorded (see example on Fig 17). To determine the total level of fluorescence of certain wavelength, the integral of the obtained curve in the region of interest was calculated.

A

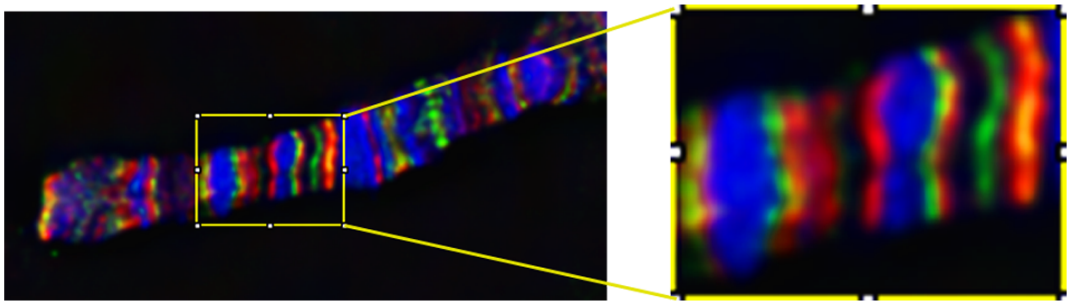

B

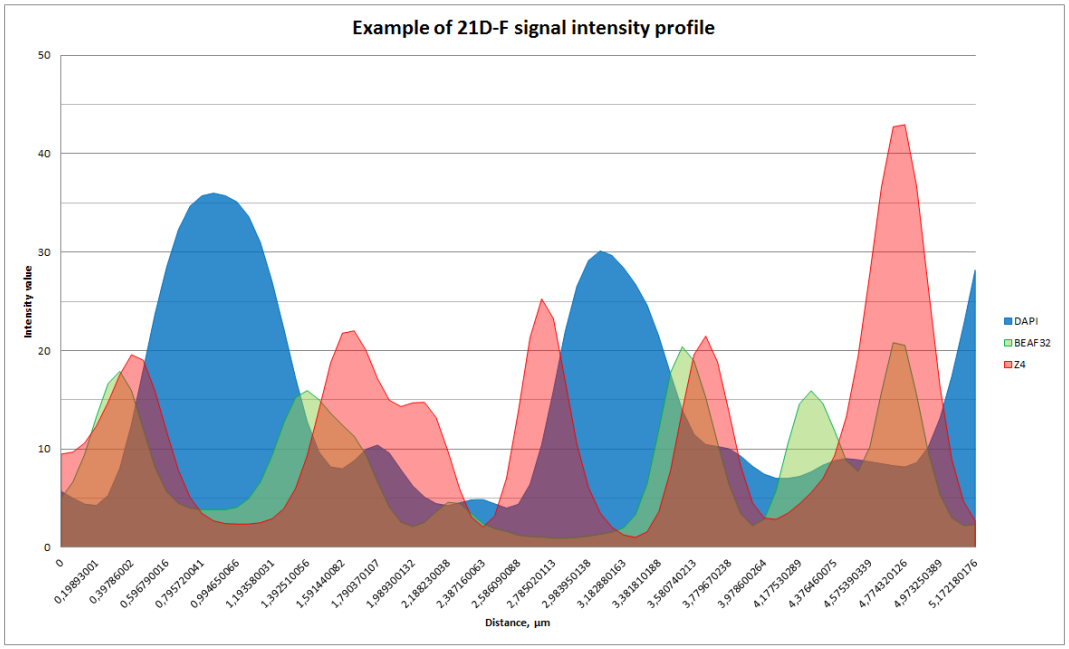

Fig. 17. Quantitative image analysis: Signal intensity profile recorded from 21F-D locus. A – Image used for quantification. Yellow frame indicates area selected for analysis; magnified selection is shown at the right side. B – Profile of fluorescent intensities in selected area for three wavelengths. Blue – DAPI, red – Z4, green – BEAF-32.

To consider the contribution of background level of the signal, for each wavelength the total fluorescence level of the area out of chromosome was subtracted from the total fluorescence level of the chromosomal signal (see example on Fig. 18).

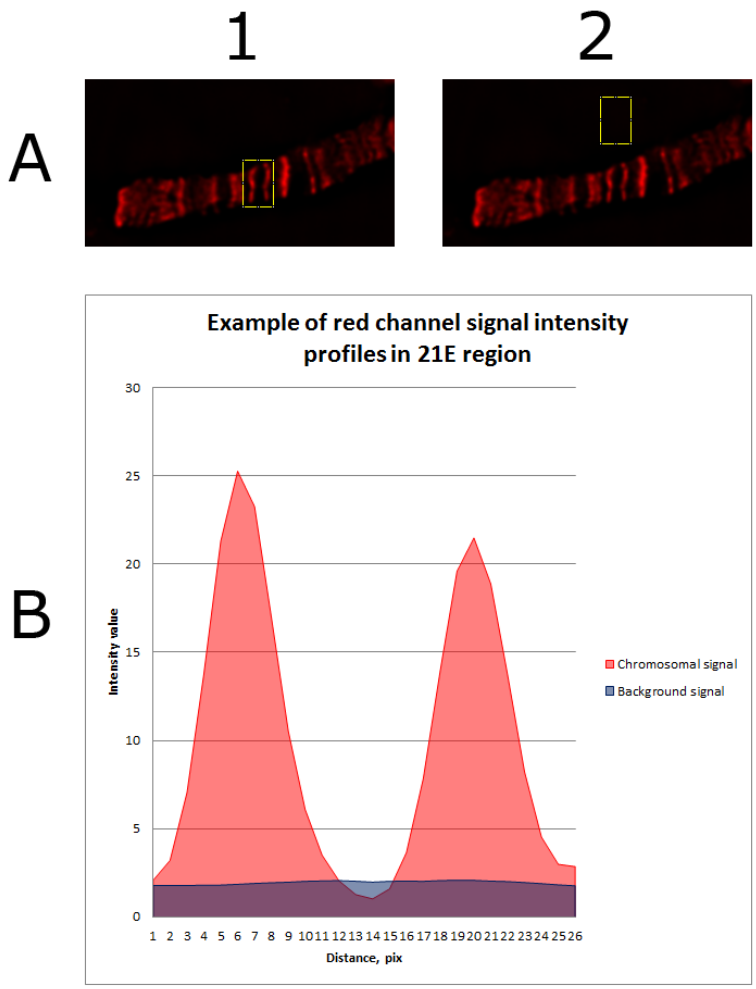

Fig. 18. Quantitative image analysis: Example of image background subtraction. A – Image used for quantification; 1 – example of chromosomal area selection; 2 – example of selection area out of chromosome. B – fluorescent intensity profile of selected area. Red – chromosomal signal profile, Blue – background signal profile.

2.2.11 Calculation of correlation coefficient

The correlation coefficient, or Pearson product-moment correlation coefficient (PMCC) is a numerical value between -1 and 1 that expresses the strength of the linear relationship between two variables. When correlation coefficient (r) is closer to 1 it indicates a strong positive relationship. A value of 0 indicates that there is no relationship. Values close to -1 signal a strong negative relationship between the two variables.

Correlation coefficient formula:

$$r = \frac{n\sum_{i=1}^{n} x_i y_i - \sum_{i=1}^{n} x_i \sum_{i=1}^{n} y_i}{\sqrt{(n\sum_{i=1}^{n} x_i^2 - (\sum_{i=1}^{n} x_i)^2)(n\sum_{i=1}^{n} y_i^2 - (\sum_{i=1}^{n} y_i)^2)}}$$

where n is the total number of samples, xi (x1, x2, ... ,xn) are the x values and yi are the y values (http://www.alcula.com/calculators/statistics/correlation-coefficient/).

2.2.12 Establishing of 42patt61C_BEAF1+2 fly strain

Pattp61C plasmid with a part of 61C7-8 interband sequence was used as a BEAF-motif containing sequence. PCR with phosphorylated primers, containing motif mutations at 5' ends was performed followed by self-ligation to produce the plasmid where two BEAF-32 binding motifs in the cluster 1 were mutated from CGATA to CGGAC (1') or CGCAG (2') (See Fig 42). Fly strain 42pattP was transfected with the resulting plasmid using ΦC31 site specific recombination. By crossing with Tft/CyO balancer fly line, homozygous stock of the positive transformant was established (fly strain 42patt61C_BEAF1+2).

3. Results

3.1 Chriz complex contributes to chromatin structure and histone modifications

3.1.1 Knockdown of Chriz complex in S2 cells

3.1.1.1 Chriz RNAi affects the amount of Z4 and the Jil-1 kinase.

To study the role of Chriz and Z4 in the complex, double-stranded RNA-induced gene silencing (RNAi) in *Drosophila* S2 cells was performed. Short sequences of Chriz and Z4 were transcribed from both directions and the resulting dsRNA was added to the S2 cells. Transfection and selection of knockdown time was performed as described in Materials and Methods. Cell lysates from the knockdowns were assayed on Western blots. (see Fig. 19)

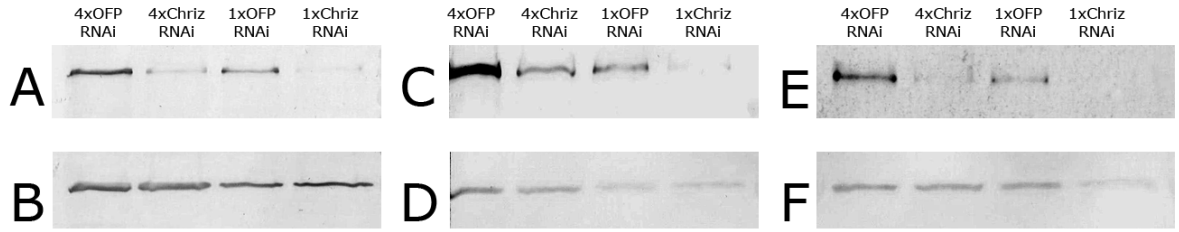

Fig. 19. Western blot from S2 cell lysates with Chriz RNAi. Cell lysates from Chriz RNAi and control OFP RNAi were loaded in two dilutions each - 4% and 1% for comparison (see text for details). Membrane was probed with the following antibodies: A) anti-Chriz; C – anti-Z4; E) anti-Jil1; B) ,D), F) anti-Tubulin loading control.

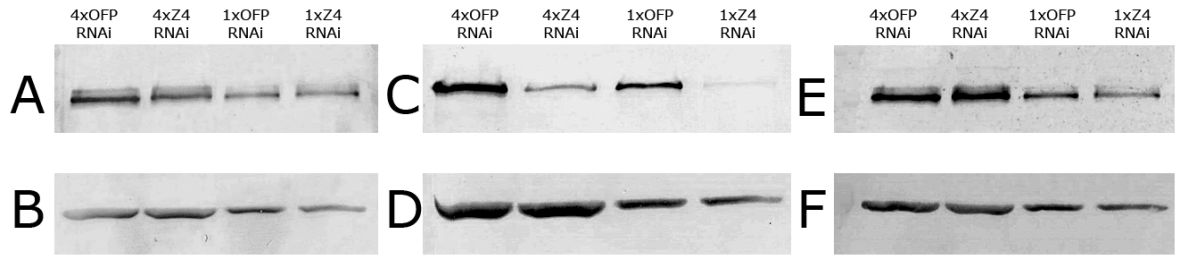

Fig. 20. Western blot from S2 cell lysates with Z4 RNAi. Cell lysates from Z4 RNAi and control OFP RNAi were loaded in two dilutions each - 4% and 1% for comparison (see text for details). Membrane was probed with the following antibodies: A) anti-Chriz; C – anti-Z4; E) anti-Jil1; B), D), F) anti-Tubulin loading control.

To achieve a semi-quantitative estimation of the knockdown efficiency, the cell lysates were loaded in two dilutions – 4x and 1x. As can be seen on western blot (Fig. 19), the 25% of control OFP probe gives stronger signal than 100% of Chriz knockdown probe, therefore the

efficiency of Chriz knockdown can be estimated as more than 75%. In Z4 RNAi knockdown efficiency (Fig. 20) was estimated to similar extend.

As can be seen from Fig. 19, RNAi knockdown of Chriz resulted in strong (75%) downregulation of Z4. However, the Z4 RNAi-mediated knockdown in contrast does not affect Chriz protein (Fig. 20).

3.1.1.2 Chriz RNAi affects interphase H3S10 phosphorylation state

RNAi knockdown of Chriz, but not of Z4 leaded to strong reduction of Jil-1 kinase level in the cells (See Fig, 19). Since Jil-1 is the only kinase which performs H3S10 phosphorylation during the interphase, we questioned whether Chriz knockdown also affects this histone modification in S2 cells. Unfortunately, it was not possible to analyze H3S10P levels quantitatively by western blot due to strong phosphorylation of H3S10 in mitotic cells by Aurora kinase, which overshadowed the possible change in interphase phosphorylation (see Suppl. Fig. 1). Therefore, to overcome this problem and to see the effect of knockdown on the level of single cells, we performed immunofluorescent staining of S2 cells following RNAi knockdown.

As can be seen on Fig 22 a, Chriz and Z4 are highly co-localized in S2 cell nuclei of control cells. In cells with Chriz knockdown, downregulation of Chriz correlates with loss of Z4 protein. This can be clearly seen at higher magnification (Fig. 22). The images of controls and Chriz RNAi for both antibodies were made with same exposure time, therefore the intensities of fluorescence can be compared. However, not all cells demonstrate the same response to RNAi. In around 20 % of cells Chriz, and therefore Z4, was still found in amounts comparable with control cells (Fig. 21, suppl. Fig. 3). This number is in agreement with semi-quantitative estimation of knockdown efficiency by western blot.

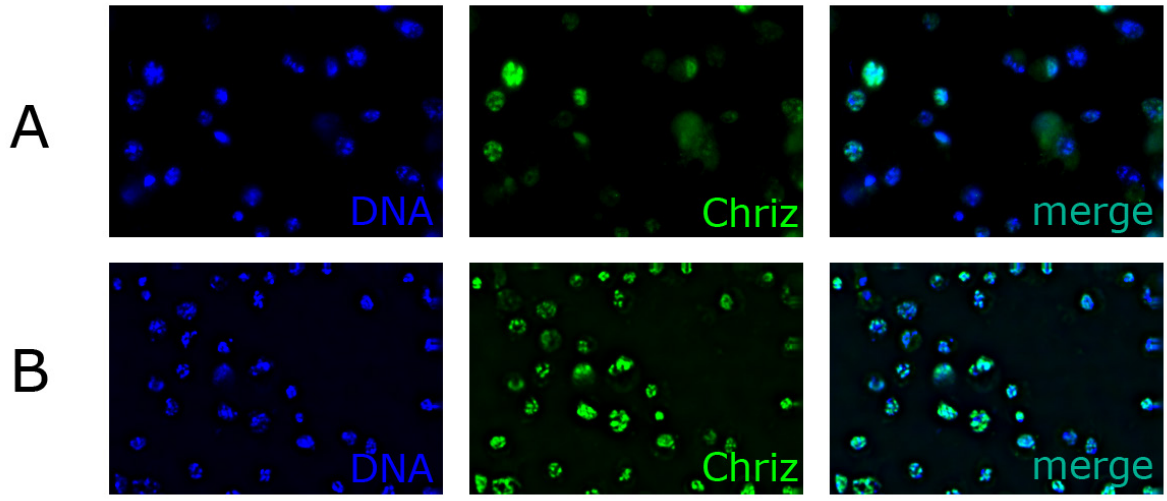

Fig. 21. Chriz RNAi in S2 cells resulted in 80% knockdown efficiency. IIF staining of S2 cells. A) Chriz RNAi; B) OFP control. 1 – Hoechst staining (blue); 2 –Chriz (green); 3 – merge.

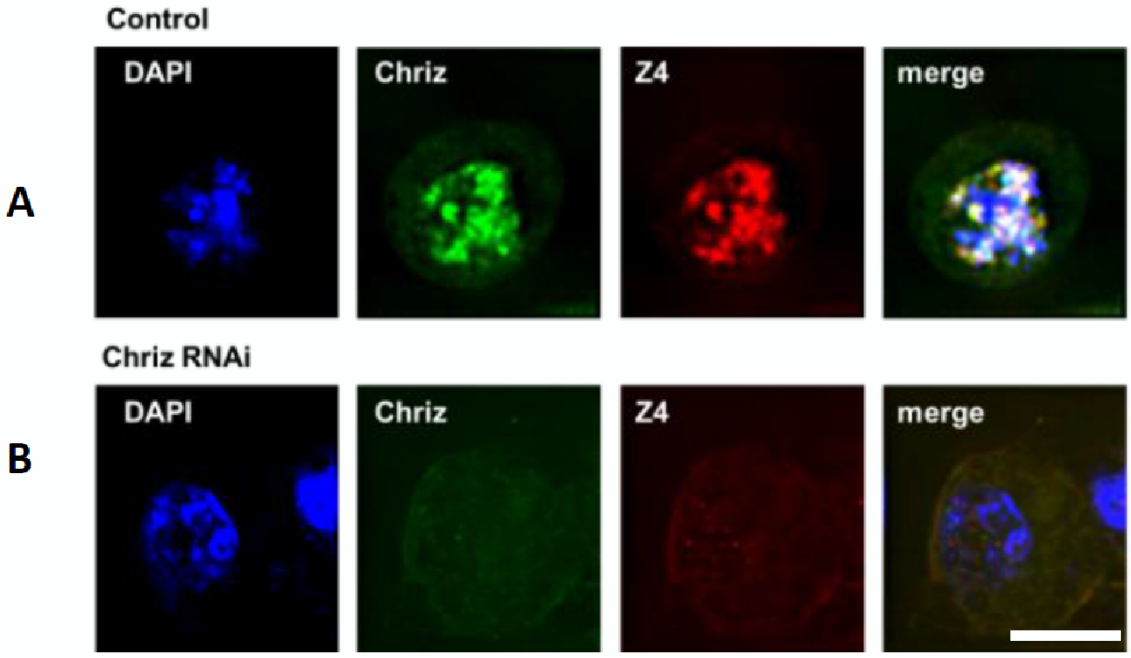

Fig.22. Knockdown of Chriz in S2 cells affects Z4 chromatin binding. IIF staining of S2 cells. A) OFP control; B) Chriz RNAi. 1 – Hoechst staining (blue); 2 –Chriz (green); 3 - Z4 (red); 4 – merge. Scale bar 4 µm

To see the effect of Chriz knockdown on H3S10 phosphorylation, immunofluorescent staining of Chriz RNAi and control cells was performed (Fig. 23, 24). It can be seen that in cells, transfected with Chris dsRNA, H3S10p level in interphase is strongly reduced. However, during the mitosis, H3S10 is still heavily phosphorylated (see Suppl. Fig. 7), which demonstrates that only Jil1- mediated H3S10 phosphorylation is affected by Chriz knockdown.

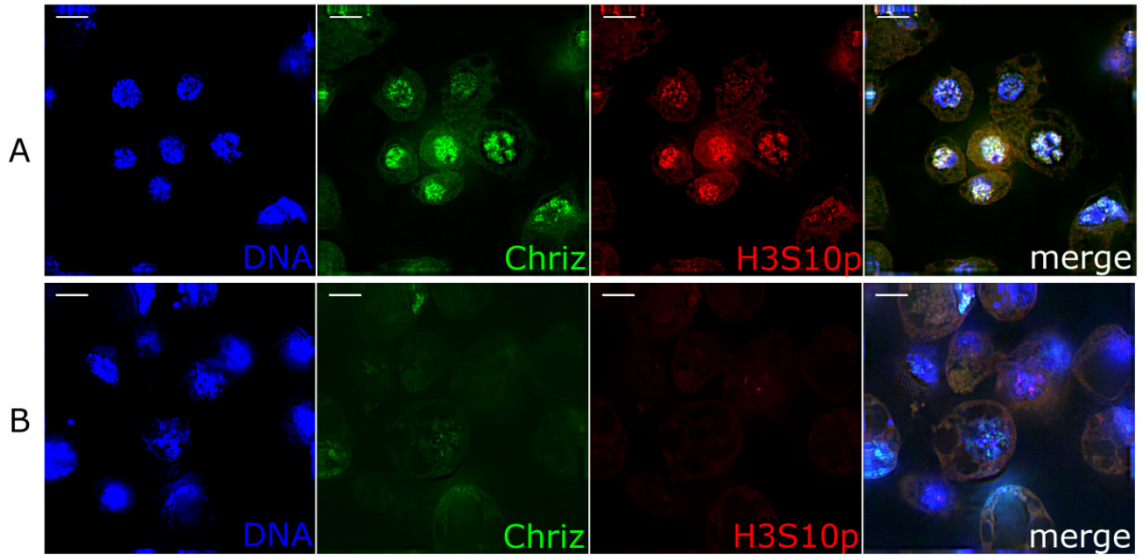

Fig. 23. Knockdown of Chriz in S2 cells affects histone H3S10 phosphorylation. IIF staining of S2 cells. A – OFP control; B – Chriz RNAi. 1 –Chriz (green); 2 - H3S10ph (red); 4 – merge with Hoechst (blue). Scale bar 4 µm

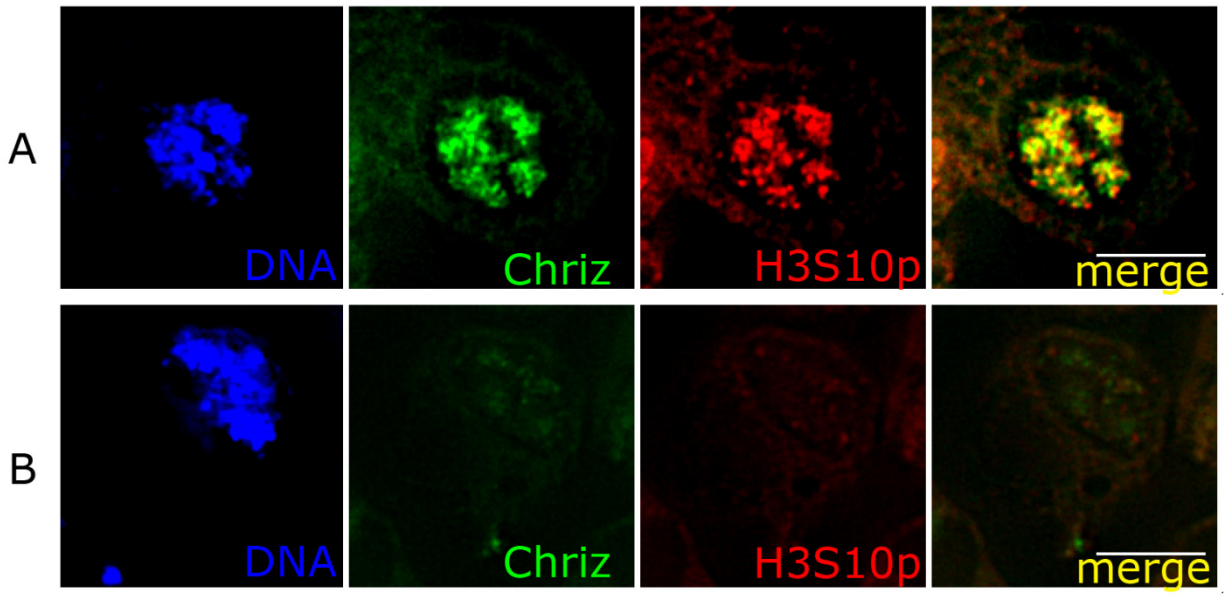

Fig. 24. Knockdown of Chriz in S2 cells affects histone H3S10 phosphorylation (High magnification imaging). IIF staining of S2 cells. A – OFP control; B – Chriz RNAi. 1 –Chriz (green); 2 - H3S10ph (red); 4 – merge with Hoechst (blue). Scale bar 4 µm

3.1.2 Chriz RNAi knockdown in salivary glands

In order to investigate Chriz effect on chromatin structure we performed RNAi in 3rd instar larvae salivary glands targeted by UAS/Gal4 system. As can be seen on Fig. 25, Chriz level is significantly reduced comparing to wildtype. However, apparently due to long half-life or high stability of Chriz protein in non-cycling cells, remaining Chriz was still detectable on polytenes. We also did not observe a disruption of chromosomal band/interband pattern as reported by Rath and colleagues for a combination of Chriz hypomorphic mutations (Rath et al. 2006). Therefore, for investigation of the structural role of Chriz, we sought to use alternative methods to obtain more severe reduction of Chriz protein in salivary glands.

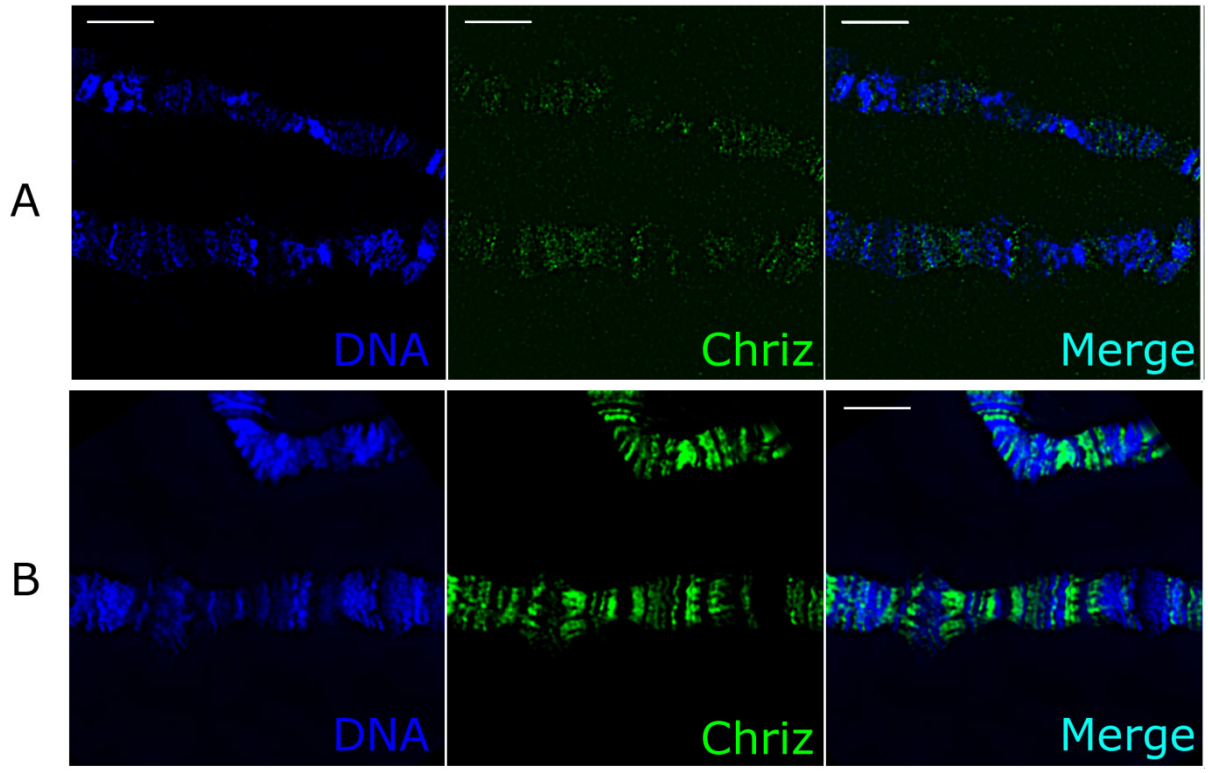

Fig. 25. Chriz knockdown by RNAi did not lead to disruption of chromosomal band/interband pattern. IIF staining of polytene chromosomes from 3rd instar larvae salivary glands. A) Chriz RNAi; B) Wild type control. DNA – blue, Chriz – green. Scale bar 2μm.

3.1.3 DeGradFP protein knockout of Chriz in salivary glands

To analyze the role of Chriz in chromatin structure, deGradFP, a novel method of GFP-tagged protein knockout was employed (see Discussion).

We made use of ΔKG12 homozygous lethal deletion of ~1.5kb Chriz genomic region, generated by P-element hop-out (Gortchakov et al. 2005). The ΔKG12 deletion was fully rescued by ΦC31 site specific insertion of a plasmid containing GFP-tagged Chriz under endogenous promoter (see crossing scheme in Materials and Methods).

Precise mapping of the deletion was performed by PCR using primers located in Chriz genomic region followed by sequencing of the product. As can be seen on the figure 26, PCRs with F3-R3 and F3-R4 primer pairs amplify from wildtype genomic DNA products of 4,8 kbp and 3,2 kbp respectively. In PCR with F3-R4 primers using genomic DNA from ChrizGFP/ChrizGFP; ΔKG12/ΔKG12 strain as a template, only 2,1 kbp was amplified, F3-R3 PCR gave no product. This fragment indicates the location of 3' end of deletion between R3 and R4 primers and at the same time demonstrates that the analyzed strain is homozygous for the deletion. The sequencing of F3-R4 PCR product detected the deletion of 2737 bp (Fig. 26 A).

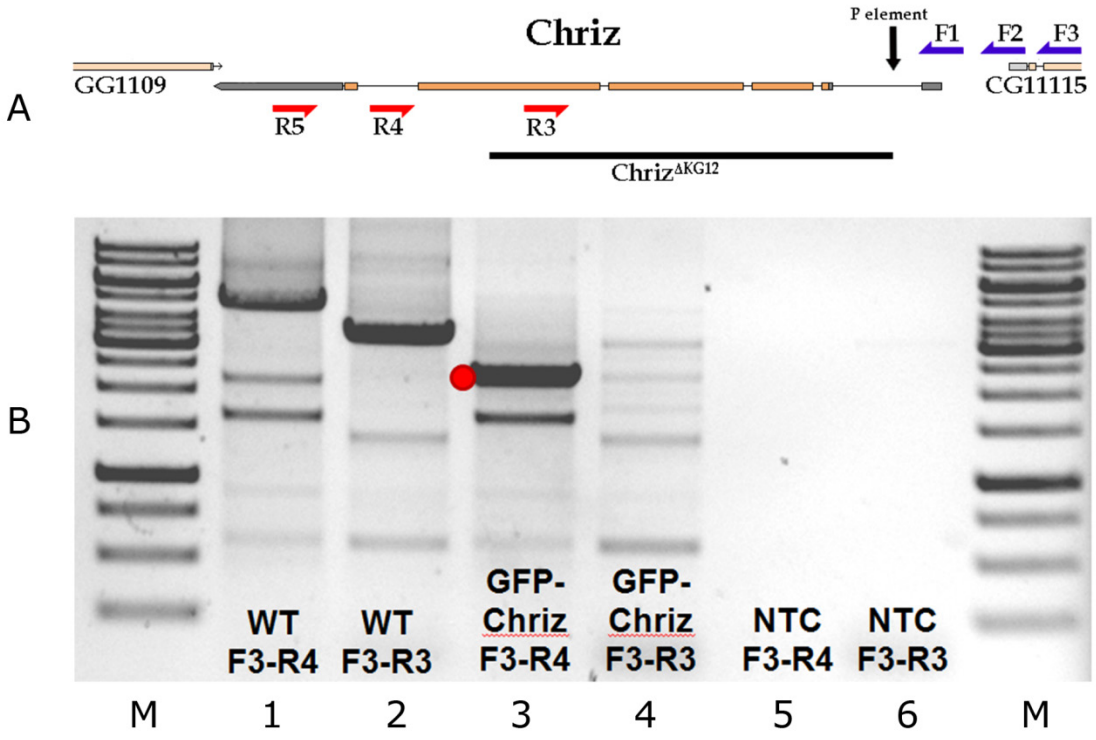

Fig. 26. Mapping of Chriz deletion in ChrizGFP/ChrizGFP; ΔKG12/ΔKG12 strain. A) Schematic picture of Chriz genomic region indicating the extent of deletion. Black vertical arrow indicates position of P-element used for mobilization. Blue and red horizontal arrows show locations of forward and reverse primers respectively, used for mapping. Black horizontal bar indicates the sequence deleted in ΔKG12 strain. B - Agarose gel showing results of PCR using F3, R3 and R4 primers. M- 1 kb DNA ladder; 1,2 – PCR from Oregon wild type genomic DNA using F3-R4 and F3-R3 primer pairs respectively. ; 3,4 – PCR from ChrizGFP/ChrizGFP; ΔKG12/ΔKG12 genomic DNA using F3-R4 and F3-R3 primer pairs respectively; 5,6 non-template controls. Red dot points to shortened PCR product from the locus with deletion.

We mapped the available Chriz deletion and rescued it by transgenic insertion of construct expressing Chriz-GFP under the control of endogenous promoter sequence. The Chriz 3' UTR was also included to the construct to avoid possible misregulation in Chriz-GFP expression as well as to keep the stability of the transcript. GFP-tagged Chriz expression in ChrizGFP/ChrizGFP; ΔKG12/ΔKG12 strain was validated by western blot and by direct fluorescence analysis of the GFP-Chriz fusion protein. As can be seen on Fig. 27, only GFP-tagged Chriz is expressed in ChrizGFP/ChrizGFP; ΔKG12/ΔKG12 strain, resulting in a shift of the Chriz band on a western blot to higher position relative to endogenous Chriz.

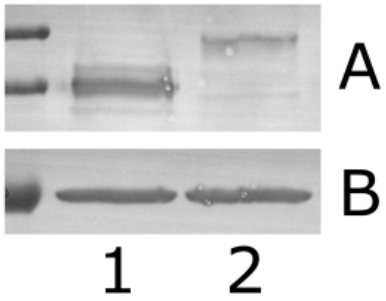

Fig. 27. Expression of GFP-tagged Chriz in ChrizGFP/ChrizGFP; ΔKG12/ΔKG12 strain. Western blot from 3rd instar larvae salivary glands. 1 – protein extract from Oregon wild type; 2- protein extract from ChrizGFP/ChrizGFP; ΔKG12/ΔKG12 strain. A) anti-Chriz antibody; B) loading control: anti-tubulin antibody.

To see the localization of GFP-tagged Chriz in the cells, direct fluorescence imaging was performed. Salivary glands were dissected and stained for 10 min in 1:10000 Hoechst solution to visualize the nucleus. Afterwards glands were mounted to slides and imaged. As can be seen on Fig. 28, GFP-Chriz is ubiquitously expressed and localized to nucleus.

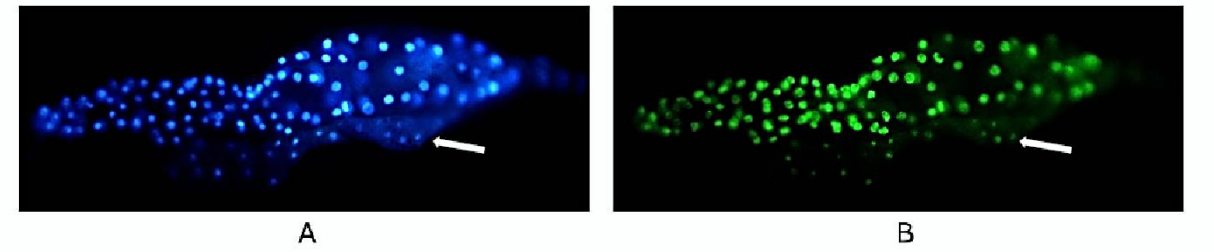

Fig. 28. Direct fluorescence imaging of a salivary glands from ChrizGFP/ChrizGFP; ΔKG12/ΔKG12 strain. A) Hoechst staining; B) GFP signal. Arrows indicate fat body cells, that are also stained indicating global GFP-Chriz expression.

To define the localization of GFP-tagged Chriz on polytene chromosomes, IIF staining of squash preparations from ChrizGFP/ChrizGFP; ΔKG12/ΔKG12 strain was performed. As can be seen on Fig 29 A1, A2 C1, C2, Chriz-GFP is located in interbands of polytene chromosomes, in a pattern identical to endogenous Chriz. Z4 protein which is known to be recruited by Chriz fully co-localize with GFP-Chriz as well (Fig. 29, A3, A4, C3, C4).

To perform GFP-Chriz protein knockout using DeGradFP nanobody system, two fly strain were generated (see cross schemes in Materials and methods). The first strain contained homozygous ΔKG12 Chriz deletion rescued by homozygous Chriz-GFP insertion and combined with G61 salivary gland specific Gal4 driver. The second strain contained homozygous NSlmb-vhhGFP4 insertion under the control of UAS promoter and heterozygous ΔKG12 Chriz deletion balanced over TM6 (Tb phenotype) chromosome. After crossing this two strains, all non-Tb larvae had the genotype “G61 Gal4 driver; UAS-NB/ChrizGFP;

ΔKG12/ΔKG12" (Chriz deGradFP strain) and were further analyzed. Interestingly, Chriz deGradFP larvae demonstrated significant developmental delay and small salivary gland phenotype, which was more severe than RNAi knockdown induced by the same G61 driver (see Fig. 30)

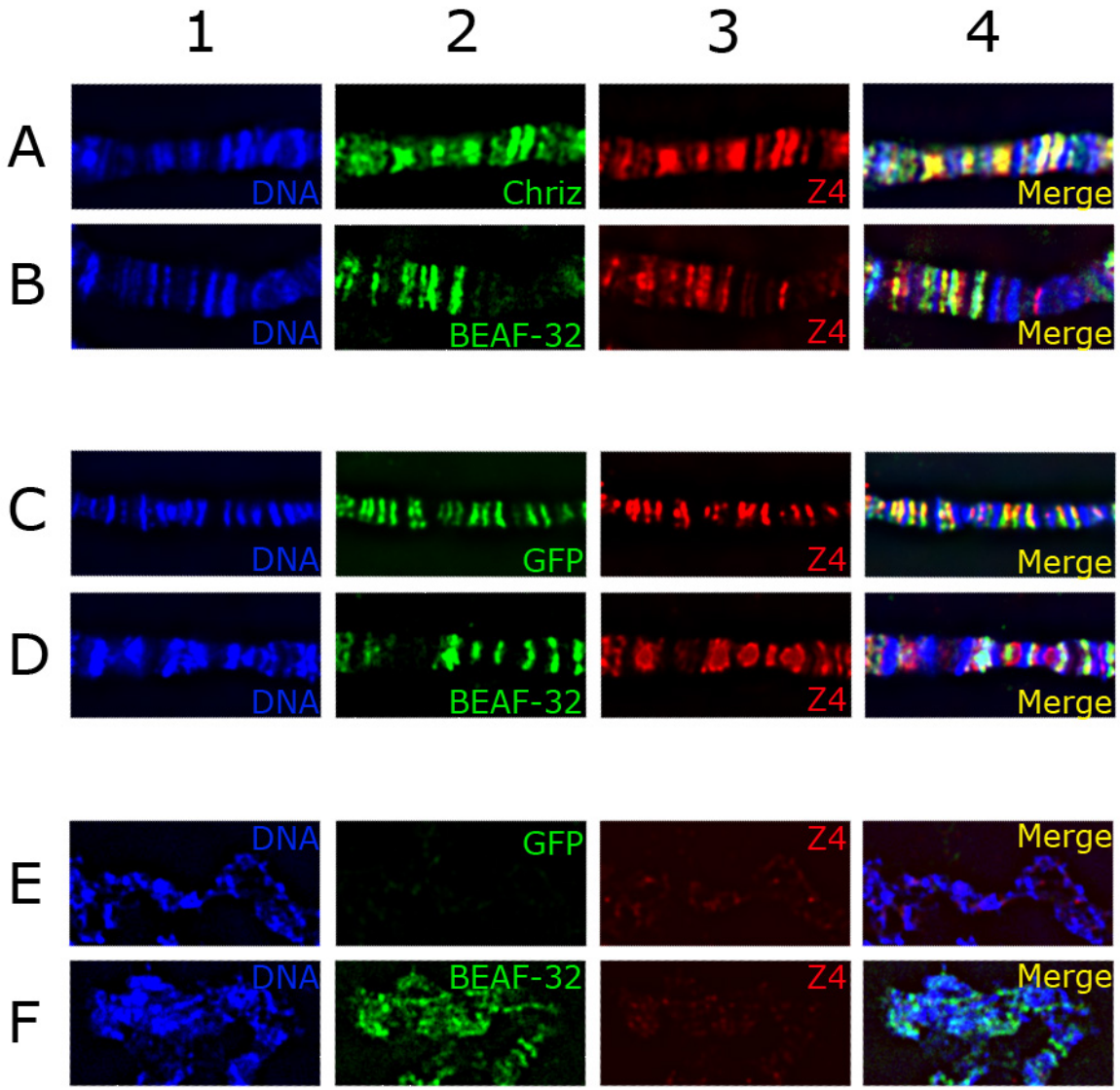

Figure 29. Chromatin protein binding in Chriz deGradFP experiments. IIF staining of polytene chromosomes from 3rd instar larvae salivary glands. A), B) wild type, stained with A2) Chriz-antiserum (green) B2) BEAF-32 antiserum (green) and A3), B3) Z4 antibody (red); C),D) Chriz-GFP strain, stained with C2) Chriz-antiserum (green) D2) BEAF-32 antiserum (green) and C3), D3) Z4 antibody (red); E),F) - Chriz deGradFP strain, stained with E2) anti-GFP antiserum (green) F2) BEAF-32 antiserum (green) and E3), F3) Z4 antibody (red). Scale bar 2μm.

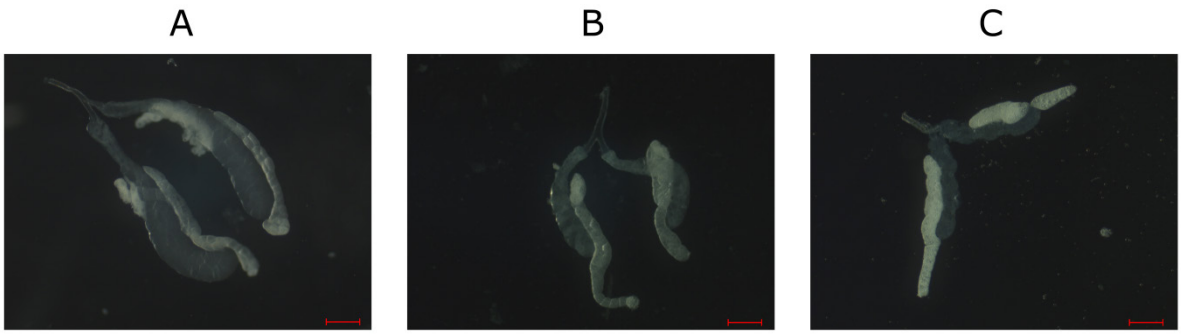

Fig. 30. Size of salivary glands is reduced following Chriz knockdown. Salivary glands with fat bodies dissected from A) Oregon wild type; B) Chriz RNAi/Gal4 G61 strain; C) Chriz deGradFP strain. Scale bar 200 µm.

To estimate the extent and specificity of Chriz-GFP knockdown, we performed direct fluorescent imaging of Chriz deGradFP tissues. As can be seen at Fig. 31, GFP signal is depleted selectively in salivary gland tissue, but still can be detected in nuclei of fat body cells. Unfortunately, it was not possible to assay the extent protein knockout by western blot. Due to extreme fragility and small size of salivary glands under ChrizGFP knockout, separation of fat body cells from salivary glands was not possible without complete distruction of gland tissue.

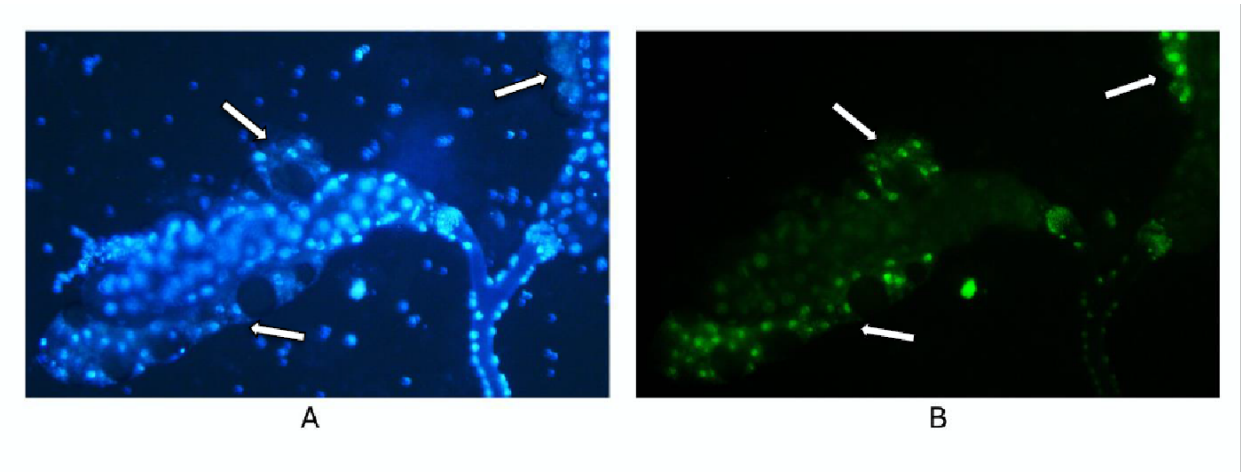

Fig. 31. Direct fluorescence imaging of Chriz deGradFP salivary glands. A) Hoechst staining; B) GFP signal. Arrows indicate fat body cells, that are not affected by DeGradFP knockdown.

Further we asked whether the Chriz protein knockout would affect the binding of Chriz complex components like Z4 and the interband/boundary protein BEAF-32. For this purpose we performed IIF staining of squash preparations from Chriz deGradFP salivary glands with a Chriz, BEAF-32 and Z4 antibodies. Fig. 29 E1,F1 shows that structure of polytene chromosomes is strongly affected, the band/interband pattern is completely corrupted. As expected, Chriz and Z4 binding to chromatin in Chriz deGradFP strain is significantly reduced.

Nevertheless, BEAF-32 was still found to bind chromatin, but due to severe structural defects it was not possible to define whether the pattern of BEAF-32 binding was affected.

To summarize, the results of Chriz and Z4 RNAi and Chriz protein knockout experiments point to an important role of Chriz complex for maintaining chromatin structure. It was found that Chriz occupies central role in the complex and is responsible for recruitment of zinc-finger protein Z4 an H3S10 kinase Jil-1. Depletion of Chriz in vivo leads to small tissue phenotype, developmental delay and loss of chromatin structure.

3.2 Role of Chriz complex in gene expression

3.2.1 Chriz and Z4 RNAi in S2 cells

3.2.1.1 Chriz and Z4 RNAi modulate the expression of many genes.

Publicly available genome-wide data shows a tendency of BEAF-32, Chriz and CP190 to bind near TSSs and promoter regions (Jiang et al. 2009; Bushey et al. 2009). Current data from our previous work and the literature suggest that the complex is involved in modification of active chromatin and as a consequence in transcription regulation (Gan et al. 2011). To figure out the contribution of Chriz complex to regulation of gene activity, we selected 42 genes containing significant Chriz enrichment at their promoter regions and performed qRT-PCR of these genes, using cDNA from cells transfected with Chriz dsRNA or Z4 dsRNA. Control cells were transfected with OFP dsRNA. The results normalized to EF1 gene expression are shown in Fig. 32. As can be seen, for the half of analyzed genes (22 of 42), the depletion of Chriz resulted in significant (more than 30%) reduction of expression, 13 genes showed no or mild downregulation, 7 genes were up-regulated 1,5-2 fold.

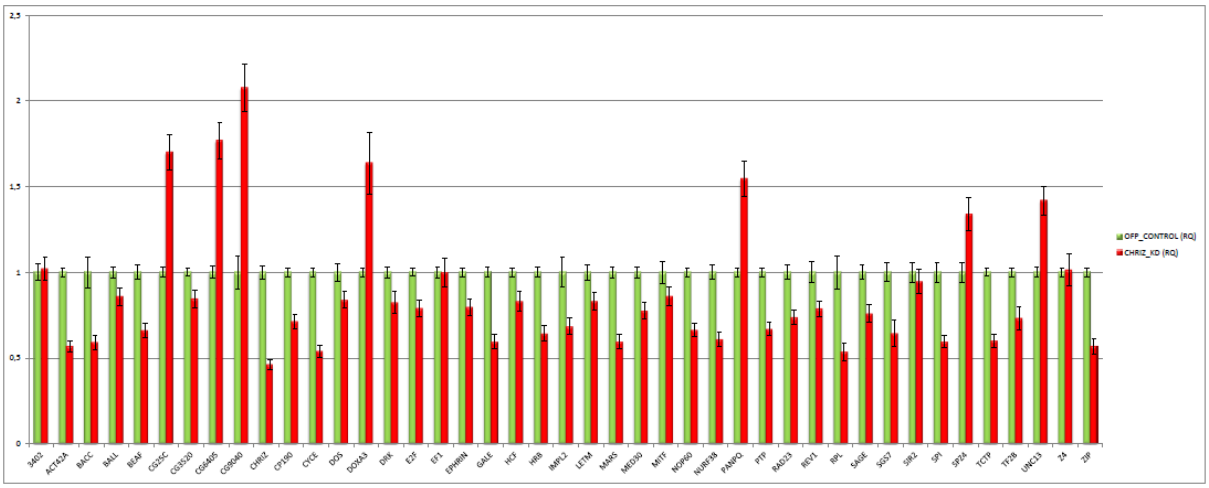

Fig. 32. Chriz knockdown reduced expression of many genes. Diagram shows qRT-PCR of 42 genes in Chriz RNAi cells (red bars), standardized to OFP control (green bars). Y axis – fold change.

Transfection of S2 cells with Z4 dsRNA for the majority (30 of 42) of analyzed genes lead to a reduction of expression similar as in Chriz RNAi (Fig. 33). However, none of the genes was found to be upregulated and 12 genes demonstrated no change in expression.

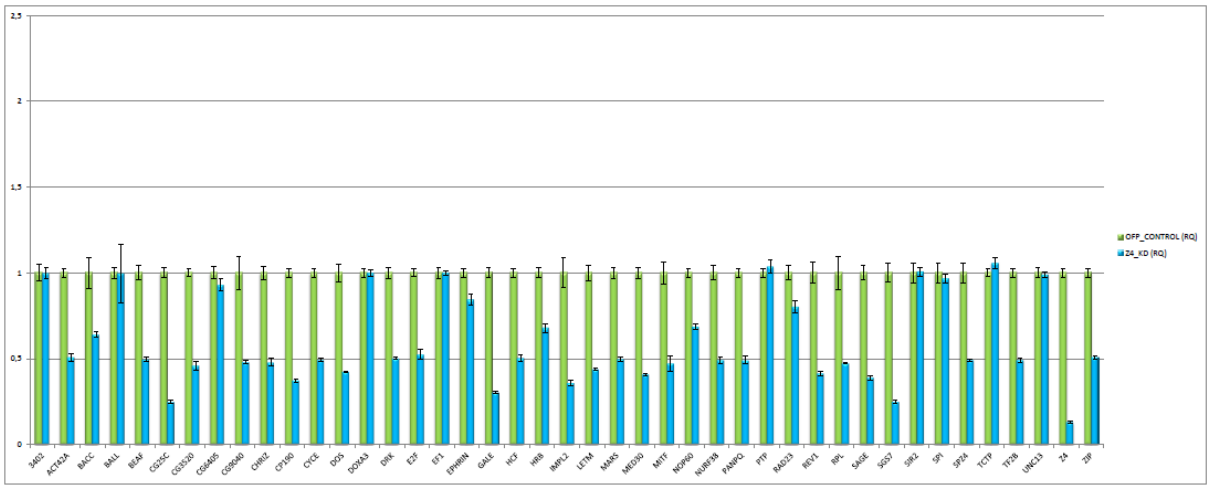

Fig. 33. Chriz knockdown reduced expression of many genes. Diagram shows qRT-PCR of 42 genes in Z4 RNAi cells (blue bars), standardized to OFP control (green bars). Y axis – fold change.

The results from both RNAi experiments are compared in Fig 34. It can be seen, that among 7 genes upregulated in Chriz RNAi experiment, 4 remain unchanged during Z4 RNAi, and 3 shows at least 50% downregulation.

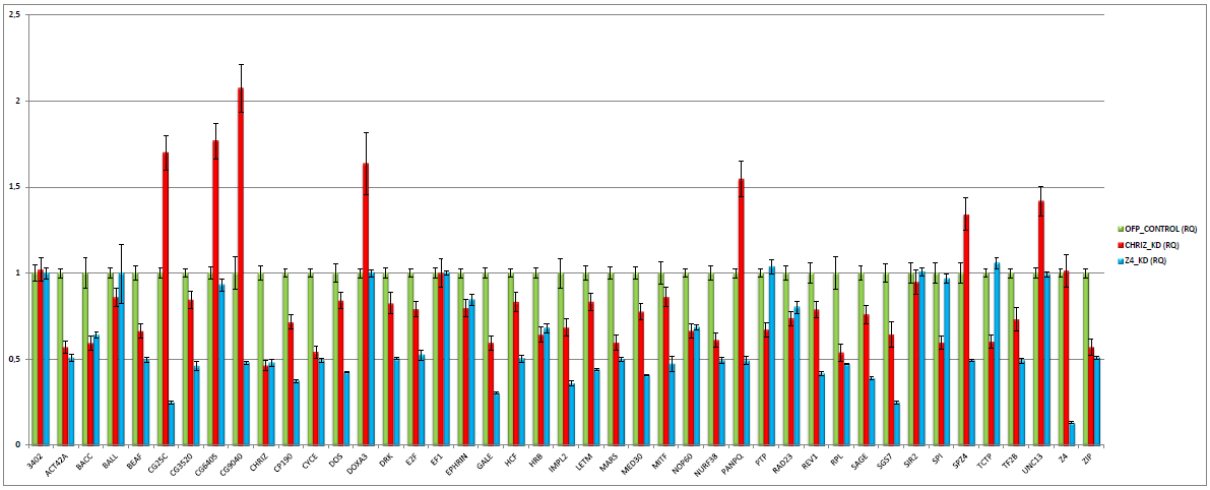

Fig. 34. The comparison of epression level of genes in Chriz RNAi and Z4 RNAi experiments. Diagram shows qRT-PCR of 42 genes in Chriz RNAi cells (red bars) and Z4 (blue bars), standardized to OFP control (green bars). Y axis – fold change.

In summary, the results of expression analysis revealed a general, mainly identical repressive effect of both Chriz and Z4 knockdowns. However, for 15% of genes Chriz depletion lead to increased expression.

3.2.2 Correlation of Chriz binding with gene expression

Analysis of genome-wide datasets of modENCODE database (http://modencode.oicr.on.ca) shows a clear tendency of Chriz to bind in a close proximity of active genes. We therefore were interested whether the amount of Chriz bound to TSSs or promoter regions of same genes in different tissues correlates with the tissue-specific level of expression of these genes. For the comparison study embryonic S2 cells and 3rd instar salivary gland tissue were selected. Using the information from FlyAtlas database (www.flyatlas.org) we chose 7 genes, depending on tissue-specific expression scores. In addition, we took for analysis 4 genes from 61C region (*Gale, CG3402, Rev1* and *Med30*). Selected genes were classified into four groups, according to expected difference in tissue-specific expression (see Table 2). Group A contaied 2 genes with a low expression score in both tissues (*CG6405* and *spz4*). *CG3523* and *tctp* together with 61C7-8 gene *gale*, which are expressed in both tissues in moderate amounts were classified to group B. Group C combined the genes CG9040 and sage that are specifically expressed in salivary glands. Bacc, which is expressed preferentially in S2 cells was classified to Group D. Three 61C7-8 genes CG3402, rev1 and med30, that are more expressed in S2 cells than in glands were also assigned to the group D.

Group	Gene	Expression	
		SG	S2
A	CG6405	no	no
	spz4		
B	CG3523	yes	yes
	tctp		
	gale		
C	CG9040	yes	no
	sage		
D	bacc	no	yes
	CG3402		
	rev1		
	med30		

Table 2. Classification of genes selected for analysis into groups according to expression values in S2 cells and in salivary glands.

To verify the expression level of selected genes in S2 cells and 3rd instar larvae salivary glands qRT-PCR was employed. We made use of FlyPrimerBank database (www.flyrnai.org/FlyPrimerBank) for designing primers for qPCR. Actin42a was used as the endogenous control. Fig 35 show the resulting heatmap displaying expression levels of the selected genes. Deviation between two biological replicas can be seen at Suppl. Fig. 8.

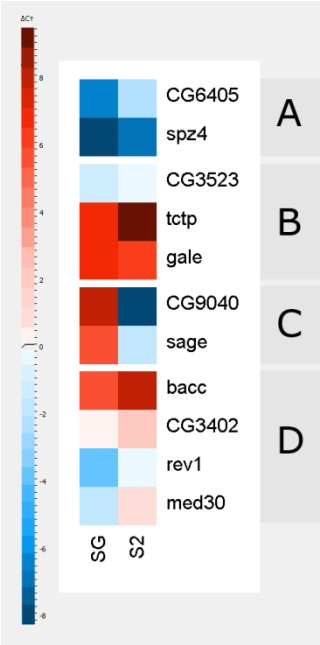

Figure 35. Heatmap of the results of qRT PCR from S2 cells (S2) and 3rd instar larvae salivary glands (SG). The gradient scale on left side indicates the expression level. A),B),C),D) – Classification groups of genes. Actin42a was used as the endogenous control.

As can be seen, all genes in group A show low expression scores in both tissues, except *CG6405*, which is weakly expressed in S2 cells. The expression levels of 2 genes in group B are high in both S2 cells and in glands. *CG3523* gene is expressed moderately. The transcript was present in approximately same amount in both tissues, with slight difference between replicas (see suppl. Fig. 8) . Heatmap profile of the 2 group C genes demonstrates a strong difference between tissues, confirming the expected expression ratios for the two salivary gland specific genes. *bacc* gene from the group D, as well as *CG3402* (to a less extent), shows unexpectedly high expression level. The genes rev1 and *Med30* demonstrated higher expression scores in S2 cells compared to salivary glands.

To determine the level of Chriz binding in certain region, chromatin immunoprecipitation with the following qPCR was performed. For the design of primers for ChIP we used the information about peaks coordinates from available Chriz profile in modENCODE database (Fig 36 A). In cases where no Chriz binding was detected near 5' end of selected genes (*spz4*, *CG9040*, *sage*, *bacc*), primers were positioned within the upstream 500 bp from TSS (see Fig. 36 B) where we expected to detect Chriz binding.

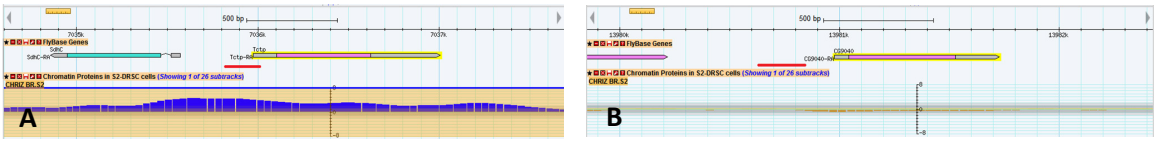

Figure 36. Scheme with examples of probe selection for ChIP based on modENCODE Chriz binding profile in S2 cells. Red bars indicate probe position. A) Example of probe selection for the gene with Chriz enrichment in promoter region. B – Example of probe selection for the gene with the absence of Chriz binding.

It can also be seen, that all genes for which the exact peak position in S2 cells was not detectable (marked on a diagram with stars) show rather low general enrichment.

The relative ChIP to control enrichment can be seen on Fig. 37.

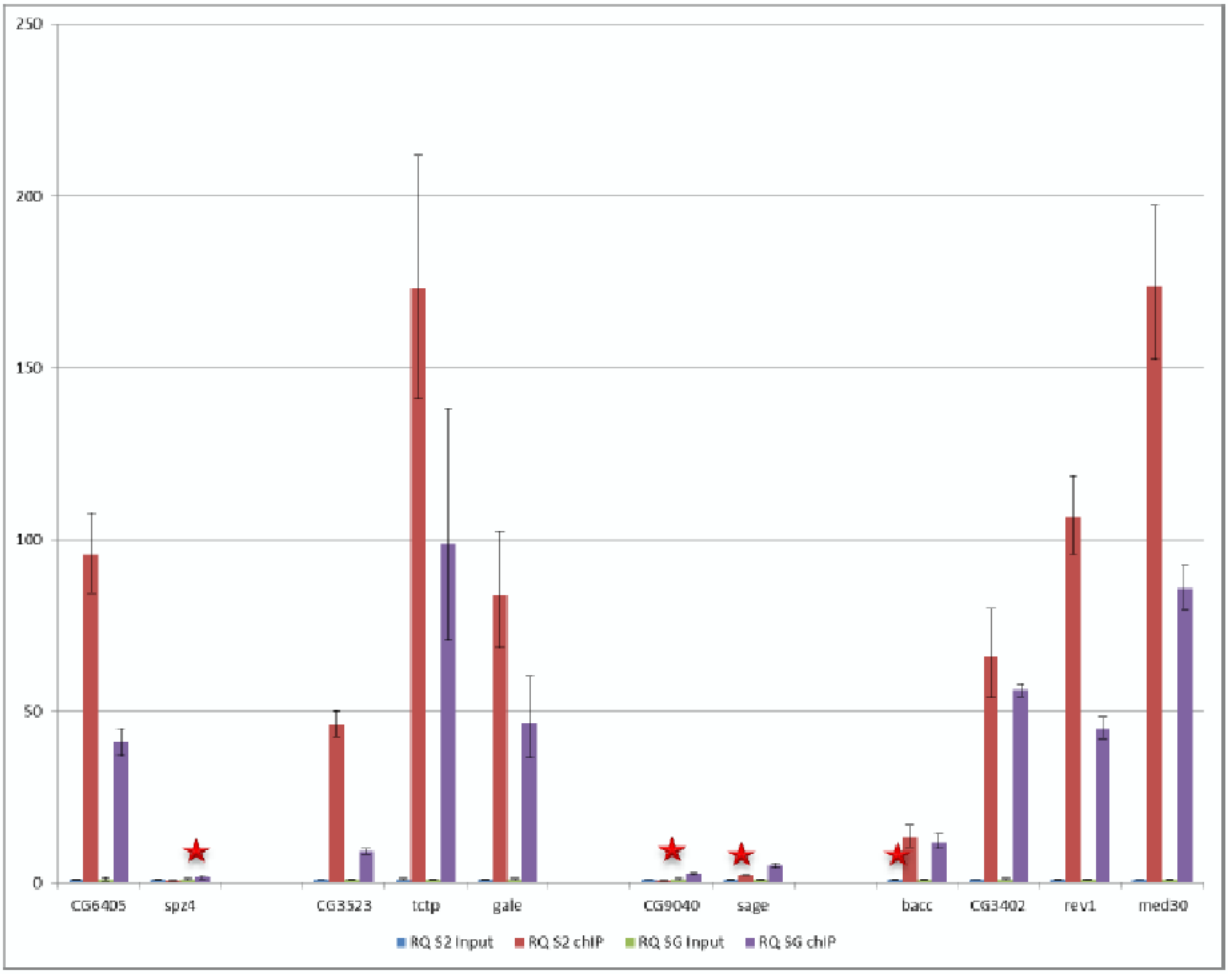

Figure 37. ChIP results for selected set of genes from S2 cells (red) and 3rd instar larvae salivary glands (violet) normalized over mock control. A), B), C), D) Classification groups of genes.

Five genes from groups A, B and D, more expressed in S2 cells (*CG6405, CG3523, tctp, rev1* and *Med30*) show higher Chriz enrichment in their promoter regions. The gene *Spz4* with lowest expression in both tissues was found to contain no Chriz at promoter region. Genes from group C (*CG9040* and *sage*) with higher expression level in salivary glands demonstrated very low Chriz enrichment in general; nevertheless it was found that Chriz is more bound to promoters of these genes in salivary glands. However, relatively different expression levels of *bacc* and *CG3402* from group D goes together with similar Chriz enrichment. The opposite situation was observed in case of *Gale* – 1,5 fold difference in Chriz enrichment between tissues with similar expression scores. For 3 genes from 11 (*bacc*, *CG3402* and *gale*) no obvious correlation between Chriz enrichment and expression level can be detected.

To estimate the level of correlation, we calculated Pearson correlation coefficient between expression change in 11 analyzed genes (SG/S2 ratio) and change in Chriz enrichment (SG/S2

ratio) for these genes (see Materials and Methods for details). Correlation coefficient was identified as 0,79011, which indicates positive relationship between given samples (see Table 3).

Gene	Chriz enrichment sg/s2	Expression level sg/s2
CG6405	0,4288	0,0668
spz4	2,1995	0,4875
CG3523	0,1990	0,6104
tctp	0,5710	0,1803
gale	0,5593	1,8327
bacc	0,9038	0,2273
CG3402	0,8533	0,3662
rev1	0,4231	0,0897
med30	0,4946	0,1576
CG9040	3,7226	82989,623
sage	2,1024	133,7242
	Pearson collelation coefficient	0,79011

Table 3. Calculation of Pearson correlation coefficient between expression change (SG/S2 ratio) and change in Chriz enrichment (SG/S2 ratio).

The correlation of Chriz binding to promoter regions of 11 differentially expressed genes with the expression of these genes in two tissues was investigated. The comparison of qRT-PCR data with levels of Chriz enrichment showed that for 8 genes of 11 stronger relative expression correlated with the higher levels of Chriz enrichment at promoter region. Person correlation coefficient analysis confirmed positive correlation between Chriz enrichment ratio in two tissues and expression ratio (calculated as 0,79011)

3.3 Insulator proteins BEAF-32 and CP190 interact with the Chriz complex

3.3.1 Co-immunoprecipitation

Previous co-immunopurifications performed by our group identified Z4 and Jil-1 kinase as interaction partners of Chriz protein (Eggert et al. 2004; Gortchakov et al. 2005). To gain further insight the composition of Chriz complex, we performed a number of Co-IPs from *Drosophila* Kc cell nuclear extract using α-Chriz, α-Z4, α-BEAF-32 and α-CP190 antibodies. IP with rabbit pre-immune serum was done as a control for unspecific binding. After immunoprecipitation, 8% of elution fraction, 1% and 3% of input from each IP were applied to the SDS gel, blotted to nitrocellulose membrane and probed with antibodies against Chriz, Z4, Jil-1, CP190 and BEAF-32. We were also interested to check the elution fractions for the presence of MBD-R2 protein, a subunit of the NSL complex, which binds at many sites in close proximity to Chriz complex (modENCODE database, http://modencode.oicr.on.ca) to determine a possible interaction between these two protein complexes. Furthermore, IPs

were probed with α-NonA, which is not co-localized with Chriz complex and was used as a control for specificity of IP. The results are shown on Figure 38.

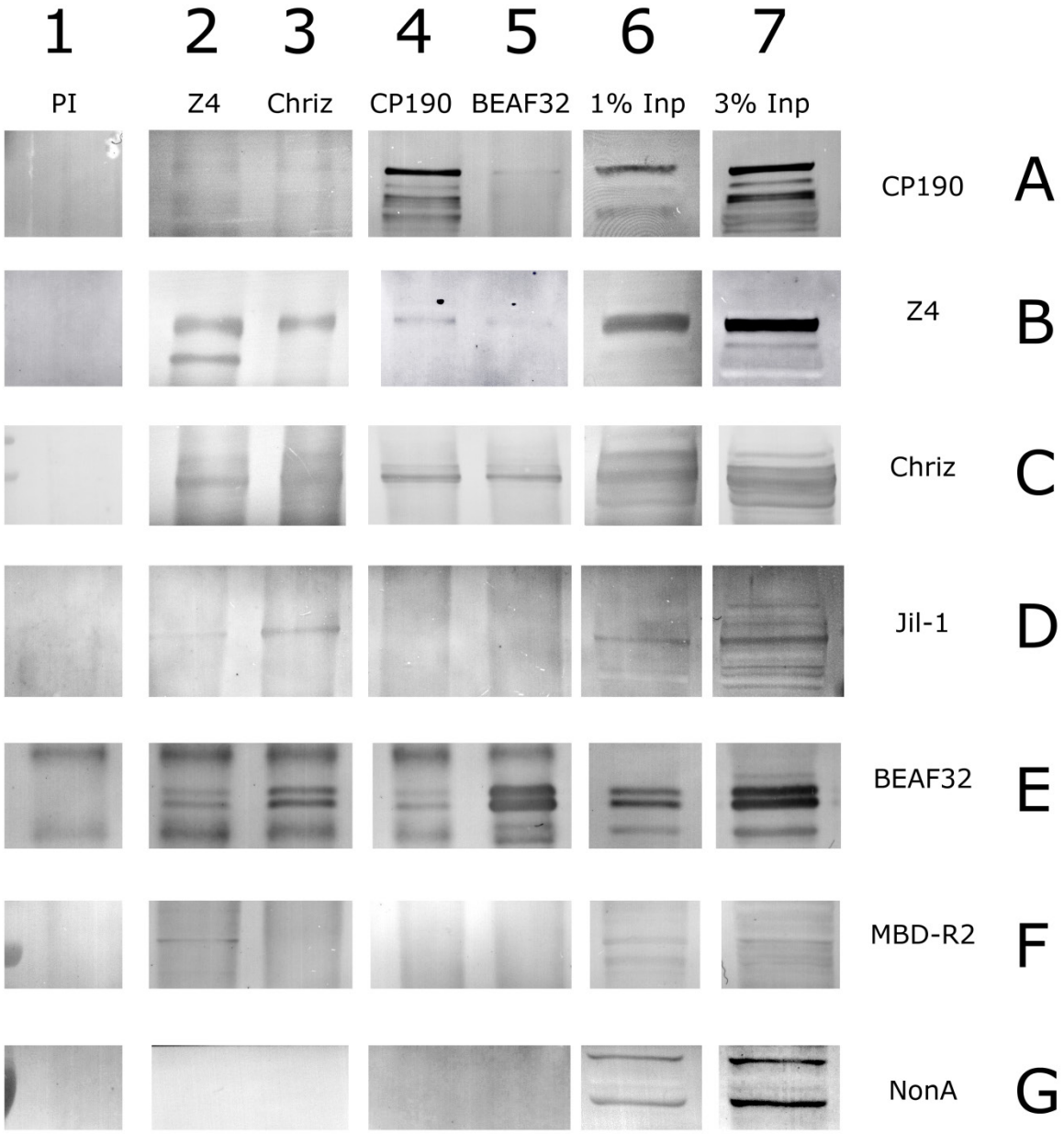

Figure 38. Co-immunoprecipitation of putative Chriz interactors from Kc cell nuclear extract. Lane 1 – coIP with pre-immune serum; Lane 2 – coIP with anti-Z4 rabbit antibody; Lane 3 – coIP with anti-Chriz rabbit antibody; Lane 4 – coIP with anti-CP190 mouse antibody; Lane 5- coIP with anti-BEAF-32 rabbit antibody; Lanes 6 and 7 shows 1% and 3% of input respectively. For every line 9% of elution fraction was loaded. CoIPs were probed with the following antibodies: A) anti-CP190 mouse; B) anti-Z4 mouse; C) anti-Chriz rabbit; D) anti-Jil1 rabbit; E) anti-BEAF-32 rabbit; F) anti-MBD-R2 rabbit; G) anti-NonA mouse.

As expected, zink finger protein Z4 and Jil-1 kinase were coprecipitated with Chriz (see Fig 38, 3B, 3D). Interestingly, insulator protein BEAF-32 (Fig. 38, 3E) showed significant presence in the elution fraction, in contrast to CP190 (Fig. 38, 3A), which was identified in minor amounts only. MBD-R2 as well as NonA were not detected (Fig. 38, 3F, 3G).

Z4 coIP resulted in strong presence of Chriz in elution fraction (Fig. 38, 2C), however Jil-1 and BEAF are found in reduced amounts compared to Chriz. CP190 band is weakly detectable. Surprisingly, MBD-R2 was identified to be coimmunoprecipitated with Z4. The NonA control showed no signal.

Both CP190 and BEAF-32 IPs were found to contain Chriz protein (Fig. 38, 4C, 5C) and Z4, however, Z4 in BEAF-32 IP was presented rather weakly. CP190 and BEAF also coIP each other to some extent (see 4E, 5A). Jil-1, MBD-R2 and NonA signals were absent.

Pre-immune serum IP showed no presence of any tested proteins. The extra bands which can be seen in E1 at a size around 55 and 25 kDa apparently reflects the heavy and light chains of IgG, which were detected by secondary anti-rabbit antibody.

3.3.2 Pulldown assay

In order to test for direct interactions between the proteins of the complex, pulldown experiments of CP190, BEAF, Chriz and Z4 were performed. The practical part of pull-down experiments was executed by M. Rehanek under my direct supervision.

Full-length or truncated ORFs of BEAF-32, Chriz and CP190 proteins were cloned to expression plasmids pRK, pMH or pGEX-6p1, in frame with MBP, Myc or GST tags respectively. BL-21 cells were transformed by the resulting constructs and fusion proteins were expressed (for example see Suppl. 6). GST and MBP epitopes were also expressed independently as controls for unspecific interaction. As a positive control, pull-down between GST-Z4-FL and Myc-Chriz-FL was performed.

GST-tagged or MBP-tagged constructs were bound to glutathione magnet beads or to amylose sepharose respectively (“bait” proteins), washed and incubated with bacterial lysates containing possible interacting protein (“prey” proteins). After washing, the proteins were eluted by SDS sample buffer and analyzed by western blotting using protein-specific or epitope-specific antibodies.

	Myc-Chriz -FL	Myc-Chriz (29-710)	Myc-Chriz (29-291)	Myc-Chriz (600-926)	GST-CP190 -FL	GST-CP190 (1-610)	GST-CP190 (500-1096)	GST-CP190 (800-1096)	GST-CP190 (600-840)	MBP-BEA F-FL	MBP-BEAF (77-283)	MBP-BEAF (1-78; 201-283)	GST	MBP
Myc-Chriz-FL					+	+	-	-	-	+	+	+	-	-
GST-CP190-FL	+	+	-	+						+	+	+		-
MBP-BEAF-FL	+	+	-	+	+	+	-	-	-				-	
GST	-	-	-	-						-	-	-		-
MBP	-	-	-	-	-	-	-	-	-				-	

Table 4. Protein-protein interactions detected by pull-down experiments between full-length- and truncated proteins Chriz, BEAF-32 and CP190. "+" indicates interaction detected, "-" indicates absence of interaction. Boxes shaded: interaction not tested.

A list of constructs tested and interactions detected by pull-down assay is shown on Table 4. As can be seen, direct interactions between Chriz and BEAF-32, between BEAF-32 and CP190 and between Chriz and CP190 were identified.

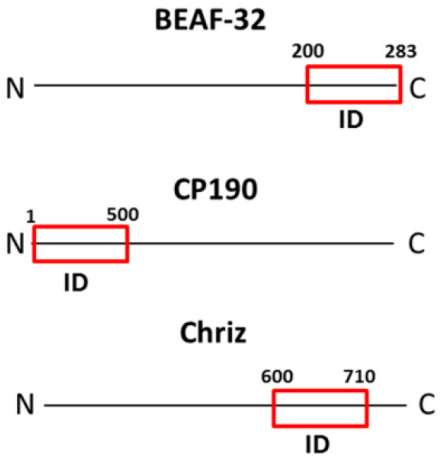

Fig. 39. Schematic position of domains, responsible for interactions between Chriz, CP190 and BEAF-32. Interaction domains are marked with red blocks. The numbers of first and last amino acids in interaction domains are subscribed. Proportions between lengths of listed proteins are not considered.

The table also shows the results of pull-down experiments between full-length and shortened proteins. As summarized in Fig. 39, the same regions (C-terminal part of BEAF-32 (200-283 aa), N-terminal part of CP190 (1-500 aa) and C-terminal part of Chriz (600-710)) are required and sufficient for interaction between Chriz, BEAF-32 and CP190 (Fig. 39).

The composition of Chriz complex was investigated by co-immunoprecipitation and pull-down experiments. The results confirmed the presence of Z4 and Jil-1 kinase in a complex as well as insulator protein BEAF-32, which was reported to interact with Chriz during the run of current project. The combination of interactors identified by coIPs points to possible co-existence of several protein complexes, one of which may include Chriz together with Z4, Jil-

1 kinase and BEAF-32, another – BEAF-32, Chriz and CP190. The significance of MBD-R2, co-immunoprecipitated with Z4 will be discussed. Pull-down experiments confirmed direct interactions between CP190 and BEAF-32, CP190 and Chriz and between Chriz and BEAF-32. It was identified that C-terminal part of BEAF-32 (200-283 aa), N-terminal part of CP190 (1-500 aa) and C-terminal part of Chriz (600-710) are responsible for mutual interaction.

3.4 BEAF-32 contributes to recruitment of Chriz complex

3.4.1 RNAi in S2 cells

Analysis of Chriz, CP190 and BEAF-32 ChIP-chip genome-wide data from modENCODE database showed significant overlap between binding sites of these proteins (Vogelmann et al. 2014). Coimmunoprecipitation and pulldown experiments of Chriz and insulator protein BEAF-32 pointed to an interaction between these two proteins. Since Chriz protein is not known so far to bind DNA directly, we examined the possibility for recruitment of Chriz complex by BEAF-32.

RNAi knockdown of BEAF-32 was performed in S2 cell culture. Cell lysates were analyzed by western blot in 72 h after transfection with BEAF dsRNA. As can be seen on Fig. 40, BEAF amount in RNAi cells is reduced at around 75%, however, downregulation of BEAF-32 protein did not lead to reduction of the total amount of Chriz in S2 cells. Z4 level was not affected as well (Suppl. Fig. 2)

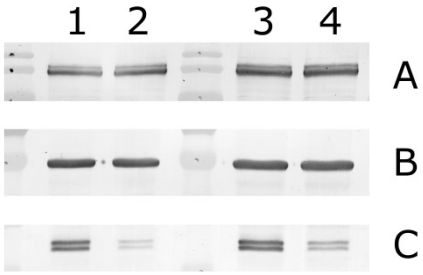

Fig. 40. Western blot from S2 cell lysates following BEAF-32 RNAi. Lanes 1 and 3 - 50% and 100% of OFP control respectively; Lanes 2 and 4 – 50% and 100% of BEAF-32 RNAi respectively. Membrane was probed with the following antibodies: A) anti-Chriz rabbit; B) anti-Tubulin loading control; C) anti-BEAF-32 rabbit.

3.4.2 BEAF-32 binding motif mutation

As could be seen in S2 cells BEAF RNAi, total level of Chriz was not dependent on chromosomally bound BEAF. To better examine the possible dependence of Chriz complex binding on BEAF-32, we compared BEAF and Chriz enrichment at the endogenous locus or at the same locus with a mutated BEAF site cluster. For this experiment we used the transgenic fly strain *42pattP* from (Zielke et al. 2014).

This strain carried an artificial chromosomal domain (*42pattP*) including a *ΦC31* recombination site that was used to integrate and test DNA sequences for ability to form decondensed chromatin. The correct position of insertion was verified by FISH using the pattp61C plasmid DNA as a probe. Fig. 41 shows images with in situ results from *42pattP* and *42patt61C_BEAF1+2* strains. Fig. 41A shows the parental transgenic strain with a condensed *42pattP* domain before recombination. Fig. 41B shows the same strain after instertion of *61C_BEAF1+2* DNA, that is able to form an open chromosomal domain as seen by the split 42attP domain, demonstrating that the *61C_BEAF1+2* DNA was recombined at the correct position.

The part tested previously to be critical for open domain formation (Zielke et al. 2014) is shown in Fig. 42. The ChIP profile shows two prominent peaks of BEAF-32 binding centered over each one pair of BEAF-32 binding sites. A broad double peak of Chriz binding overlaps the two BEAF-32 binding regions. Positions of BEAF binding sites in a sequence are marked at Fig. 42

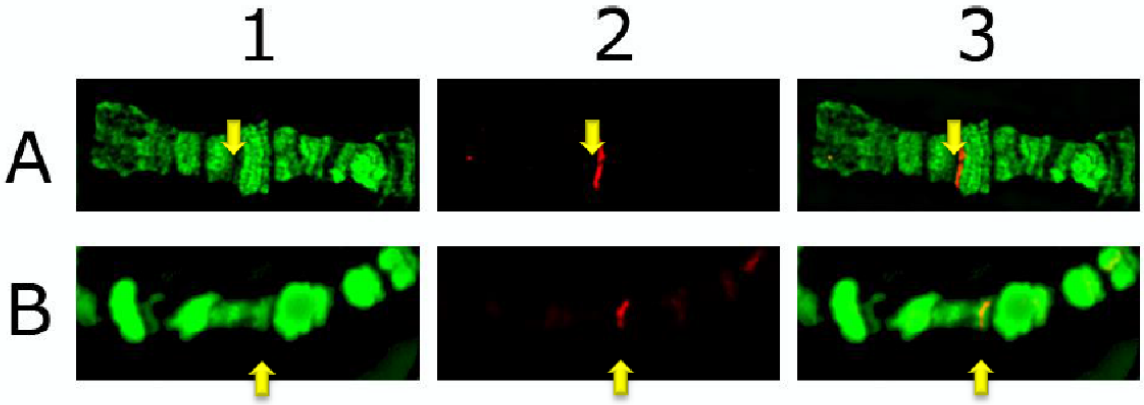

Fig. 41. Fluorescent in situ hybridization of 21f region with *pattP* plasmid. 1 –DAPI staining; 2- in situ signal; 3- merge. Arrows indicate the position of insertion. A) *42pattP* strain*;* B) *42patt61C_BEAF1+2* strain.

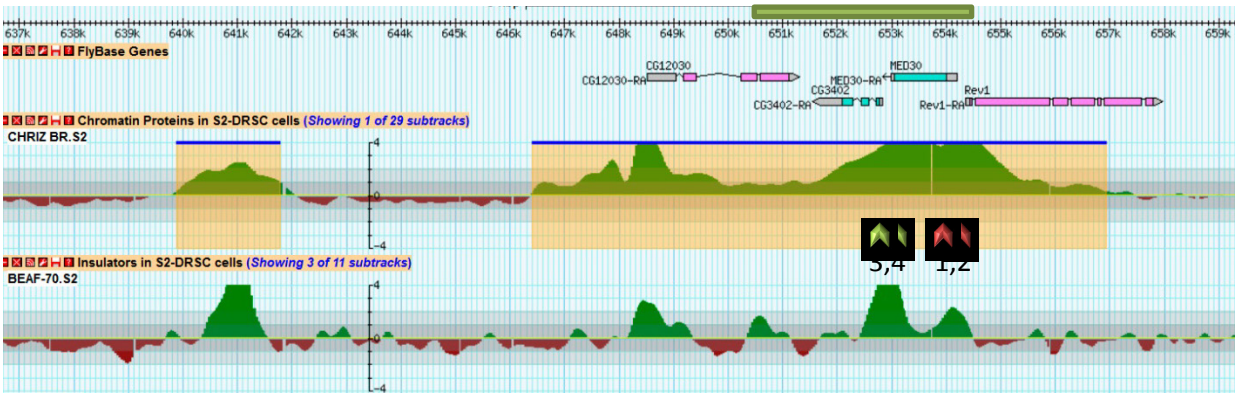

Fig. 42. Schematic position of BEAF-32 binding motifs in 61C7-8 interband relative to Chriz and BEAF-32 binding profiles of S2 cells. Red arrows indicate mutated BEAF-32 binding motifs, green arrows indicate original non-mutated motifs. Upper green bar indicates proximal part tested previously to be critical for open domain formation.

For specific PCR amplification of mutated- or non-mutated BEAF motif, specific primers which overlap each BEAF binding motif at 3' end where designed. The specificity of the primers was checked by PCR using WT genomic DNA or plasmid DNA with mutated BEAF sites as a template (see Fig. 43). As can be seen, original and mutated motifs can be specifically amplified.

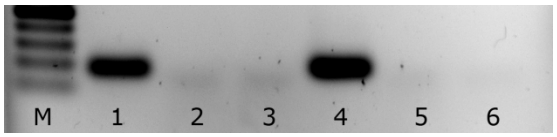

Fig. 43. PCR test for specificity of primers used for ChIP. M- 50bp marker; Lanes 1, 3 and 5 – PCR with primers for original BEAF motif; Lanes 2,4 and 6 – PCR with primers for mutated BEAF motif. For probes 1 and 2 Oregon wildtype genomic DNA was used as a template. For probes 3 and 4 *42patt61C_BEAF1+2* plasmid DNA, containing mutated sites only was used as a template. 5,6 – non-template control.

To identify a possible difference in protein binding to original and mutated BEAF motifs, we performed ChIP with BEAF-32 and Chris antiserum from 3rd instar salivary glands of the *patt61C_BEAF1+2* strain using mutation–specific and original site-specific primers. For the determination of the enrichment the standard curve experimental design was used and percent of ChIP enrichment over input was calculated. As a control ChIP from *Oregon* salivary glands with pre-immune rabbit serum was performed.

Primers for BEAF 3 motif, which was not mutated were used as a control of chromatin prep from transgenic and Oregon strains and were expected to amplify same amount of product relative to input. As can be seen on a Fig. 44, 45, BEAF motif 3 shows similar enrichments in *patt61C_BEAF1+2* to Oregon WT (14% over input of BEAF and 26-31% of Chriz).

Chriz enrichments in both WT and transgenic preps were defined at around 24%, however BEAF enrichment in WT was slightly higher than in *patt61C_BEAF1+2* (7% and 5% respectively).

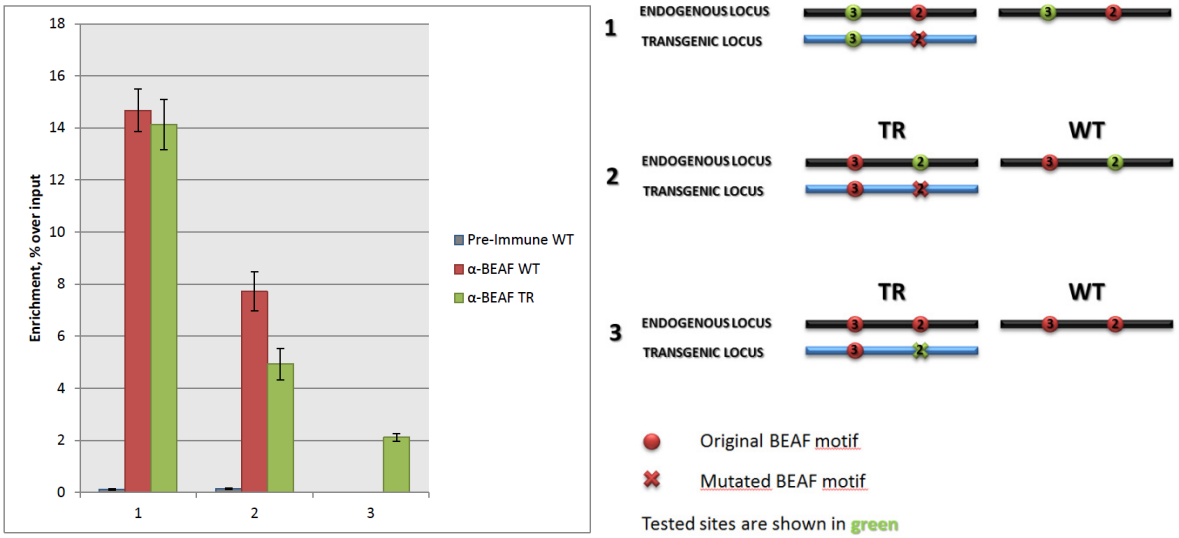

Fig. 44. ChIP results showing BEAF-32 binding to regions with original and mutated BEAF motifs in Oregon wildtyp and in *patt61C_BEAF1+2.* 1 – ChIP-qPCR using primers for original BEAF motif 3; 2 – ChIP-qPCR using primers for original BEAF motif 2; 3 – ChIP-qPCR using primers for mutated BEAF motifs 1-2.

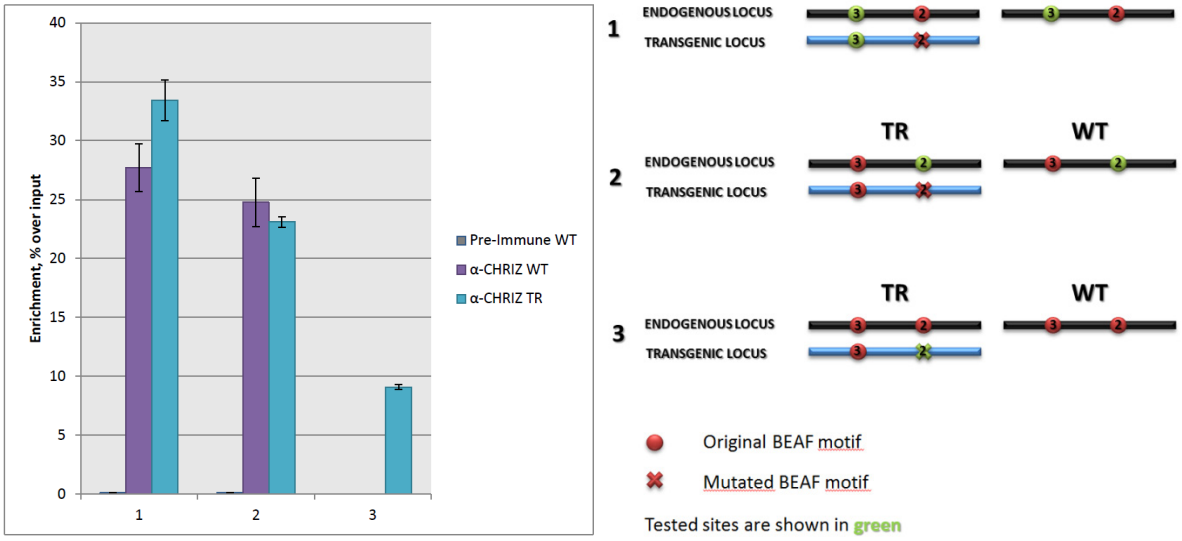

Fig. 45. ChIP results showing Chriz binding to regions with original and mutated BEAF motifs in Oregon wildtyp and in *patt61C_BEAF1+2.* 1 – ChIP-qPCR using primers for original BEAF motif 3; 2 – ChIP-qPCR using primers for original BEAF motif 2; 3 – ChIP-qPCR using primers for mutated BEAF motifs 1-2.

In case of motifs 1,2 mutation the results of chromatin immunoprecipitation from *patt61C_BEAF1+2* showed a reduction of BEAF enrichment from 5% at original motif to 2 %; Chriz binding at the respective sites was reduced from 23% to 9%. This result points to contribution of BEAF protein binding to Chriz complex localization.

3.4.3 RNAi of BEAF-32 and CP190 in salivary glands

To further characterize the contribution of insulator proteins to localization of Chriz complex, RNAi experiments were performed. Using available RNAi strains in combination with G231.1 Gal4 driver, insulator proteins BEAF-32 or CP190 were downregulated specifically in larval salivary glands. For investigating possible synergetic effect from downregulation of both insulators, we combined RNAi strains to obtain simultaneous double knockdown of BEAF-32 and CP190 (see the cross scheme in “Materials and Methods”).

Salivary glands were dissected from third instar larvae and squashed for IIF with αChriz, αZ4, αCP190 and αBEAF antibodies. Since the images of respective antibodies were made with same exposure time, the intensities of fluorescence can be compared. Fig 46 3C, 3A and Fig 47 2B, 2D, shows that in experimental strains amounts of BEAF-32 and/or CP190 were significantly reduced comparing with Oregon WT strain. The knockdown efficiency was also estimated by western blot (See Suppl. 5)

As can be seen on squashes (Fig. 46,47), in BEAF and CP190 RNAi strains, as well as in BEAF/CP190 double knockdown, Chriz and Z4 kept the typical interband-specific pattern; however the staining seemed to be slightly weaker. CP190 binding pattern was also not affected. Single BEAF and CP190 knockdowns did not lead to noticeable change in chromosomal structure, in contrast to double BEAF-32/CP190 knockdown, where band/interband pattern was generally disturbed (Fig 46, D1). Therefore, for analysis of double BEAF-32/CP190 knockdown, upper 5% in quality chromosomes were selected.

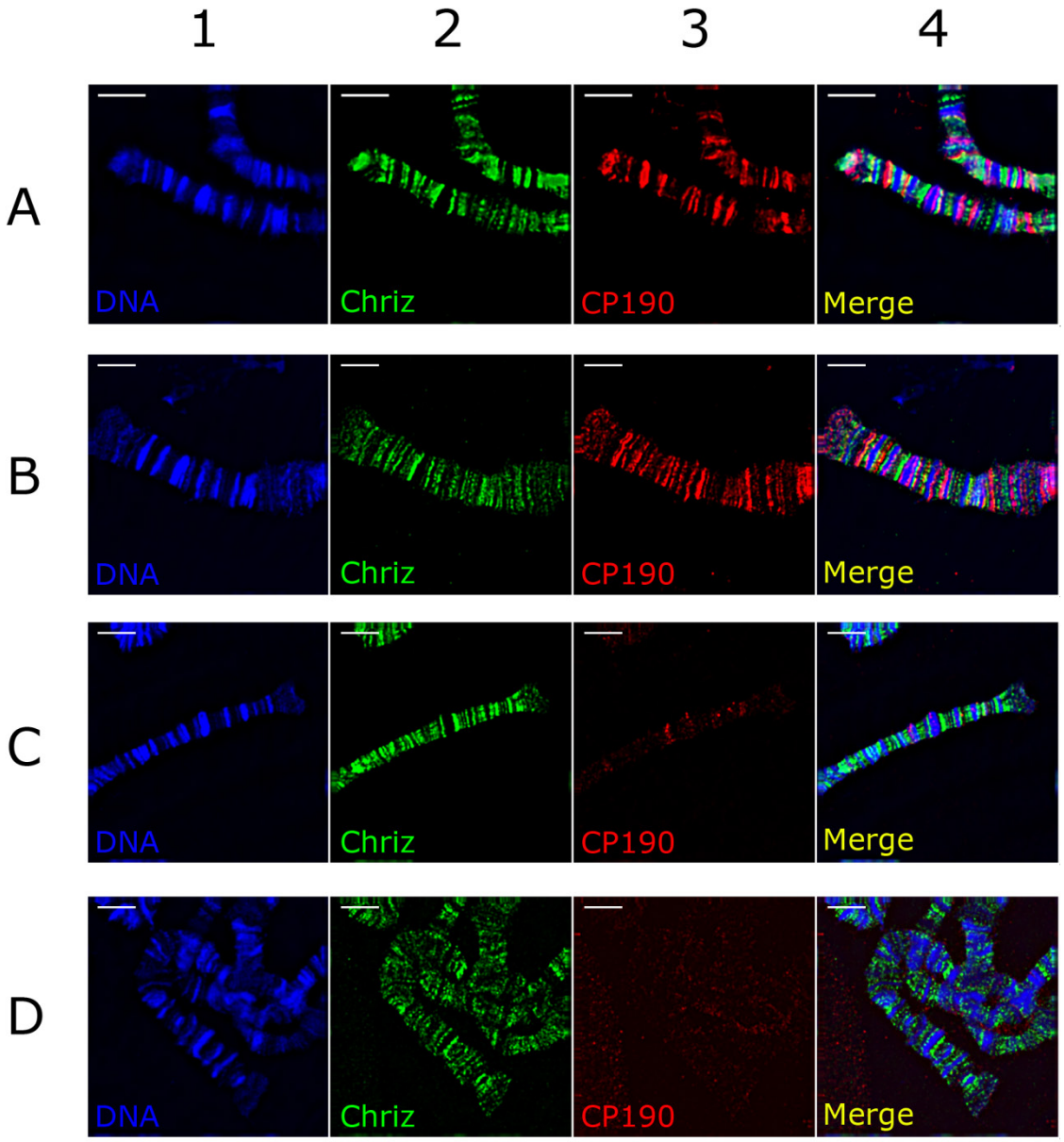

Fig. 46. Chriz and Z4 binding is reduced in BEAF-32 and CP190 RNAi experiments. IIF staining of polytene chromosomes from 3rd instar larvae salivary glands. DNA – blue, Chriz – green, CP190 – red. A) wild type; B) BEAF-32 RNAi; C) CP190 RNAi; D) BEAF-32/CP190 double RNAi. Scale bar 2μm.

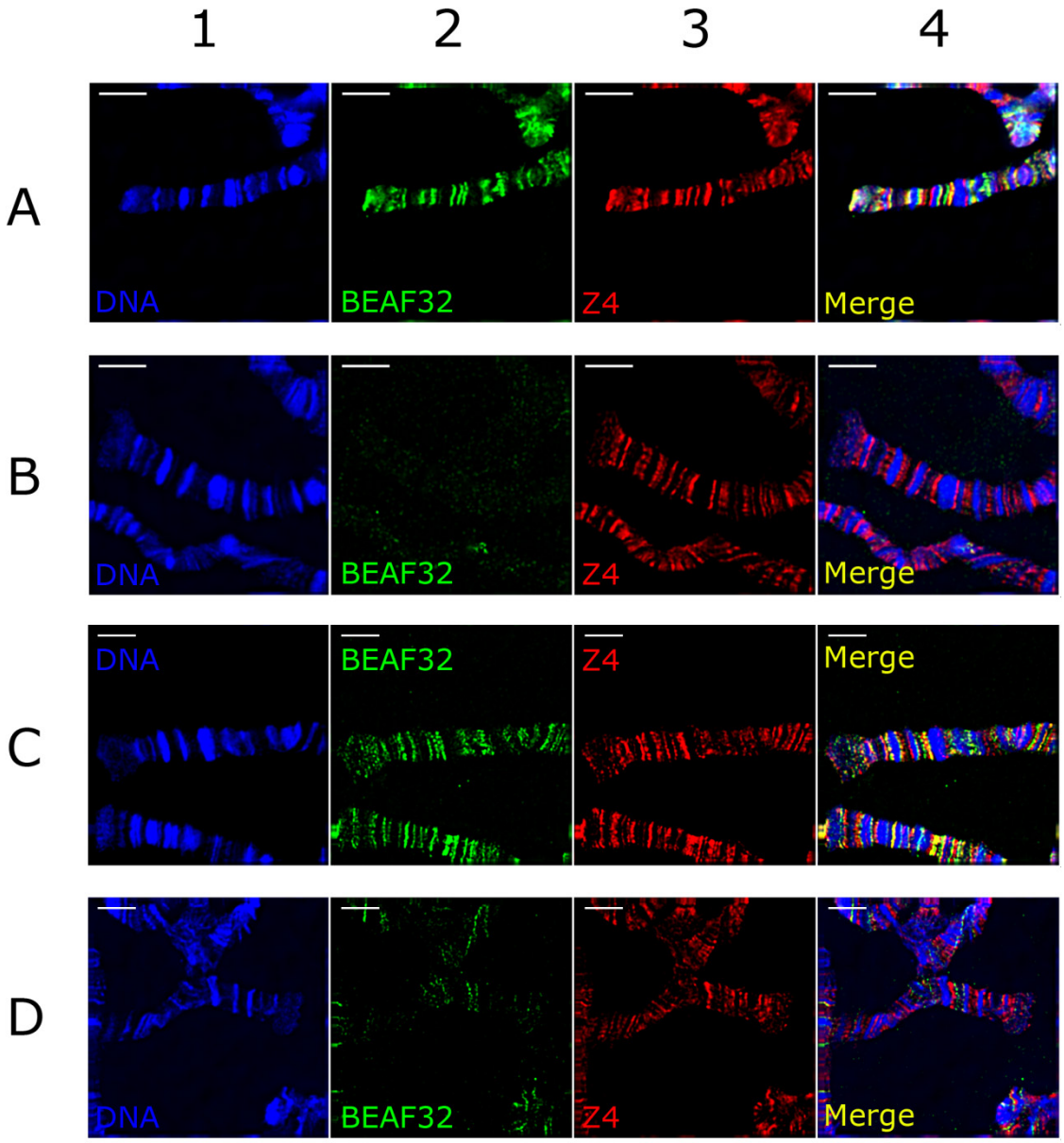

Fig. 47. Chriz and Z4 binding is reduced in BEAF-32 and CP190 RNAi experiments. IIF staining of polytene chromosomes from 3rd instar larvae salivary glands. DNA – blue, BEAF-32 – green, Z4 – red. A) wild type; B) BEAF-32 RNAi; C)CP190 RNAi; D) BEAF-32/CP190 double RNAi. Scale bar 2μm.

Visual examination of the IIF preparations could not give an exact estimation of the amounts of target proteins, therefore we performed analysis of signal intensity profiles to determine and compare the levels of fluorescence in a certain chromosomal region. Total levels of fluorescence in 21E region were measured for each wavelength in three different preps (for details see Materials and Methods). The average meanings of signal intensity levels are shown on Fig. 48. As can be seen, in Oregon wild type and in both single knockdowns of

insulator proteins DAPI levels are similar in contrast to simultaneous BEAF-32 and CP190 knockown, where the DAPI staining intensity is reduced to 30%. This may be caused by disturbance of cytological structure of polytene chromosomes in this experimental condition.

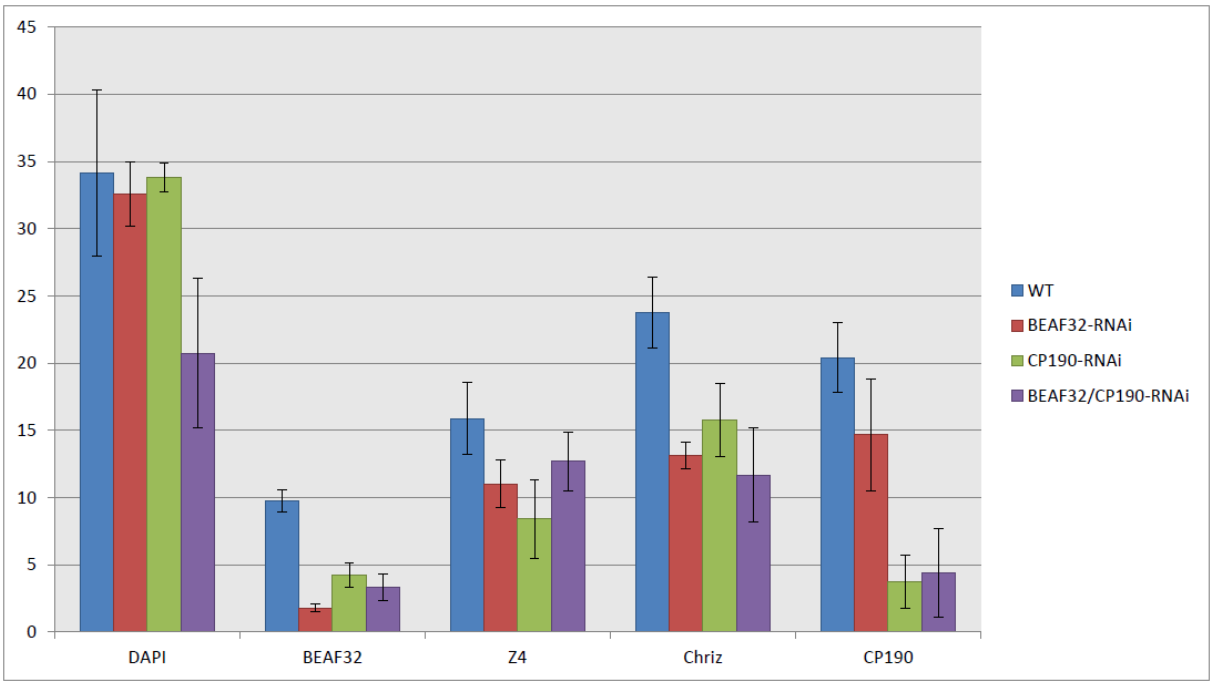

	DAPI	BEAF-32	Z4	Chriz	CP190
WT	34,15645	9,72211	15,88721	23,79341	20,39362
BEAF-32-RNAi	32,56462	1,789423	11,03715	13,12659	14,66947
CP190-RNAi	33,81828	4,228605	8,416595	15,77843	3,765334
BEAF-32/CP190-RNAi	20,74081	3,349545	12,69394	11,67971	4,389682

Fig. 48. Image analysis results from BEAF-32 and CP190 RNAi experiments. Average meanings of signal intensity levels are listed in the table.

In agreement with visual IIF inspection, BEAF-32 level was found to be strongly reduced in BEAF knockdown and, to less extent, in BEAF/CP190 combination. Unexpectedly, CP190 single knockdown also led to more than 50% decrease of BEAF binding in 21E region. Both Chriz and Z4 levels were reduced in all tested knockdown combination, however Chriz downregulation was more prominent in each of experiments. Observed reduction of CP190 signal in single CP190 knockdown as well as in double BEAF-32/CP190 combination was confirmed by quantitative measurements. Interestingly, BEAF-32 knockdown as well led to reduction of CP190 level in analyzed region. We should note that the intensity values for BEAF/CP190 double knockdown may serve only as a conservative estimate since to identify cytology the most structurally conserved chromosomes had to be used.

In summary, the results of BEAF-32 and CP190 RNAi experiments confirmed the statement that Chriz complex localization is partially dependent on BEAF-32 and CP190 binding. Simultaneous BEAF-32 and CP190 knockdown leaded to disturbing of chromatin structure. In 21E locus BEAF-32 and CP190 demonstrated interdependence in their binding to chromatin.

3.5 Role of Chriz in open chromatin domain formation.

The analysis of publicly available genome-wide datasets of chromatin proteins binding shows a tendency of such Chriz associated components as BEAF-32, Chriz, CP190 to bind preferentially to promoters of active genes and to so called transition sites with sudden changes in enrichment of histone modification as, for example, H3K27me3, H3K4me or H3K9ac (Van Bortle et al. 2012). Assuming the high level of similarity in chromatin domain organization between different cell types (Demakov et al. 2011), we asked whether the binding pattern of Chriz would also be conserved.
Since a lot of interesting research work that attempted to compare the cytological structure of polytene chromosomes with a molecular biology data obtained from different cell types has been published in previous years (Zhimulev et al. 2014), we decided to compare the similarity of binding profiles of Chriz complex components between 3rd instar larvae salivary glands and S2 cells within a defined chromosomal interval. Well studied 61C7-8 interband appeared to be a suitable cytogenetic locus for such comparative analysis.

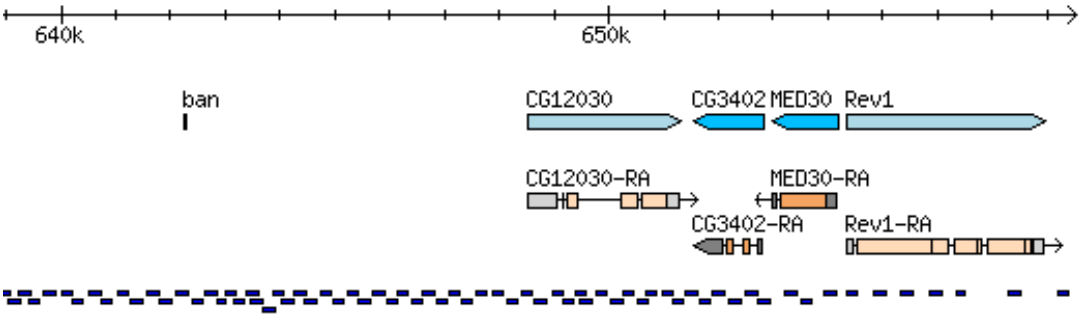

Fig. 49. The location of probes for ChIP in 61C7-8 chromatin region. A) genes located in the region of interest; B) location of probes for ChIP.

For high resolution protein binding analysis by ChIP/qPCR we designed a number of primers, covering 25 kbp of 61C7-8 open chromatin domain (Zielke et al. 2015, in press) (see Fig. 49). To estimate the reliability of our ChIP method, we performed a comparison of ChIP-chip profile of Chriz binding in S2 cells from modENCODE database with our data from the same cell type. In our result the pattern of Chriz enrichment listed in modENCODE was fully reproduced (Fig. 50 B, C). In S2 cells ChIP revealed that Chriz is bound in three broad regions in the 61C7-8 interband: distally a smaller peak between 640-642 kbp followed by a prominent binding region between 647-650 kbp and a double-peak region at 652-655 kbp.
Interestingly, ChIP performed on salivary gland cell chromatin revealed that the distal Chriz peak at 640-642 kbp is not formed in this cell type (Fig. 50 D).

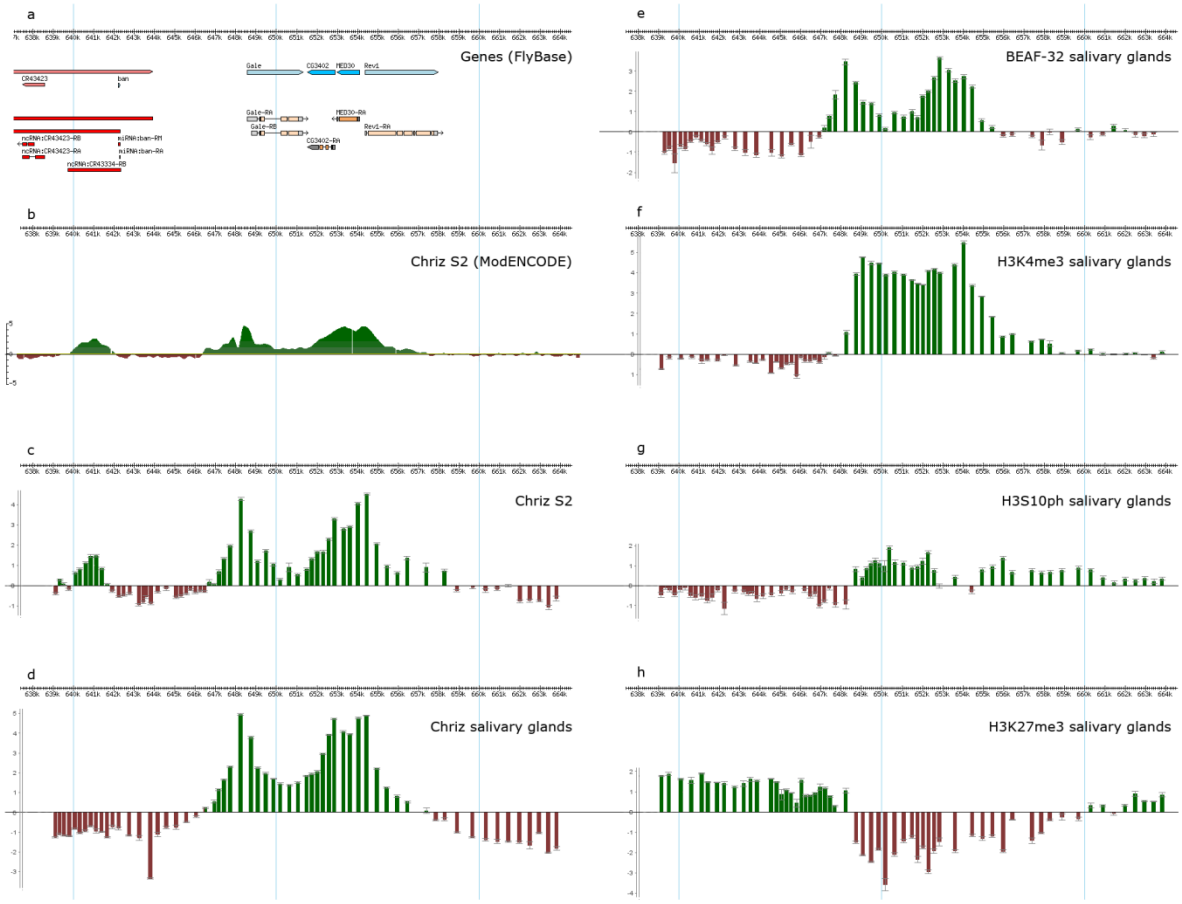

Figure 50. Comparison of the Chromatin state of the 61C7-8 open domain in diploid and polytene cells: ChIP/qPCR was performed on S2 cell and salivary gland chromatin and data for the 61C7-8 open chromatin domain were plotted against genomic coordinates of distal 3L; S) location of genes in the region of interest; B) ChIP profile for Chriz (flybase/modENCODE (http://modencode.oicr.on.ca/fgb2/gbrowse/fly) binding in S2 cells; C) ChIP profile for Chriz binding in S2 cells (own data); D) ChIP profile for Chriz binding in salivary gland cells; E) ChIP profile for BEAF-32 binding in salivary gland cells; F) ChIP profile forH3K4me3 histone modification in salivary gland cells; G) ChIP profile for H3S10ph histone modification in salivary gland cells; H) ChIP profile for H3K27me3 histone modification in salivary gland cells. Values plotted above zero line in green and below zero line in red indicate enrichment depletion of histone modification/protein binding respectively as log SD.

In S2 cells BEAF-32 showed four binding peaks in the 61C7-8 in open domain: at 640-642 kbp, 647-649 kbp and 652-654 kbp partially overlapping a peak at 655 kbp. We questioned whether BEAF-32 would show similar difference in binding at the distal locus of 61C7-8 interband. Similarly to Chriz binding, the distal BEAF peak at 640-642 kbp was not detectable in ChIPs from salivary gland cell chromatin (Fig. 50 E). In the remaining part of the 61C7-8 domain the binding of BEAF-32 and Chriz in salivary glands was found to be indistinguishable from the binding in S2 cells.

To figure out whether the 61C7-8 domain differs in pattern of chromatin modifications between two given cell types, we analyzed the binding profiles of H3K27me3, H3S10ph and H3K4me3 within the domain.

Similarly to Chriz complex components, the pattern chromatin modifications present on S2 cell chromatin differed in the distal region from those detected on salivary gland cell chromatin. In S2 cells H3K27me3 was depleted in the whole 61C7-8 open domain (639-659 kbp). In contrast, in salivary gland cell chromatin H3K27me3 modification spreaded into the distal part of the domain up to position 648 kbp, restricting the H3K27me3 depleted zone to 649-659 kbp (Fig. 50 F). On the opposite, H3K4me3, a mark for transcriptionally active open chromatin that was found in the S2 cells between the coordinates 639-656 was restricted in salivary gland cells to the proximal part of the domain, between 648-656 kbp (Fig. 50 G). H3S10ph in salivary glands it was detected between the coordinates 648-660 kbp. This corresponds well to the distribution of the Jil-1 kinase in salivary gland chromatin, which is the enzyme responsible for this modification in interphase. Unfortunately, there are no data on H3S10ph distribution in S2 interphase cells. However, Jil-1 kinase showed a binding region between the coordinates 639-642 in these cells (see Cai et al. 2014).

A consequence for the observed difference in the chromatin structure between S2 cells and salivary gland cells in distal part of 61C7-8 may be a different transcriptional state in the genes located in this part of the domain. According to ModENCODE database (http://modencode.oicr.on.ca/fgb2/gbrowse/fly), CR43334-RA and CR43334-RB non-coding transcripts were located in distal part of the interband, therefore we compared the transcription within their intervals by RT-qPCR of total RNA isolated from S2 cells and salivary glands (Fig. 51). The coding genes in the proximal region were transcribed in both tissues to similar rates except *CG12030/Gale* that was ~2-fold higher expressed in salivary glands (FlyAtlas database). Interestingly, qRT-PCR with primer pairs specific for the CR43334-RB transcript in the distal part of 61C7-8 showed, that this transcript was robustly expressed in S2 cells but not in salivary glands (Fig. 51). CR43334-RA non-coding transcript was found to be expressed as well, but to less extent. (Fig. 51)

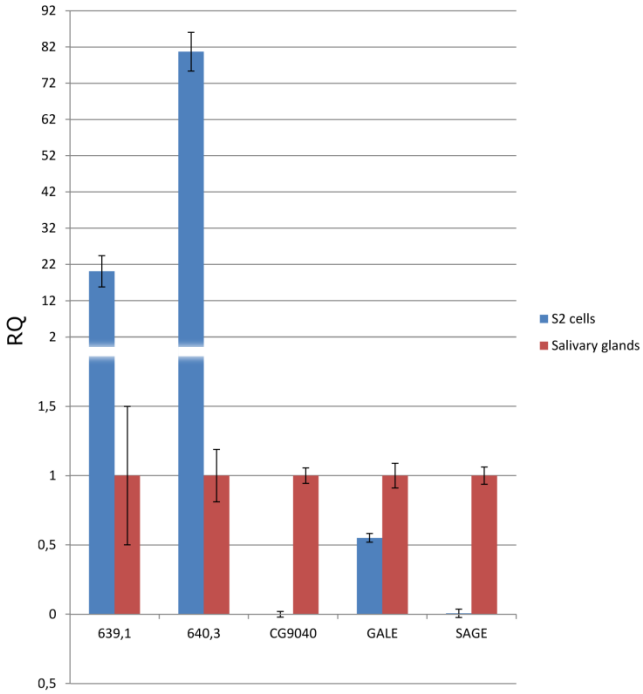

Fig. 51. Transcription of genes in the 61C7-8 domain in S2 cells and salivary gland cells: Total RNA isolated from salivary glands or S2 cells was investigated by qRT-PCR using seven primer pairs covering the noncoding transcript CR43334-RB between 640.1 -641.7. The expression values obtained were normalized relative to actin42a (1.0) and plotted on the abscissa for each primer pair side by side for expression in S2 cells (blue) and salivary glands (red).

In summary, comparative analysis of Chriz complex binding and epigenetic modifications in 61C7-8 locus between salivary gland chromatin and S2 cell chromatin was performed. It was found that Chriz pattern within the domain differs in distal part and is conserved in proximal. Similar observations were made for BEAF-32 and selected histone modifications – H3K4me3, H3S10ph and H3K27me3. Expression levels of transcript located in distal part of 61C7-8 domain were found to differ in analyzed tissues.

4. Discussion

4.1 Chriz complex contributes to chromatin structure and histone modifications

Gan and colleagues showed that Z4 and Jil-1 are dependent on Chriz for specific chromatin binding (Gan et al. 2011). We asked whether the function of Chriz complex is conserved between cell types and performed double-stranded RNA-induced gene silencing (RNAi) in *Drosophila* S2 cells. We found that, in agreement with previous data, knockdown of Chriz results in strong (80%) downregulation of Z4 and Jil-1 protein level. However, the expression of these genes was found to be not affected. This points to the fact that the observed downregulation takes place at the protein level due to increased instability of Z4 and Jil-1 dissociated from chromatin. Z4 RNAi-mediated knockdown in contrast does not affect Chriz and Jil-1 protein and transcript levels. Further, by IIF we showed that the H3S10 phosphorylation level is dramatically decreased in S2 cells after Chriz knockdown. This for a long time was obscure in biochemical approach of diploid cells for the dominant activity of the Aurora H3S10 kinase during mitosis. This data confirms the observations, done in salivary gland tissue of 3rd instar larvae (Gan et al. 2011) and points to general role of Chriz in the complex and to common mechanism of maintaining interphase chromatin structure in diploid and polytene cells.

Analysis of mutant combination and RNAi knockdown experiments, performed in salivary glands of 3rd instar larvae demonstrated essential role of Chriz protein for maintenance of chromatin structure (Rathet al. 2006; Gortchakov et al. 2005). Using S2 cells as a model, we observed general repressive effect of Chriz and Z4 RNAi knockdowns. However, due to high stability of the Chriz protein, the RNAi knockdown required at least 72 hours to obtain 70-80% of protein reduction. Therefore, the change in expression of analyzed genes which we detected could also be influenced by a number of secondary events. To monitor the primary effect of Chriz depletion on expression of bound genes, we initially attempted to use the novel promising method of protein knockout via ubiquitin degradation pathway – deGradFP (Caussinus et al. 2011; Caussinus et al. 2013). This method is based on the inducible expression of NSlmb-vhhGFP4, a fusion of F-box protein which determines the substrate specificity for poly-ubiquitinilation with a single-domain antibody fragment VhhGFP4, which binds to GFP protein and its close derivatives (Venus, YFP and EYFP). Thus, upon NSlmb-vhhGFP4 expression, GFP fusion proteins are recognized, bound and poly-ubiquitililated for further degradation by proteasome machinery. If the only source of target protein is fused with GFP, the loss-of-function effect will be obtained. The advantage of using deGradFP system is in short time of protein degradation – up to two hours (Caussinus et al. 2011). To our knowledge, this system was not yet explored for the knockdown of chromatin proteins.

In order to obtain tissue-specific expression, the NSlmb-vhhGFP4 strain had to be combined with suitable Gal4 driver. Due to high complexity of crossing scheme, we were limited in choice of a driver, which had to be located on X chromosome. Unfortunately, no strains containing inducible drivers on X chromosome were available in Bloomington fly stock

center for that time, therefore, to observe the effect of a protein knockout on gene expression as well on chromosomal structure, we chose salivary-gland specific G61 Gal4 driver. Taking into consideration that this driver starts to induce expression during embryonic stage, which is too early for the purpose of primary effect analysis, we attempted to delay the expression of NSlmb-vhhGFP4 by keeping the strain at reduced temperature until second instar larvae had developed. Then, the Gal4 expression could be induced by simply rising up the temperature from 18˚C to 25˚C(McGuire et al. 2004). Unfortunately, this approach was not efficient – we could not observe reasonable protein degradation within 6 h after increasing the temperature. This may be caused by several factors. First, low accessibility of Chriz-GFP in the protein complex might make the binding of NSlmb-vhhGFP4 difficult. In contrast to cycling cells, where Chriz is relieved from the chromatin during mitosis and re-localized to mitotic spindle, in salivary gland cells, which are non-cycling, Chriz remains bound to chromatin during whole time of knockout induction. Second, since NSlmb-vhhGFP4 is delivered to the nucleus by free diffusion (the fusion protein is smaller than 55 kDa and can freely penetrate the nuclear pores), its concentration in the nucleus is too low to initiate the degradation of all Chriz-GFP within short time. This problem can be overcome by adding NLS sequence to NSlmb-vhhGFP4 that it can be targeted to the nucleus.

Chriz-GFP combined with the homozygous lethal ΔKG12 Chriz deletion showed ubiquitous expression, correct localization to the nucleus, expected interband pattern on polytene chromosomes and a capacity to recruit zinc-finger protein Z4, which is known component of Chriz complex and requires it for binding to chromatin (Gan et al. 2011). In western analysis the expression of Chriz-GFP protein in rescue strain was somewhat less than endogenous Chriz in the wild type, possibly due to position effect of transgenic insertion. However, the strain did not demonstrate any phenotype in development or in chromatin structure.

After the final deGradFP fly cross, non-Tb larvae, which don't contain endogenous Chriz, were analyzed (see cross scheme in Materials and Methods for details). The experimental strain showed a delay in development and lower mobility comparing to parental strains. These effects, together with small size of salivary glands in Chriz protein knockout experiments are similar to those that were described before by Kugler and colleagues for the Z4 mutant phenotype (Kugler et al. 2007).

The total BEAF-32 binding was not affected in ChrizGFP protein knockout, confirming the Chriz-independent direct binding of BEAF-32 to chromatin. However, due to severe corruption of chromosome structure, it was not possible to measure by quantitative image analysis the amounts of BEAF-32 bound and, therefore, to exclude the contribution of Chriz to BEAF-32 localization to chromatin.

4.1 Role of Chriz complex in gene expression

Chriz complex is known to bind open chromatin in salivary gland polytene chromosomes (Gortchakov et al. 2005) and available genome-wide data points to close proximity of Chriz binding peaks to many active promoters. Therefore, in RNAi experiments we more expected to see repressive effect on gene activity. It was indeed the case for a majority of genes in Z4 and Chriz knockdown, which lead to a decrease in expression of 70% (Z4 RNAi) and 52% (Chriz RNAi) of analyzed genes.

We should note that the fact of a general decrease in expression lead to difficulties in the selection of reference gene. Initially, we tested several recommended (Ponton et al. 2011) housekeeping genes to choose a reliable control for our experiments. All recommended genes contained a Chriz binding peak at their promoters. Therefore, there was a risk of choosing a control which is affected by Chriz RNAi. To select a suitable control gene, we compared the expression levels of reference genes in Chriz- and Z4- RNAi using RNA from same cell number. Unfortunately, all of the control genes showed a decrease in expression during Chriz or Z4 RNAi (data not shown). EF1 gene which was finally selected as endogenous control demonstrated the least difference between experimental and control conditions. Nevertheless, the shift of amplification curve in Chriz RNAi is still noticeable, it is around one cycle (Suppl. 4). This fact might explain the discrepancy in estimation of knockdown efficiency of Chriz RNAi between western blot (80-85% dowregulation) and qRT-PCR (55% downregulation). Thus, the repressive effect of Chriz knockdown on expression of selected group of genes might be much stronger than it was defined by qRT-PCR. Probably, for further experiments, different way of qRT-PCR data normalization (for example, by cell number or DNA concentration) would give more real estimate of expression levels.

The role of Z4 in regulation of several groups of genes was already investigated by Kugler and colleagues (Kugler et al. 2011). The analyzed Z4 deletion mutants evolved melanotic tumors and showed up-regulation of several immune response genes. The authors suggested that Z4 is an essential co-factor of NURF. We still do not know the Z4 function unless that it is not involved in Jil-1 binding. However, Z4 could recruit other histone modifiers, like HATs that would give the way for NURF binding. Juxtaposing this observation with our findings that Z4 requires Chriz to bind chromatin, we can assume a basic role of Chriz protein as a platform for recruitment factors required for open chromatin formation.

We did not observe any significant tendency of certain ontological group of genes to be more affected by the knockdown comparable to others (GeneOntology database used, http://geneontology.org/). This observation points to general role of Chriz and Z4 in regulation of expression of the screened genes, probably by keeping chromatin at their promoter regions in decondensed state. This feature can be accomplished by a complex of nucleosome-remodeling factors, which are known to be recruited to the chromatin by Z4 protein (Kugler et al. 2011). Therefore, the effect of Chriz RNAi on the expression change might consist of two element. The simultaneous Z4 knockdown would affect the NURF-

binding and the loss of Jil-1, which requires Chriz to bind chromatin, would result in decreased H3S10 phosphorylation that is required for open chromatin formation (Deng et al. 2009). Such global repression of the activity of a wide group of genes in a long run will result in secondary effects in the knockdown cells. It may be that the observed up-regulation in 15% of analyzed genes is possibly reasoned by secondary events. However, we cannot exclude the contribution of so far unknown components recruited by Chriz which can be responsible for observed effect.

As can be seen on ChIP-chip genome-wide datasets, Chriz binding peaks are preferentially present at genes in gene rich regions, with a strong overlap with epigenetics marks, typical for open chromatin, as H3K4me3 or H3K9Ac. Jil-1 kinase which phosphorylates histone H3 at serine 10 is recruited by Chriz to chromatin (Gan et al. 2011), therefore suggesting role of Chriz in regulation of expression. Our results sa well as observations of Vogelmann and coworkers demonstarted that Chriz forms a complex and directly interacts with insulator proteins BEAF-32 and CP190 (Vogelmann et al. 2014), which are enriched at chromatin domain boundaries and at promoter regions of active genes (Emberly et al. 2008). Earlier, the research of Jiang revealed the change of expression in a number of genes following BEAF-32 and CP190 knockdowns (Jiang et al. 2009).

We already demonstrated a role of the Chriz complex in gene expression. To strengthen our argument for a distinct role of the Chriz complex in gene activity we performed the comparison of Chriz enrichment in promoter regions and transcriptional activity for the same group of genes in two different tissues. For 8 of 11 selected genes the analysis revealed that stronger relative expression of the gene was correlated with the higher levels of Chriz enrichment at promoter region. Person correlation coefficient analysis confirmed positive correlation between Chriz enrichment ratio and expression ratio in two tissues.

However, for analyzed genes the single ChIP probe did not give information about total amount of Chriz bound to promoter region Therefore, general high levels of expression were not always coincidence with high Chriz enrichment. This can be seen on the example of genes from the group D, which contains *CG90490* and sage, highly expressed in 3rd instar salivary-glands. According to ChIP-chip ModENCODE dataset, Chriz was not present at their promoters in S2 cells, same results were obtained by our ChIP-qPCR analysis. In salivary glands enrichment was found to be higher relative to S2 cells, but nevertheless, far from the enrichment level of the genes expressed in similar amounts (*gale*, *tcpt*). These factors refer to difficulties in selection of the probe position for indicated genes and to general limitation of the method used. Current experiment represents pilot approach in identifying possible correlation between the amounts of Chriz protein bound to promoter of a gene with its expression level. We see identified correlation as a promising start for expanding the analysis to genome-wide format using microarray techniques.

4.3 Insulator proteins BEAF-32 and CP190 interact with the Chriz complex

Chromodomain protein Chriz is ubiquitous, essential and is required for maintaining the structure of polytene chromosomes (Gortchakov et al., 2005). It directly interacts with a number of proteins, forming a complex, which is localized in open chromatin domains which correspond to interband regions of polytene chromosomes. Earlier interaction studies of Chriz complex were concentrated either on Z4/Jil-1 as complex components (Gortchakov et al. 2005; Rath, 2006) or on associated insulator proteins (Vogelmann et al. 2014). In order to identify and summarize the interactions between known components of Chriz complex – Z4, Jil-1, BEAF-32, Chriz and CP190, we performed a number of co-immunoprecipitation experiments.

Zinc-finger protein Z4 and Chriz were shown to co-localize and directly interact by their N-terminal and central domains respectively. The N-terminal domain of Z4 is required for Chriz-mediated targeting to interbands (Gan et al. 2011). Direct interaction with Chriz in vitro was demonstrated also for H3S10-specific kinase Jil-1 (Rath et al. 2006). Chriz was shown to recruit Jil-1 to chromatin and therefore, to be essential for H3S10 phosphorylation during interphase (Gan et al. 2011). In agreement to these findings, both the zinc-finger protein Z4 and the H3S10 kinase Jil-1 were co-immunoprecipitated with Chriz, while in the elute fraction of Z4 co-IP we identified Chriz and Jil-1. Pull-down experiments performed earlier in our group did not detect any direct interaction between Z4 and Jil-1 (data not shown), pointing to the fact that their co-precipitation as a complex is mediated by Chriz protein.

Significant co-localization between Z4 and insulator protein BEAF-32, identified by Gan and coworkers as well as co-IP results obtained by them, pointed to interaction between BEAF-32 and the Chriz complex, which was recently confirmed in the work of Vogelmann and colleagues (Vogelmann et al. 2014). Consistently with their observations, BEAF-32 was identified in relatively high amounts in our elute fraction of co-IP performed with Chriz antisera (BEAF-32 signal from 9% of elute fraction is comparable with 1% of input), pointing to their interaction in the majority of co-localization sites seen in ChIP of S2 cells and in immunostaining on polytene chromosomes. BEAF-32 was also found to be present in Z4 and CP190 elute fractions, however in fewer amounts.

Genome-wide analysis of CP190 binding revealed over 5 thousand sites (ModENCODE database, http://modencode.oicr.on.ca), some which were later found to be overlapped by a number of insulator proteins, such as Su(Hw), dCTCF, GAGA factor. It was shown that these factors are responsible for CP190 recruitment at co-localized sites (Schwartz et al. 2012). Recently, additional DNA-binding proteins Pita, ZIPIC, IBF1 and IBF2 which target CP190 to the sites, previously considered independent, were discovered (Maksimenko et al. 2015; Cuartero et al. 2014). It was shown that Chriz interacts directly with CP190 and shares around 3000 binding sites (Vogelmann, 2014). Interestingly, >80% of Chriz/CP190 overlapped sites are also bound by BEAF-32. In our co-IP experiments CP190 was found to be precipitated by BEAF-32 and, to less extent, by Chriz and Z4. Consistently with this finding,

BEAF-32, Chriz and Z4 were identified in elute fraction of co-IP, performed with anti-CP190 antibody. Interestingly, Jil-1 was not co-precipitated neither by CP190 nor by BEAF-32, pointing to the co-existing of different Chriz-associated protein complexes, one of which may include Chriz together with Z4, Jil-1 kinase and BEAF-32, another – Chriz and Z4 together with insulator proteins BEAF-32 and CP190 .

Histone acetylation plays an important role in keeping the chromatin structure. It has been shown, that acetylation at different lysine residues can be specifically recognized by distinct protein domains (e.g. bromodomains), which in turn recruit chromatin-remodeling factors (Ruthenburg et al. 2011). MOF, a MYST family histone acetyltransferase was shown to be associated with NSL – Non-Specific Lethal complex, bound to majority of constitutively active gene promoters (Raja et al. 2010). The complex is composed of seven proteins: NSL1, NSL2, NSL3, MCRS2, MBD-R2, WDS and MOF (Mendjan et al. 2006). Genome-wide comparative analysis of NSL-3 and MBD-R2 binding between 3rd instar larvae salivary glands and S2 cell line, performed by Lam and coworkers, revealed high similarity in profiles of these proteins (Lam et al. 2012). Similarly to Chriz complex, NSL was shown to localize in a close proximity (within 800 bp) to transcriptional start sites. Taking into consideration also functional generality of these two complexes in regulation of gene activity, we sought to investigate the possibility of their physical interaction. For this purpose, we analyzed the elute fractions of Chriz, Z4, BEAF-32 and CP190 for the presence of MBD-R2. Co-IPs of insulator proteins CP190 and BEAF-32 did not contain MBD-R2, but, interestingly, we found it to be co-immunoprecipitated with zinc-finger protein Z4. In contrast to our expectations, MBD-R2 was not found in Chriz co-IP fraction. It can be explained either by competing of Chriz antibody with MBD-R2 for the same binding site on the surface of Chriz molecule, which results in selective precipitation of Chris not associated with MBD-R2 or by postulating a fraction of Z4 chromosomal loci with higher affinity to MBD-R2 then to Chriz. Generally, we assume the possibility of Z4-mediated association between Chriz complex and NSL.

Pull down experiments, aimed to identify whether the co-immunoprecipitation of Chriz, CP190 and BEAF-32 is reasoned by direct interaction, revealed that these proteins interact with each other and protein fragments required for interaction were determined. We found that C-terminal part of Chriz protein (600-710 aa) is responsible for direct interaction with BEAF-32 and CP190. These results are in agreement with observations of Vogelmann and coworkers, who recognized same domains involved in interaction between BEAF-32 and Chriz (Vogelmann et al. 2014) The identified region partially overlaps with 500-768aa self-interaction part of Chriz protein, defined by Gan and coworkers (Gan et al 2011) and, interestingly, is also contained in 329-926 aa region, required for Jil-1 recruitment to chromatin (Rath et al. 2006). Taking into consideration the results of co-IP, which show that Jil-1 can be co-immunoprecipitated exclusively by Chriz or Z4, but not by BEAF-32 or CP190, we can assume that identified region may be required for selective interaction either with Jil-1 kinase or with insulator proteins depending on so far unknown chromatin context.

The interaction between BEAF-32 with CP190 as well as with Chriz was found to be mediated by 83 amino acid residues in C-terminal part of BEAF-32 (200-283 aa). The identified region contains 40 aa long BESS domain, known to mediate protein-protein interactions (Hart et al. 1997) and coiled-coil domain (200-230 aa), which was described to be necessary for BEAF self-interaction (Hart et al. 1997; Gilbert et al. 2006). Since we did not use BEAF-32 constructs missing CC-domain in our pull-down experiments, we cannot estimate the contribution of BEAF-32 self-interaction to Chriz or CP190 binding.

In the work of Vogelmann and coworkers, direct interaction between BEAF-32 and C-terminal (599-1096 aa) CP190 region was demonstrated (Vogelmann et al. 2014). This region contains glutamate-rich domain, which is required for CP190 essential function (Oliver et al. 2010). However, in our experiments N-terminal CP190 construct (1-500), containing BTB/POZ and D-rich domains was found to directly interact with BEAF-32 and Chriz proteins. Oliver and colleagues showed that BTB/POZ domain of CP190 is necessary for its association with BEAF-32 sites and CP190 fragment that lacks the whole E-rich region was still localized to all the tested CP190 wild-type containing Su(Hw), CTCF and BEAF sites in ChIP assays (Oliver et al. 2010). Due to inability of CP190 to bind chromatin directly (Vogelmann et al. 2014), interaction with insulator proteins appears to be necessary for correct targeting to co-localized sites, therefore, we would favor the results of Oliver et al. pointing to the role of BTB/POZ domain in interaction of CP190 with BEAF-32.

4.4 BEAF-32 contributes to recruitment of Chriz complex

Chriz is known to be localized to interband regons of polytene chromosomes with a preference to bind active gene regions (Eggert et al. 2004). Previous studies showed co-localization of Chriz with insulator protein BEAF-32 and demonstrated their presence in the same complex with Z4 (Gan et al. 2011). Later, Vogelmann with coworkers found BEAF-32 to be co-immunoprecipitated and interact directly with c-terminus domain of Chriz. It was also shown that Chriz possesses low affinity for DNA and, therefore is unlikely to bind chromatin independently (Vogelmann et al. 2014). Gan and colleagues hypothesized the possibility of BEAF-32 to be responsible for targeting of Chriz complex to open chromatin (Gan et al. 2011).

Taking into consideration, that over 90% BEAF-32 binding sites contain Chriz (Vogelmann et al. 2014), it was suggested, that BEAF-32 may be responsible for recruitment of Chriz complex to chromatin. However, downregulation of BEAF-32 to 80% in our RNAi experiments did not affect total amount of Chriz and Z4 in S2 cells. This result still did not exclude the role of BEAF-32 in targeting, since the remaining 20% could still be sufficient for the recruitment of complex. Alternatively, due to relatively long turnover period, Chriz may still form a stable complex with Z4 remaining dissociated from chromatin.

Therefore, to better examine the role of BEAF-32 in targeting of Chriz complex, we tested the binding of both to a site with mutated BEAF-32 motifs and compared it with enrichment at original motif. For this purpose we selected well studied 61C7-8 interband (Semeshin et al. 1989; Demakov et al. 1993; Zielke et al. 2014). It contains two clusters of BEAF-32 motifs are located in proximal part, coinciding with two binding peaks in ChIP-chip profiles of BEAF-32 and Chriz. ChIP-qPCR analysis revealed more than 50% decrease in BEAF-32 (from 5% to 2%) and, interestingly, decrease in Chriz enrichments (from 23% to 9%) at the mutated motif. However, we still observed 2% and 9% of precipitated DNA over input at mutated motif for BEAF-32 and Chriz respectively. This may be explained by a nearby high affinity cluster of two BEAF-32 original motifs (3,4) located in close proximity to mutated BEAF-32 motifs (less than 1 kbp), which could be present and co-precipitated at some DNA fragments after sonication step of ChIP.

The possibility of Chriz complex recruitment by insulator proteins was further analyzed on polytene squash preparations from BEAF-32 and CP190 RNAi fly strains using quantitative fluorescent microscopy. Since the images were acquired by DeltaVision image restoration microscopy they retain information of the recorded fluorescence intensity and therefore allow quantitative evaluation of intensity profiles across the recorded signals. (Zielke et al. 2015, in press). By analyzing deconvolved images, we measured total levels of fluorescence for each wavelength (see Materials and Methods for details).

The quantitative comparison of signal intensity profiles in 21E region of BEAF RNAi strain revealed 30% and 40% reduction of Z4 and Chriz levels respectively. Surprisingly, CP190 RNAi leaded to similar decrease in amounts of Chriz and Z4. These observations are in agreement with analysis of BEAF-32 mutated motif, strengthening the hypothesis of BEAF-32 contribution to Chriz complex targeting.

Interestingly, simultaneous BEAF-32 and CP190 RNAi knockdown, demonstrated severe disruption of chromosomal structure, in contrast to single knockdowns where the band-interband pattern remained intact. This finding points to synergetic effect from downregulation of both insulator proteins. In our measurements Chriz and Z4 were reduced to extent similar to single BEAF23 or CP190 knockdowns. However, this is the conservative estimatesince the analysis required recognition of cytology which was not possible on 95% of chromosomes most altered by the knockdown.

BEAF-32 was suggested to be responsible for recruitment of CP190 to chromatin (Bushey et al. 2009). However, Schwartz and coworkers later demonstrated no change in CP190 binding at sites colocalized with BEAF-32 in BEAF-32 RNAi knockdown (Schwartz et al. 2012). In contradiction with this statement, we observed reduction of CP190 level in BEAF RNAi. Unexpectedly, in the analyzed 21E region BEAF-32 binding following CP190 RNAi was also decreased.

The results of RNAi experiments are in agreement with the suggestion that insulator protein BEAF-32 is at least partially responsible for Chriz complex localization and point to possible

role of other factors such as CP190 in Chriz targeting. However, since the collected data describe the situation only at a single locus, we cannot extrapolate it to the whole genome as a general model.

4.5 Role of Chriz complex in open chromatin domain formation.

Over 2,000 of genome-wide studies, followed by research groups all over the world revealed high complexity pattern of proteins and epigenetic modifications of chromatin during development and between different cell types (Brown et al. 2015). To better understand the principles of chromatin structure formation, numerous attempts to classify the chromatin according to unique conjunctions of proteins bound were performed recent years (Filion et al. 2010; Kharchenko et al. 2011; Zhimulev et al. 2014). This analysis lead to the important finding that the genome is structured into chromatin domains with certain typical combinations of epigenetic factors. By juxtaposing the locations of P-element insertions and proteins bound in defined chromosomal regions with the pattern of epigenetic factors bound, Zhimulev and his colleagues proposed high level of correlation between epigenetic states of 3rd instar larvae salivary glands and cell culture (Vatolina et al. 2011, Demakov et al. 2011; Zhimulev et al. 2012).

Our group is interested to elucidate mechanisms responsible for open chromatin domain formation by an experimental approach. 61C7-8 interband was chosen for our comparative analysis as one of the best-studied cytological regions in *Drosophila* (Semeshin et al. 1989; Demakov et al. 1993; Zielke et al. 2014). High resolution mapping of the 61C region by in situ hybridization walk, performed in our group, determined the extent of decondensed 61C7-8 domain as 640-660+2 kbp. (Zielke et al. 2015, in press). This borders, defined cytologically on salivary gland chromosomes coincide with borders of open region mapped according to epigenetic modifications in S2 cells. Assuming that the epigenetic state is conserved between both cell types we would expect to observe the binding of open chromatin proteins within the mapped cytogenetic interval.

Such proteins as BEAF-32, Chriz and CP190 were found to be located within mapped region in S2 cells, according to IIF analysis However, high resolution comparative analysis of Chriz complex binding and epigenetic modifications in 61C7-8 locus between salivary gland chromatin and S2 cell chromatin revealed that Chriz pattern within the domain differs in distal part and is conserved in proximal. Similar observations were made for BEAF-32 and selected histone modifications – H3K4me3, H3S10ph and H3K27me3. To our surprise, the distalmost 642 kbp peak of BEAF-32- and Chriz-binding was not observed in salivary gland chromatin, although this chromatin section clearly belonged to the open domain according to *in situ* mapping (Zielke et al. 2015, in press).

Both enrichment for H3K4me3- and depletion for H3K27me3-chromatin in S2 cells correspond well with the extent of the open domain mapped by *in situ* approach (640-660

kbp), but this was not the case for salivary gland cell chromatin. Here presence/absence of these modifications is restricted to the proximal part of the domain (H3K27me3-enrichment: 649-659 kbp; H3K4me3-depletion: 648-660 kbp). Therefore, we can conclude that these two epigenetic modifications might not be involved in formation of open domain boundary and their function could be more related to transcription process. The difference in the expression levels of transcript located in distal part of 61C7-8 domain between two tissues is consistent with this statement (Zielke et al. 2015, in press).

Therefore, we assume that Chriz complex binding at the distal part of 61C7-8 domain in S2 cells plays a role in expression of CR43334 non-coding transcript. However, it is remained unclear whether the binding of the Chriz complex is a consequence of started transcription event or Chriz complex function is limited to maintaining the open state of chromatin region by associated nucleosome remodeling factors, keeping it available for regulatory factors.

5. Conclusion

Organization of DNA in the nucleus is a key for understanding how the correct expression of genetic material is executed. Recent identification of chromatin domains as fundamental units of genome architecture was a significant step forward in chromatin biology which brought us to the idea that many gene functions operate at the domain level (White 2012). Therefore, the studies related to mechanisms of domain organization are of actual interest today.

Current work emphasized architectural function of Chriz protein complex in establishing and maintenance of the chromatin domains. Our results obtained on different tissues revealed a distinct role of Chriz complex in transcription. Observed effects as well as tissue-specific correlation between Chriz binding and expression appears to be a promising start for expanding the analysis to genome-wide format.

Protein interactions, analyzed in current work identified insulator proteins BEAF-32 and CP190 as Chriz complex components. However, the complexity of carried functions points to existence of so far unknown proteins which may contribute to Chriz complex activity. In this context, we see tandem affinity purification of Chriz complex or such techniques as QUICK-SILAC as perspective steps in the investigation of interplay of chromatin factors.

Continuing technical advances together with the accumulated knowledge on the *Drosophila* genome represent the interphase polytene chromatin with the high cytological resolution as perspective model for the analysis of many remaining questions concerning how genome structure relates to genome function.

Literature

Ahanger, S. H., Shouche, Y. S., & Mishra, R. K. (2013). Functional sub-division of the *Drosophila* genome via chromatin looping: The emerging importance of CP190. Nucleus, 4(2), 115–122. http://doi.org/10.4161/nucl.23389

Alcover A, Izquierdo M, Stollar BD, Kitagawa Y, Miranda M, Alonso C (1982) In situ immunofluorescent visualization of chromosomal transcripts in polytene chromosomes. Chromosoma 87:263-277.

Avramova Zoya, Alexander Tikhonov (1999), Are *scs* and *scs*' 'neutral' chromatin domain boundaries of the 87A7 locus in vivo?, Trends in Genetics, Volume 15, Issue 4, 1 April, Pages 138-139, ISSN 0168-9525, http://dx.doi.org/10.1016/S0168-9525(99)01712-6.

Ausio Juan, Feng Dong, K.E. van Holde, (1989) Use of selectively trypsinized nucleosome core particles to analyze the role of the histone "tails" in the stabilization of the nucleosome, Journal of Molecular Biology, Volume 206, Issue 3, 1989, Pages 451-463, ISSN 0022-2836

Allfrey, V. G., Faulkner, R. and Mirsky, A. E. (1964): Acetylation and Methylation of Histones and Their Possible Role in the Regulation of Rna Synthesis. Proc Natl Acad Sci U S A, 51, 786-94

Amber R. Cutter, Jeffrey J. Hayes (2015) A brief review of nucleosome structure, FEBS Letters, Available online 14 May 2015, ISSN 0014-5793, http://dx.doi.org/10.1016/ j.febslet.2015.05.016.

Aravind L, (2000) The BED finger, a novel DNA-binding domain in chromatin-boundary-element-binding proteins and transposases, Trends in Biochemical Sciences, Volume 25, Issue 9, 1 September, Pages 421-423, ISSN 0968-0004, http://dx.doi.org/10.1016/S0968-0004(00)01620-0.

Ashburner M. (1967). Patterns of puffing activity in the salivary gland chromosomes of *Drosophila*. I. Autosomal puffing patterns in a laboratory stock of *Drosophila* melanogaster. Chromosoma 21(4) 398-428.

Ashburner M. (1998). *Drosophila*: A Laboratory Manual. New York: Cold Spring Harbor Laboratory. 1989.

Ashburner M. (1970) The genetic analysis of puffing in polytene chromosomes of *Drosophila*. Proc R Soc Lond B Biol Sci. 1970 Dec 1;176(1044):319-27.

Bannister, A. J., & Kouzarides, T. (2011). Regulation of chromatin by histone modifications. Cell Research, 21(3), 381–395. http://doi.org/10.1038/cr.2011.22

Bartkuhn M., Straub T., Herold M., Herrmann M., Rathke C.,Saumweber H., Gilfillan G.D., Becker P.B. and Renkawitz R. (2009). Active promoters and insulators are marked by the centrosomal protein 190. EMBO J. 28 877–888

Beermann W. (1972). Chromomeres and genes. in: Results and Problems in Cell Differentiation, 4. Developmental studies on giant chromosomes (eds. W. Beermann, J. Reinert, H. Ursprung), pp.1-34, Berlin: Springer Verlag.

Besant PG, Attwood PV. (2012) Histidine phosphorylation in histones and in other mammalian proteins. Methods Enzymol;471:403–26.

Bian, Q., & Belmont, A. S. (2012). Revisiting Higher-order and Large-scale Chromatin Organization. Current Opinion in Cell Biology, 24(3), 359–366. http://doi.org/10.1016/j.ceb.2012.03.003

Bell A.C., West A.G.,Felsenfeld G. (2001). Insulators and Boundaries: Versatile Regulatory Elements in the Eukaryotic Genome. Science 291, 447.

Berkaeva M, Demakov S, Schwartz YB, Zhimulev I. (2009). Functional analysis of *Drosophila* polytene chromosomes decompacted unit: the interband. Chromosome Res. 2009;17(6):745-54. doi: 10.1007/s10577-009-9065-7. Epub 2009 Aug 21.

Bickmore Wendy A., Bas van Steensel, (2013) Genome Architecture: Domain Organization of Interphase Chromosomes, Cell, Volume 152, Issue 6, 14 March 2013, Pages 1270-1284, ISSN 0092-8674, http://dx.doi.org/10.1016/j.cell.2013.02.001.

Bridges C.B. (1935). Salivary chromosome maps with a key to the banding of the chromosomes of *Drosophila* melanogaster. J. Hered. 26: 60-64.

Boros Imre M. Histone modification in *Drosophila* (2012)BRIEFINGS IN FUNCTIONAL GENOMICS. VOL 11. NO 4. 319 331 doi:10.1093/bfgp/els029

Brown JB, Celniker SE. (2015) Lessons from modENCODE. Annu Rev Genomics Hum Genet. 2015 Aug 24;16:31-53. doi: 10.1146/annurev-genom-090413-025448. Epub 2015 Jun 26.

Brower-Toland, B., Riddle, N. C., Jiang, H., Huisinga, K. L., & Elgin, S. C. R. (2009). Multiple SET Methyltransferases Are Required to Maintain Normal Heterochromatin Domains in the Genome of *Drosophila* melanogaster. Genetics, 181(4), 1303–1319. http://doi.org/10.1534/genetics.108.100271

Bushey A.M., Ramos E., Corces V.G. (2009). Three subclasses of a *Drosophila* insulator show distinct and cell type-specific genomic distributions. Genes Dev. 2009 Jun 1;23(11):1338-50. doi: 10.1101/gad.1798209. Epub 2009 May 14.

Cai H., Levine M. (1995). Modulation of enhancer-promoter interactions by insulators in the *Drosophila* embryo. Nature. 1995 Aug 10;376(6540):533-6.

Cai, W., Wang, C., Li, Y., Yao, C., Shen, L., Liu, S., … Johansen, K. M. (2014). Genome-wide analysis of regulation of gene expression and H3K9me2 distribution by JIL-1 kinase mediated histone H3S10 phosphorylation in *Drosophila*. Nucleic Acids Research, 42(9), 5456–5467. http://doi.org/10.1093/nar/gku173

Cohen, I., Poręba, E., Kamieniarz, K., & Schneider, R. (2011). Histone Modifiers in Cancer: Friends or Foes? Genes & Cancer, 2(6), 631–647. http://doi.org/10.1177/1947601911417176

Callaini G, M.G. Riparbelli (1990) Centriole and centrosome cycle in the early *Drosophila* embryo Journal of Cell Science 1990 97: 539-543;

Caelin Cubeñas-Potts, Victor G. Corces, (2015) Architectural proteins, transcription, and the three-dimensional organization of the genome, FEBS Letters, Available online 22 May 2015, ISSN 0014-5793, http://dx.doi.org/10.1016/j.febslet.2015.05.025.

Caussinus E., Oguz Kanca, Markus Affolter (2013) Protein Knockouts in Living Eukaryotes Using deGradFP and Green Fluorescent Protein Fusion Targets Current Protocols in Protein Science UNIT 30.2 DOI: 10.1002/0471140864.ps3002s73

Caussinus E., Oguz Kanca& Markus Affolter (2011) Fluorescent fusion protein knockout mediated by anti-GFP nanobody Nature Structural & Molecular Biology 19,117–12 doi:10.1038/nsmb.2180

Cuartero, S., Fresán, U., Reina, O., Planet, E., & Espinàs, M. L. (2014). Ibf1 and Ibf2 are novel CP190-interacting proteins required for insulator function. The EMBO Journal, 33(6), 637–647. http://doi.org/10.1002/embj.201386001

Daban Joan-Ramon. (2000) Physical Constraints in the Condensation of Eukaryotic Chromosomes. Local Concentration of DNA versus Linear Packing Ratio in Higher Order Chromatin Structures, Biochemistry 2000 39 (14), 3861-3866 DOI: 10.1021/bi992628w

Demakov S. A., Semeshin V. F., Zhimulev I. F. (1993). Cloning and molecular genetic analysis of *Drosophila* melanogaster interband DNA. Mol Gen Genet. 238(3) 437-443.

Demakov, S.A., Gortchakov, A. A., Schwartz, Y. B., Semeshin, V.F. , Campuzano, S., Modolell, J. und Zhimulev, I.F. (2004). Molecular and genetic organization of *Drosophila* melanogaster polytene chromosomes: evidence for two types of interband regions. Genetica 122, 311-324.

Demakov, S.A., Vatolina, T.Y., Babenko, V.N., Semeshin, V.F., Belyaeva, E.S. und Zhimulev, I.F. (2011). Protein composition of interband regions in polytene and cell line chromosomes of *Drosophila* melanogaster. BMC Genomics 12, 566-579.

Dekker J., Karsten Rippe, Martijn Dekker, and Nancy Kleckner (2002) Capturing Chromosome Conformation Science 15 February 2002: 295 (5558), 1306-1311. [DOI:10.1126/science.1067799]

Dekker J., Edith Heard, (2015) Structural and functional diversity of Topologically Associating Domains, FEBS Letters, Available online 5 September 2015, ISSN 0014-5793, http://dx.doi.org/10.1016/j.febslet.2015.08.044.

Deng H., Bao X., Cai W., Blacketer M.J., Belmont A.S., Girton J., Johansen J., Johansen K.M. (2008). Ectopic histone H3S10 phosphorylation causes chromatin structure remodeling in *Drosophila*. Development. 2008 Feb;135(4):699-705. doi: 10.1242/dev.015362. Epub 2008 Jan 16.

Deng H., Cai W., Wang C., Lerach S., Delattre M., Girton J., Johansen J., Johansen K.M. (2010). JIL-1 and Su(var)3-7 interact genetically and counteract each other's effect on position-effect variegation in *Drosophila*. Genetics. 2010 Aug;185(4):1183-92. doi: 10.1534/genetics.110.117150. Epub 2010 May 10.

Deng H., Zhang W., Bao X., Martin J.N., Girton J., Johansen J., Johansen K.M. (2005). The JIL-1 kinase regulates the structure of *Drosophila* polytene chromosomes. Chromosoma. 2005 Aug;114(3):173-82. Epub 2005 Jun 29.

Dixon J.R., Selvaraj S., Yue F., Kim A., Li Y., Shen Y., Hu M., Liu J.S., Ren B. (2012). Topological domains in mammalian genomes identified by analysis of chromatin interactions. Nature. 485(7398):376-80. doi: 10.1038/nature11082.

Eggert H., Gortchakov A. und Saumweber H. (2004). Identification of the *Drosophila* interband–specific protein Z4 as a DNA-binding zinc-finger protein determining chromosomal structure. J. Cell Sci. 117, 4253-4264.

E. Emberly, R. Blattes, B. Schuettengruber, M. Hennion, N. Jiang, CM Hart, E. Käs, O. Cuvier (2008) BEAF regulates cell-cycle genes through the controlled deposition of H3K9 methylation marks into its conserved dual-core binding sites. PLoS Biol. 6(12):2896-910

Filion G.J., van Bemmel J.G., Braunschweig U., Talhout W., Kind J., Ward L.D., Brugman W., de Castro I.J., Kerkhoven R.M., Bussemaker H.J., van Steensel B. (2010). Systematic protein location mapping reveals five principal chromatin types in *Drosophila* cells. Cell. 2010 Oct 15;143(2):212-24. doi: 10.1016/j.cell.2010.09.009. Epub 2010 Sep 30.

Finch J. T. und Klug A. (1976). Solenoidal model for superstructure in chromatin. Proc Natl Acad Sci USA 73(6) 1897-1901.

Finch J.T., Lutter L.C., Rhodes D., Brown R.S., Rushton B., Levitt M., Klug A. (1977). Structure of nucleosome core particles of chromatin. Nature. 269(5623):29-36.

Frasch, M., Glover, D. M. and Saumweber, H. (1986). Nuclear antigens follow different pathways into daughter nuclei during mitosis in early *Drosophila* embryos. J. Cell Sci. 82, 155-172.

Feng, S., & Jacobsen, S. E. (2011). Epigenetic modifications in plants: an evolutionary perspective. Current Opinion in Plant Biology, 14(2), 179–186. http://doi.org/10.1016/j.pbi.2010.12.002

Gan M., Moebus S., Eggert H. und Saumweber H. (2011). The Chriz-Z4 complex recruits JIL-1 to polytene chromosomes, a requirement for interband-specific phosphorylation of H3S10. J. Biosci. 36, 425-438.

Gavrilov A., Eivazova E., Priozhkova I., Lipinski M., Razin S., Vassetzky Y. (2009). Chromosome conformation capture (from 3C to 5C) and its ChIP-based modification. Methods Mol Biol. 2009;567:171-88. doi: 10.1007/978-1-60327-414-2_12.

Gaszner, M., Vazquez, J., & Schedl, P. (1999). The Zw5 protein, a component of the *scs* chromatin domain boundary, is able to block enhancer–promoter interaction. Genes & Development, 13(16), 2098–2107.

Gerasimova T.I. und Corces V.G. (2001). Chromatin Insulators and Boundarys: Effects on Transcription and Nuclear Organization. Annu. Rev. Genet. 35:193–208.

Guohong Li, Ping Zhu, (2015) Structure and organization of chromatin fiber in the nucleus, FEBS Letters, Available online 22 April 2015, ISSN 0014-5793, http://dx.doi.org/10.1016/j.febslet.2015.04.023.

Giet R, Glover DM. (2001) *Drosophila* aurora B kinase is required for histone H3 phosphorylation and condensin recruitment during chromosome condensation and to organize the central spindle during cytokinesis. J Cell Biol 2001;152: 669–82.

Goto H, Yasui Y, Nigg EA, et al. (2002) Aurora-B phosphorylates Histone H3 at serine28 with regard to the mitotic chromosome condensation. Genes Cells 2002;7:11–17.

Gilbert M.K., Tan Y.Y., Hart C.M. (2006). The *Drosophila* boundary element-associated factors BEAF-32A and BEAF-32B affect chromatin structure. Genetics. 2006 Jul;173(3):1365-75. Epub 2006 Apr 30.

A. K. Golovnin, I. S. Shapovalov, M. V. Kostyuchenko, M. F. Shamsutdinov, P. G. Georgiev, L. S. Melnikova (2014) Chromator protein directly interacts with the common part of the *Drosophila* melanogaster Mod(mdg4) family proteins doklady Biochemistry and Biophysics January 2014, Volume 454, Issue 1, pp 21-24

Gortchakov A., Eggert H., Gan M., Mattow J., Zhimulev V.F und Saumweber H. (2005). Chriz, a chromodomain protein specific for the interbands of *Drosophila* melanogaster. Chromosoma 114, 54-66.

Hart C. M., Olivier Cuvier, Ulrich K. Laemmli (1999) Evidence for an antagonistic relationship between the boundary element-associated factor BEAF and the transcription factor DREF Chromosoma November 1999, Volume 108, Issue 6, pp 375-383

Hart C. M., K. Zhao, U.K. Laemmli (1997) The *scs*' boundary element: characterization of boundary element-associated factors. Mol Cell Biol., 17(2): 999-1009

Hirose S. (1996) Transcriptional regulation through chromatin structure Tanpakushitsu Kakusan Koso. 1996 Nov;41(15 Suppl):2393-6.

Hou, C., Li, L., Qin, Z. S., & Corces, V. G. (2012). Gene Density, Transcription and Insulators Contribute to the Partition of the *Drosophila* Genome into Physical Domains. Molecular Cell, 48(3), 471–484. http://doi.org/10.1016/j.molcel.2012.08.031

Jiang N., E. Emberly, O. Cuvier, CM Hart (2009) Genome-wide mapping of boundary element-associated factor (BEAF) binding sites in *Drosophila* melanogaster links BEAF to transcription. Mol Cell Biol. (13): 3556-68

Jin, Y., Wang, Y., Walker, D. L., Dong, H., Conley, C., Johansen, J. and Johansen, K. M. (1999): JIL-1: A Novel Chromosomal Tandem Kinase Implicated in Transcriptional Regulation in *Drosophila*. Mol Cell, 4(1), 129-135

Ivaldi, M. S., Karam, C. S., & Corces, V. G. (2007). Phosphorylation of histone H3 at Ser10 facilitates RNA polymerase II release from promoter-proximal pausing in *Drosophila*. Genes & Development, 21(21), 2818–2831. http://doi.org/10.1101/gad.1604007

Kleinjan Dirk-Jan and Pedro Coutinho (2009) Cis-ruption mechanisms: disruption of cis-regulatory control as a cause of human genetic disease Briefings in Functional Genomics and Proteomics 8 (4): 317-332 first published online July 13, 2009 doi:10.1093/bfgp/elp022

Kharchenko P.V., Alekseyenko A.A., Schwartz Y.B., Minoda A., Riddle N.C., Ernst J., Sabo P.J., Larschan E., Gorchakov A.A., Gu T., Linder-Basso D., Plachetka A., Shanower G., Tolstorukov M.Y., Luquette L.J., Xi R., Jung Y.L., Park R.W., Bishop E.P., Canfield T.K., Sandstrom R., Thurman R.E., MacAlpine D.M., Stamatoyannopoulos J.A., Kellis M., Elgin S.C., Kuroda M.I., Pirrotta V., Karpen G.H., Park P.J. (2010). Comprehensive analysis of the chromatin landscape in *Drosophila* melanogaster. Nature. 2011 Mar 24;471(7339):480-5. doi: 10.1038/nature09725. Epub 2010 Dec 22.

Kellum, R., & Schedl, P. (1992). A group of *scs* elements function as domain boundaries in an enhancer-blocking assay. Molecular and Cellular Biology, 12(5), 2424–2431.

Kellum R., Paul Schedl, (1991) A position-effect assay for boundaries of higher order chromosomal domains, Cell, Volume 64, Issue 5, 8 March 1991, Pages 941-950, ISSN 0092-8674, http://dx.doi.org/10.1016/0092-8674(91)90318-S.

Kellner, W. A., Ramos, E., Van Bortle, K., Takenaka, N., & Corces, V. G. (2012). Genome-wide phosphoacetylation of histone H3 at *Drosophila* enhancers and promoters. Genome Research, 22(6), 1081–1088. http://doi.org/10.1101/gr.136929.111

Kugler, S. J., & Nagel, A. C. (2007). putzig Is Required for Cell Proliferation and Regulates Notch Activity in *Drosophila*. Molecular Biology of the Cell, 18(10), 3733–3740. http://doi.org/10.1091/mbc.E07-03-0263

Kugler, S. J., & Nagel, A. C. (2010). A Novel Pzg-NURF Complex Regulates Notch Target Gene Activity. Molecular Biology of the Cell, 21(19), 3443–3448. http://doi.org/10.1091/mbc.E10-03-0212

Kugler S.J., Gehring E.M., Wallkamm V., Krüger V., Nagel A.C. (2011).The Putzig-NURF nucleosome remodeling complex is required for ecdysone receptor signaling and innate immunity in *Drosophila* melanogaster. Genetics. 188(1):127-39. doi: 10.1534/genetics.111.127795.

Kuhn E.J., Viering M.M., Rhodes K.M., Geyer P.K. (2003). A test of insulator interactions in *Drosophila*. EMBO J. 2003 May 15;22(10):2463-71.

Kvon E.Z., Demakov S.A., and Zhimulev I.F. (2011). Chromatin Decompaction in the Interbands of *Drosophila* Polytene Chromosomes Does Not Correlate with High Transcription Level. Genetika. 2011 Jun;47(6):765-73.

Kyrchanova O. and Georgiev P. (2014). Chromatin insulators and long-distance interactions in *Drosophila*. Elsevier 588(1):8-14

Lam, K. C., Mühlpfordt, F., Vaquerizas, J. M., Raja, S. J., Holz, H., Luscombe, N. M., … Akhtar, A. (2012). The NSL Complex Regulates Housekeeping Genes in *Drosophila*. PLoS Genetics, 8(6), e1002736. http://doi.org/10.1371/journal.pgen.1002736

Legube G, McWeeney SK, Lercher MJ, Akhtar A (2006) X-chromosome-wide profiling of MSL-1 distribution and dosage compensation in *Drosophila*. Genes Dev 20:871-883.

Le, T. B. K., Imakaev, M. V., Mirny, L. A., & Laub, M. T. (2013). High-resolution mapping of the spatial organization of a bacterial chromosome. Science (New York, N.Y.), 342(6159), 731–734. http://doi.org/10.1126/science.1242059

Lee JS, Smith E, Shilatifard A. (2010) The language of histone crosstalk. Cell 2010;142:682–5.

Luger K. (2003). Structure and dynamic behavior of nucleosomes. Curr Opin Genet Dev. 2003 Apr;13(2):127-35.

Maksimenko, O., Bartkuhn, M., Stakhov, V., Herold, M., Zolotarev, N., Jox, T., … Georgiev, P. (2015). Two new insulator proteins, Pita and ZIPIC, target CP190 to chromatin. Genome Research, 25(1), 89–99. http://doi.org/10.1101/gr.174169.114

Matzat, L. H., & Lei, E. P. (2014). Surviving an Identity Crisis: A Revised View of Chromatin Insulators in the Genomics Era. Biochimica et Biophysica Acta, 1839(3), 203–214. http://doi.org/10.1016/j.bbagrm.2013.10.007

Maeda Robert K, François Karch, (2007) Making connections: boundaries and insulators in *Drosophila*, Current Opinion in Genetics & Development, Volume 17, Issue 5, October 2007, Pages 394-399, ISSN 0959-437X, http://dx.doi.org/10.1016/j.gde.2007.08.002.

McGuire Sean E, Gregg Roman, Ronald L Davis, (2004) Gene expression systems in *Drosophila*: a synthesis of time and space, Trends in Genetics, Volume 20, Issue 8, 1 August 2004, Pages 384-391, ISSN 0168-9525, http://dx.doi.org/10.1016/j.tig.2004.06.012.

Martin Cyrus & Yi Zhang (2005) The diverse functions of histone lysine methylation Nature Reviews Molecular Cell Biology 6, 838-849 (November 2005) | doi:10.1038/nrm1761

MBInfo contributors. From DNA to metaphase chromosome. In MBInfo Wiki, Retrieved 10/21/2014 from http://www.mechanobio.info/figure/figure/1389944285515.jpg.html

Methods in molecular biology. (2009) vol 536 Protein Blotting and Detection Editors: Kurien, Biji T., Scofield, R. Hal (Eds.)

Methods in molecular biology. (2012) vol 869 Protein Electrophoresis Editors: Kurien, Biji T., Scofield, R. Hal (Eds.)

Mendjan, S., & Akhtar, A. (2007). The right dose for every sex. Chromosoma, 116(2), 95–106. http://doi.org/10.1007/s00412-006-0089-x

Moon, H., Filippova, G., Loukinov, D., Pugacheva, E., Chen, Q., Smith, S. T., … Lobanenkov, V. (2005). CTCF is conserved from *Drosophila* to humans and confers enhancer blocking of the Fab-8 insulator. EMBO Reports, 6(2), 165–170. http://doi.org/10.1038/sj.embor.7400334

Muller, J., Hart, C. M., Francis, N. J., Vargas, M. L., Sengupta, A., Wild, B., Miller, E. L., O'Connor, M. B., Kingston, R. E. and Simon, J. A. (2002): Histone methyltransferase activity of a *Drosophila* Polycomb group repressor complex. Cell, 111(2), 197-208

North JA, Javaid S, Ferdinand MB, et al. (2011) Phosphorylation of histone H3(T118) alters nucleosome dynamics and remodeling. Nucleic Acids Res 2011;39:6465–74.

Nowak, S. J. and Corces, V. G. (2004): Phosphorylation of histone H3: a balancing act between chromosome condensation and transcriptional activation. Trends Genet, 20(4), 214-220

Nègre, N., Brown, C. D., Shah, P. K., Kheradpour, P., Morrison, C. A., Henikoff, J. G., … White, K. P. (2010). A Comprehensive Map of Insulator Elements for the *Drosophila* Genome. PLoS Genetics, 6(1), e1000814. http://doi.org/10.1371/journal.pgen.1000814

Nora, E. P., Lajoie, B. R., Schulz, E. G., Giorgetti, L., Okamoto, I., Servant, N., … Heard, E. (2012). Spatial partitioning of the regulatory landscape of the X-inactivation center. Nature, 485(7398), 381–385. http://doi.org/10.1038/nature11049

Oliver D, B. Sheehan, H. South, O. Akbari and C.-Y. Pai (2010) The chromosomal association/dissociation of the chromatin insulator protein Cp190 of *Drosophila* melanogaster is mediated by the BTB/POZ domain and two acidic regions. BMC Cell Biology, 11:101

Painter, T. S. (1934). The Morphology of the X Chromosome in Salivary Glands of *Drosophila* Melanogaster and a New Type of Chromosome Map for This Element. Genetics, 19(5), 448–469.

Ponton Fleur, Marie-Pierre Chapuis, Mathieu Pernice, Gregory A. Sword, Stephen J. Simpson, (2011) Evaluation of potential reference genes for reverse transcription-qPCR studies of physiological responses in *Drosophila* melanogaster, Journal of Insect Physiology, Volume 57, Issue 6, June 2011, Pages 840-850, ISSN 0022-1910, http://dx.doi.org/10.1016/j.jinsphys.2011.03.014.

Qi, H., Rath, U., Ding, Y., Ji, Y., Blacketer, M. J., Girton, J., Johansen, J. and Johansen, K. M. (2005), EAST interacts with Megator and localizes to the putative spindle matrix during mitosis in *Drosophila*. J. Cell. Biochem., 95: 1284–1291. doi:10.1002/jcb.20495

Qi, H., Rath, U., Wang, D., Xu, Y.-Z., Ding, Y., Zhang, W., … Johansen, K. M. (2004). Megator, an Essential Coiled-Coil Protein that Localizes to the Putative Spindle Matrix during Mitosis in *Drosophila*. Molecular Biology of the Cell, 15(11), 4854–4865. http://doi.org/10.1091/mbc.E04-07-0579

Raja S. J., Iryna Charapitsa, Thomas Conrad, Juan M. Vaquerizas, Philipp Gebhardt, Herbert Holz, Jan Kadlec, Sven Fraterman, Nicholas M. Luscombe, Asifa Akhtar, (2010) The Nonspecific Lethal Complex Is a Transcriptional Regulator in *Drosophila*, Molecular Cell, Volume 38, Issue 6, 25 June 2010, Pages 827-841, ISSN 1097-2765, http://dx.doi.org/10.1016/j.molcel.2010.05.021.

Rath, U., Wang, D., Ding, Y., Xu, Y.-Z., Qi, H., Blacketer, M. J., Girton, J., Johansen, J. and Johansen, K. M. (2004), Chromator, a novel and essential chromodomain protein interacts directly with the putative spindle matrix protein skeletor. J. Cell. Biochem., 93: 1033–1047. doi:10.1002/jcb.20243

Rath U., Ding Y, Deng H., Qi H., Bao X., Zhang W., Girton J. Johansen J. and Johansen, K.M. (2006). The chromodomain protein, chromator , interacts with JIL-1 kinase and regulates the structure of *Drosophila* polytene chromosomes. J. Cell Sci. 119, 2332-2341.

Reitman Marc , Eric Lee, Heiner Westphal & Gary Felsenfeld (1990) Site-independent expression of the chicken βA-globin gene in transgenic mice Nature 348, 749 - 752 (27 December 1990); doi:10.1038/348749a0

Regnard C, Straub T, Mitterweger A, et al. (2011) Global analysis of the relationship between JIL-1 kinase and transcription. PLoS Genet 2011;7:e1001327.

Ruthenburg, A. J., Li, H., Milne, T. A., Dewell, S., McGinty, R. K., Yuen, M., … Allis, C. D. (2011). Recognition of a mononucleosomal histone modification pattern by BPTF via multivalent interactions. Cell, 145(5), 692–706. http://doi.org/10.1016/j.cell.2011.03.053

Schübeler Dirk (2010), Chromatin in Multicolor, Cell, Volume 143, Issue 2, 15 October 2010, Pages 183-184, ISSN 0092-8674, http://dx.doi.org/10.1016/j.cell.2010.09.045.

Sotero-Caio C, G, de Souza M, J, Cabral-de-Mello D, C, Brasileiro-Vidal A, C, Guerra M (2011) Phosphorylation of Histone H3S10 in Animal Chromosomes: Is There a Uniform Pattern? Cytogenet Genome Res 2011;135:111-117

Staynov D.Z., S. Dunn, J.P. Baldwin, C. Crane-Robinson,(1983) Nuclease digestion patterns as a criterion for nucleosome orientation in the higher order structure of chromatin, FEBS Letters, Volume 157, Issue 2, 4 July 1983, Pages 311-315, ISSN 0014-5793, http://dx.doi.org/10.1016/0014-5793(83)80567-5.

Sanyal, A., Lajoie, B., Jain, G., & Dekker, J. (2012). The long-range interaction landscape of gene promoters. Nature, 489(7414), 109–113. http://doi.org/10.1038/nature11279

Saha A1, Wittmeyer J, Cairns BR. (2006) Mechanisms for nucleosome movement by ATP-dependent chromatin remodeling complexes. Results Probl Cell Differ. 2006;41:127-48.

Swaminathan A. Ambikai Gajan, Lori A Pile (2012) Epigenetic regulation of transcription in *Drosophila* Frontiers in Bioscience 17, 909-937, January 1, 2012

Sambrook Joseph &Michael Green (2012) Molecular Cloning: A Laboratory Manual. Publisher: Cold Spring Harbor Laboratory Press; 4th edition (June 15, 2012)

Sadakierska-Chudy, A., & Filip, M. (2015). A Comprehensive View of the Epigenetic Landscape. Part II: Histone Post-translational Modification, Nucleosome Level, and Chromatin Regulation by ncRNAs. Neurotoxicity Research, 27, 172–197. http://doi.org/10.1007/s12640-014-9508-6

Schwartz, Y. B., Linder-Basso, D., Kharchenko, P. V., Tolstorukov, M. Y., Kim, M., Li, H.-B., … Pirrotta, V. (2012). Nature and function of insulator protein binding sites in the

Drosophila genome. Genome Research, 22(11), 2188–2198. http://doi.org/10.1101/gr.138156.112

Semeshin V.F., Demakov S.A., Zhimulev I.F. (1989). Characteristics of structures of *Drosophila* polytene chromosomes formed by transposable DNA fragments. Genetika. 1989 Nov;25(11):1968-78.

Semeshin V.F., Demakov S.A., Shloma V.V., Vatolina T.Y., Gortchakov, A.A. and Zhimulev, V.F. (2008). Interbands behave as decompacted units in *Drosophila* melanogaster polytene chromosomes. Genetica 132, 267-279.

Sexton T., Bantignies F. and Cavalli G. (2009). Genomic interactions: chromatin loops and gene meeting points in transcriptional regulation. Semin. Cell Dev. Biol. 20, 849-855.

Sexton T., Yaffe E., Kenigsberg E., Bantignies F., Leblanc B., Hoichman M., Parrinello H., Tanay A., Cavalli G. (2012). Three-dimensional folding and functional organization principles of the *Drosophila* genome. Cell. 148(3):458-72. doi: 10.1016/j.cell.2012.01.010. Epub 2012 Jan 19.

Sims, R. J., 3rd, Nishioka, K. and Reinberg, D. (2003): Histone lysine methylation: a signature for chromatin function. Trends Genet, 19(11), 629-39

Silva-Sousa, R., López-Panadès, E., Piñeyro, D., & Casacuberta, E. (2012). The Chromosomal Proteins JIL-1 and Z4/Putzig Regulate the Telomeric Chromatin in *Drosophila* melanogaster. PLoS Genetics, 8(12), e1003153. http://doi.org/10.1371/journal.pgen.1003153

Turner B.M., Andrew J. Birley, Jayne Lavender, (1992) Histone H4 isoforms acetylated at specific lysine residues define individual chromosomes and chromatin domains in *Drosophila* polytene nuclei, Cell, Volume 69, Issue 2, 17 April 1992, Pages 375-384, ISSN 0092-8674, http://dx.doi.org/10.1016/0092-8674(92)90417-B.

Turner B.M. (2000). Histone acetylation and an epigenetic code. Bioessays. 2000 Sep;22(9):836-45.

Thoma F, Koller T, Klug A. (1979). Involvement of histone H1 in the organization of the nucleosome and of the salt-dependent superstructures of chromatin. The Journal of Cell Biology, 83(2), 403–427.

Udvardy Andor, Eleanor Maine, Paul Schedl, (1985) The 87A7 chromomere: Identification of novel chromatin structures flanking the heat shock locus that may define the boundaries of higher order domains, Journal of Molecular Biology, Volume 185, Issue 2, 20 September 1985, Pages 341-358, ISSN 0022-2836, http://dx.doi.org/10.1016/0022-2836(85)90408-5.

Valenzuela L and Rohinton T. Kamakaka (2006) Chromatin Insulators Annual Review of Genetics Vol. 40: 107-138 (Volume publication date December 2006) DOI: 10.1146/annurev.genet.39.073003.113546

Van Bortle K., Nichols M.H., Li L., Ong C.T., Takenaka N., Qin Z.S., Corces V.G. (2014). Insulator function and topological domain border strength scale with architectural protein occupancy. Genome Biol. 15(6):R82. doi: 10.1186/gb-2014-15-5-r82.

Van Bortle K. and Corces V.G. (2012). Nuclear organization and genome function. Ann Rev. Cell Dev. Biol. 28, 163-187.

Van Holde E. (1988). Histon modifications in chromatin. Springer Verlag, New York pp. 111-148P.

Van Holde K.E., Shaw B.R., Lohr D., Herman T.M. and Kovacic R.T. (1975). Organization and expression of the eukaryotic genome. In Tenth FEBS Meeting, G. Bernardi and F. Gros, eds. (Amsterdam: North Holland/American Elsevier), pp. 57–72.

Vatolina T.Y., Bolyreva L.V., Demakova O.V., Demakov S.A., Kokoza E.B., Semeshin V.F., Babenko V.N., Goncharov F.P., Belyaeva E.S. and Zhimulev I.F. (2011). Identical functional organization of nonpolytene and polytene chromosomes in *Drosophila* melanogaster. PLoS one 6, e25960.

Vogelmann J., Le Gall A., Dejardin S., Allemand F., Gamot A., Labesse G., Cuvier O., Nègre N., Cohen-Gonsaud M., Margeat E., Nöllmann M.. (2014). Chromatin insulator factors involved in long-range DNA interactions and their role in the folding of the *Drosophila* genome. PLoS Genet. 2014 Aug 28;10(8):e1004544. doi: 10.1371/journal.pgen.1004544. eCollection 2014.

Vogelmann J., Valeri A., Guillou E., Cuvier O., Nöllmann M. (2011). Roles of chromatin insulator proteins in higher-order chromatin organization and transcription regulation. Nucleus. 2011 Sep-Oct;2(5):358-69. doi: http://dx.doi.org/10.4161/nucl.2.5.17860. Epub 2011 Sep 1.

Walker, D. L., Wang, D., Jin, Y., Rath, U., Wang, Y., Johansen, J., & Johansen, K. M. (2000). Skeletor, a Novel Chromosomal Protein That Redistributes during Mitosis Provides Evidence for the Formation of a Spindle Matrix. The Journal of Cell Biology, 151(7), 1401–1412.

White R. (2012) Packaging the fly genome: domains and dynamics.Brief Funct Genomics. 2012 Sep;11(5):347-55. doi: 10.1093/bfgp/els020. Epub 2012 Sep 3.

Wang C., Cai W., Li Y., Deng H., Bao X., Girton J., Johansen J., Johansen K.M. (2011). The epigenetic H3S10 phosphorylation mark is required for counteracting heterochromatic spreading and gene silencing in *Drosophila* melanogaster. J Cell Sci. 2011 Dec 15;124(Pt 24):4309-17. doi: 10.1242/jcs.092585.

Whitfield W. G. F., M. A. Chaplin, K. Oegema, H. Parry, D. M. Glover (1995) The 190 kDa centrosome-associated protein of *Drosophila* melanogaster contains four zinc finger motifs and binds to specific sites on polytene chromosomes. Journal of Cell Science 108, 3377-3387

Widom, J., Finch, J. T., & Thomas, J. O. (1985). Higher-order structure of long repeat chromatin. The EMBO Journal, 4(12), 3189–3194.Worcel et al. 1981

Wasser M, Zalina Bte Osman, William Chia, (2007) EAST and Chromator control the destruction and remodeling of muscles during *Drosophila* metamorphosis, Developmental Biology, Volume 307, Issue 2, 15 July 2007, Pages 380-393, ISSN 0012-1606, http://dx.doi.org/10.1016/j.ydbio.2007.05.001.

Xu, Q., Li, M., Adams, J., & Cai, H. N. (2004). Nuclear location of a chromatin insulator in *Drosophila* melanogaster. Journal of Cell Science, 117(0 7), 1025–1032. http://doi.org/10.1242/jcs.00964

Yang, J., Ramos, E., & Corces, V. G. (2012). The BEAF-32 insulator coordinates genome organization and function during the evolution of *Drosophila* species. Genome Research, 22(11), 2199–2207. http://doi.org/10.1101/gr.142125.112

Yao, C., Ding, Y., Cai, W., Wang, C., Girton, J., Johansen, K. M., & Johansen, J. (2012). THE CHROMODOMAIN-CONTAINING NH2-TERMINUS OF CHROMATOR INTERACTS WITH HISTONE H1 AND IS REQUIRED FOR CORRECT TARGETING TO CHROMATIN. Chromosoma, 121(2), 209–220. http://doi.org/10.1007/s00412-011-0355-4

Yun Ding, Changfu Yao, Mariana Lince-Faria, Uttama Rath, Weili Cai, Helder Maiato, Jack Girton, Kristen M. Johansen, Jørgen Johansen, (2009) Chromator is required for proper microtubule spindle formation and mitosis in *Drosophila*, Developmental Biology, Volume 334, Issue 1, 1 October 2009, Pages 253-263, ISSN 0012-1606, http://dx.doi.org/10.1016/j.ydbio.2009.07.027

Ye Jin, Yanming Wang, Diana L Walker, Hao Dong, Cherice Conley, Jørgen Johansen, Kristen M Johansen, (1999) JIL-1: A Novel Chromosomal Tandem Kinase Implicated in Transcriptional Regulation in *Drosophila*, Molecular Cell, Volume 4, Issue 1, July 1999, Pages 129-135, ISSN 1097-2765, http://dx.doi.org/10.1016/S1097-2765(00)80195-1.

Zhang W., Deng H., Bao X., Lerach S., Girton J., Johansen J., Johansen K.M. (2006). The JIL-1 histone H3S10 kinase regulates dimethyl H3K9 modifications and heterochromatic spreading in *Drosophila*. Development. 2006 Jan;133(2):229-35. Epub 2005 Dec 8.

Zhao K., Hart C.M. and Laemmli U.K. (1995). Visualization of chromosomal domains with boundary element-associated factor BEAF-32. Cell 81, 879-889.

Zhimulev I.F., Zykova T.Y., Goncharov F.P., Khoroshko V.A., Demakova O.V., Semeshin V.F., Pokholkova G.V., Boldyreva L.V., Demidova D.S., Babenko V.N., Demakov S.A.,

Belyaeva E.S. (2014). Genetic organization of interphase chromosome bands and interbands in *Drosophila* melanogaster. PLoS One. 9(7):e101631. doi: 10.1371/journal.pone.0101631. eCollection 2014.

Zhuimulev I.F., Beliaeva E.S., Zykova T.I., Semeshin V.F., Demakov .SA., Demakova O.V., Goncharov F.P., Khoroshko V.A, Boldyreva L.V., Kokoza E.B., Pokholkiova G.V.(2013) Chromomeric organization of interphase chromosomes in *Drosophila* melanogaster Tsitologiia. 2013;55(3):144-7.

Zentgraf H., Franke W.W. (1984)Differences of supranucleosomal organization in different kinds of chromatin: cell type-specific globular subunits containing different numbers of nucleosomes.. *The Journal of Cell Biology*, *99*(1 Pt 1), 272–286.

Zielke T., Saumweber H. (2014) Dissection of open chromatin domain formation by site-specific recombination in *Drosophila*. J Cell Science (2014) 127:2365–2375.

Zielke T., Glotov A., Saumweber H. (2015) Mapping the chromosomal interval 61C7-61C8 of *Drosophila melanogaster* reveals interbands as open chromatin domains. Chromosoma. In press.

Supplementary figures

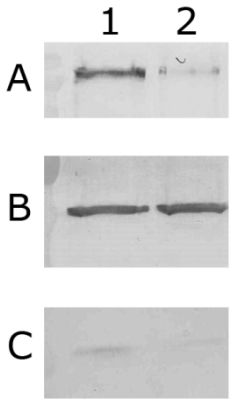

Suppl. fig. 1. Knockdown of Chriz in S2 cells affects histone H3S10 phosphorylation. Western blot from S2 cell lysates following Chriz RNAi. Lane 1 - OFP control; Lane 2 - Chriz knockdown. Membrane was probed with the following antibodies: A) anti-Chriz; B) anti-Tubulin loading control; C) anti-H3S10Ph.

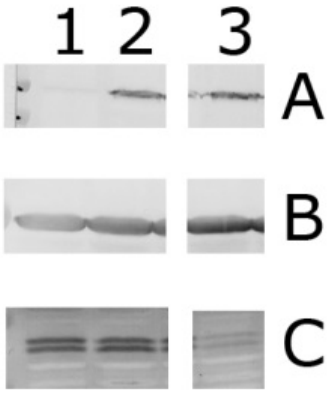

Suppl. fig. 2. Knockdown of Z4 in S2 cells does not affect BEAF-32 level and vice versa. Western blot from S2 cell lysates following Z4- and BEAF-32 RNAi. Lane 1 - Z4 RNAi; Lane 2 - OFP control; Lane 3 - BEAF-32 RNAi. Membrane was probed with the following antibodies: A) anti-Z4; B) anti-Tubulin loading control; C) anti-BEAF-32.

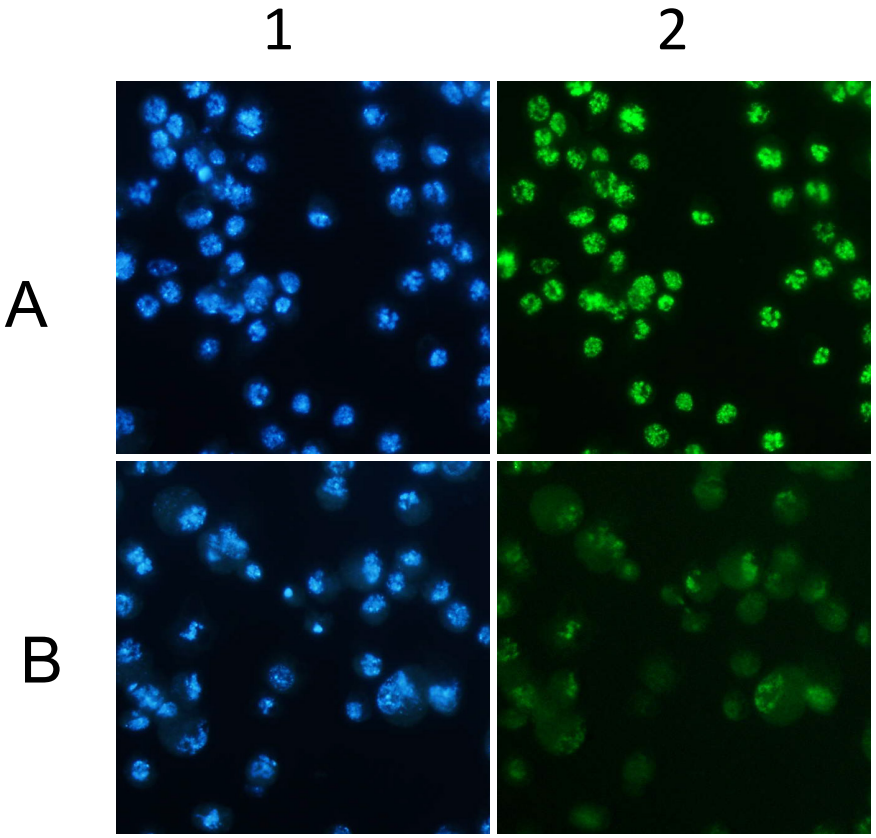

Suppl. fig. 3. Z4 RNAi in S2 cells resulted in >80% knockdown efficiency. IIF staining of S2 cells. A) OFP control; B) Z4 RNAi. 1 – Hoechst staining (blue); 2 –Z4 (green).

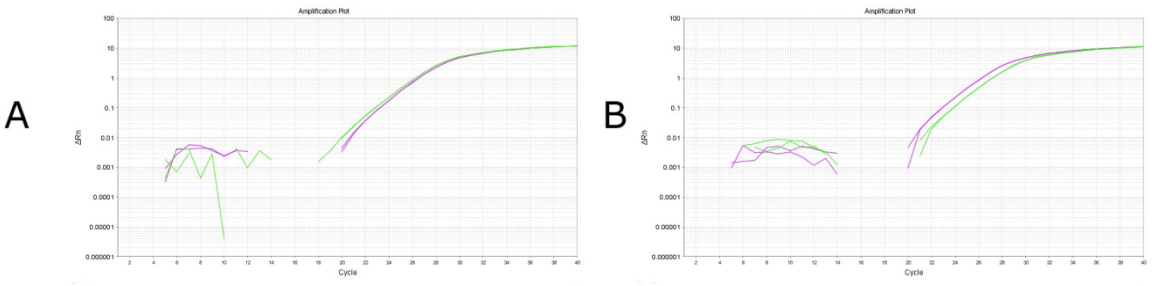

Suppl. fig. 4. Expression of EF1 reference gene is reduced following Chriz knockdown.

qPCR amplification plots of EF1 gene in Z4 RNAi (A) and Chriz RNAi (B). Green line represents knockdown, violet line – OFP control

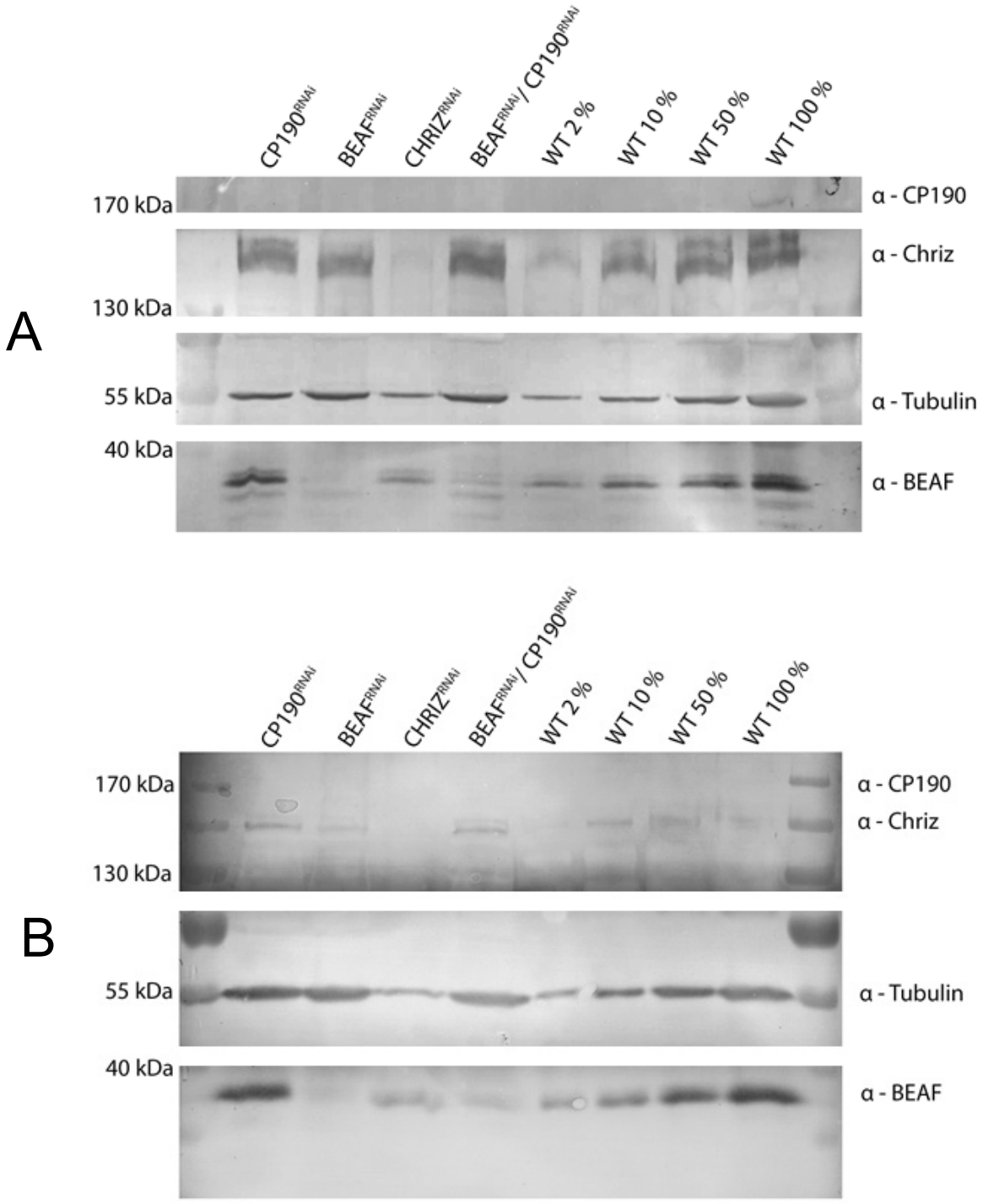

Suppl. fig. 5. Knockdown efficiencies of RNAi strains estimated by western blot. Salivary glands were dissected, cooked 10 mins in Laemmli buffer and applied to the gel. For estimation of knockdoen efficiencies, lysate from the wild type was loaded in dilutions. RNAi strains are subscribed above the respective lanes. On the left side wolecular weights of marker are subscribed. On the right side the antibodies used for western. A, B – two biological replicas.

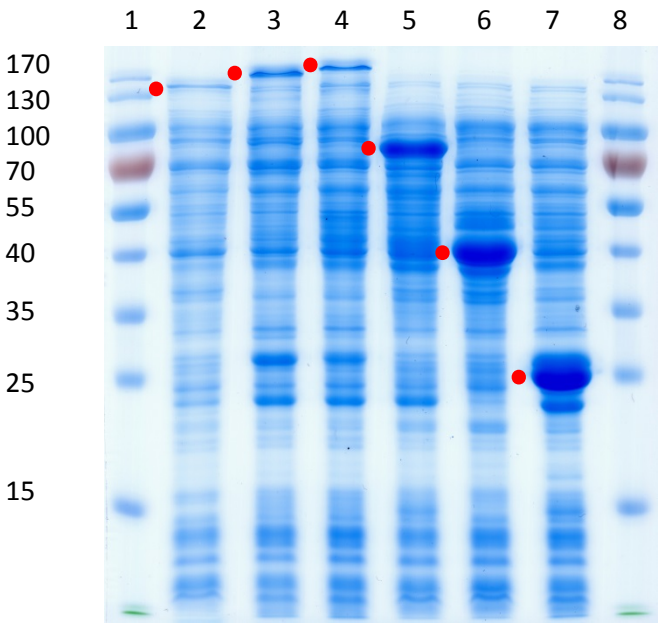

Suppl. Fig. 6. Example of expression of proteins used for pull-down assay. Transgenic constructs were expressed in BL-21 cell strain, lysates were prepared, boiled 10 mins in Laemmli buffer and applied to the gel. 1,8 – Maker; 2 – Myc-Chriz-FL; 3 – GST-Z4-FL; 4 – GST-CP190-FL; 5 – MBP-BEAF-32-FL; 6 – MBP epitope; 7- GST epitope. On the left side wolecular weights of marker is subscribed. Red dots mark the positions of expressed transgenic proteins.

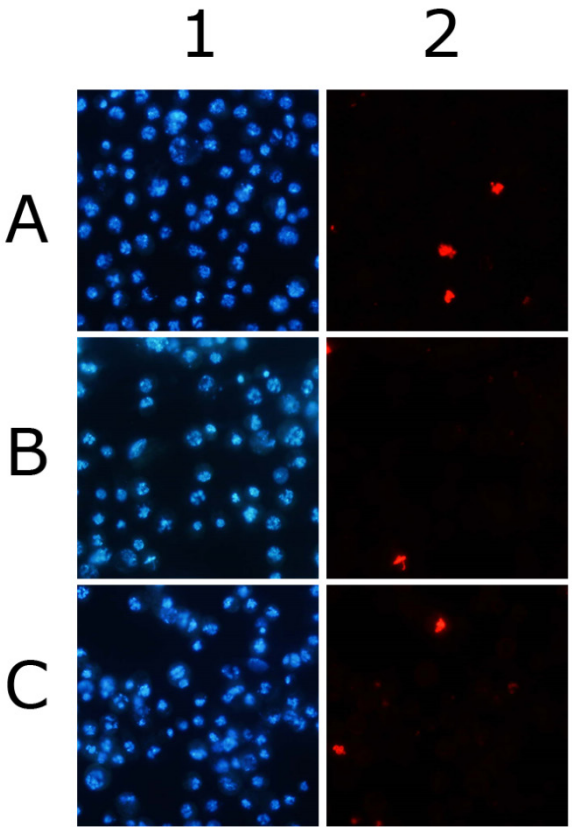

Suppl. Fig. 7. Aurora B - mediated H3S10 phosphorylation during mitosis is not affected by Chriz or Z4 knockdowns. IIF staining of S2 cells. 1 – Hoechst; 2 – anti - H310ph antibody. A) OFP control; B) Chriz RNAi; C) Z4 RNAi.

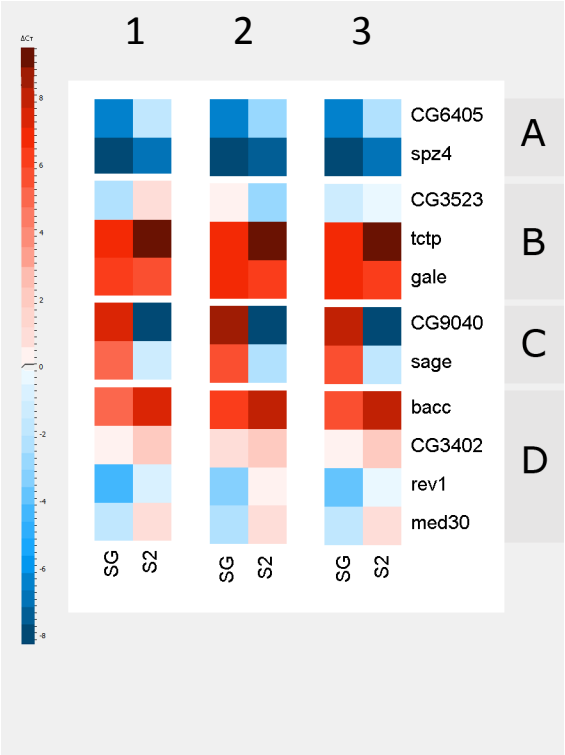

Suppl. Fig. 8. Heatmap of the results of qRT PCR from S2 cells (S2) and 3rd instar larvae salivary glands (SG). The gradient scale on left side indicates the expression level. A,B,C,D – Classification groups of genes. 1, 2 – biological replicas; 3 – average mean. Actin42a was used as the endogenous control.